Technische Universität München
TUM School of Life Sciences

The relationship between carbon isotopic composition of plant dry matter and gas exchange in near isogenic lines of maize (*Zea mays* L.)

Stella Eggels

Vollständiger Abdruck der von der TUM School of Life Sciences der Technischen Universität München zur Erlangung des akademischen Grades einer

Doktorin der Naturwissenschaften (Dr. rer. nat.)

genehmigten Dissertation.

Vorsitz: Prof. Dr. Gerd Patrick Bienert

Prüfende der Dissertation:

1. Prof. Dr. Chris-Carolin Schön
2. apl. Prof. Dr. Thorsten Grams

Die Dissertation wurde am 29.06.2022 bei der Technischen Universität München eingereicht und durch die TUM School of Life Sciences am 04.11.2022 angenommen.

Content

List of figures III
List of tables V
List of abbreviations VI
Prior publications VIII
Summary IX
Zusammenfassung XI
1 Introduction 1
1.1 Carbon fixation and water use efficiency in C_4 plants 1
1.1.1 Water use efficiency 1
1.1.2 C_4 photosynthesis 3
1.1.3 Carbon fixation in maize 4
1.2 Carbon isotope discrimination ($\Delta^{13}C$) 6
1.2.1 $\Delta^{13}C$ during photosynthesis 6
1.2.2 Connection of carbon isotopic composition ($\delta^{13}C$) and water use efficiency 9
1.2.3 Leakiness 10
1.2.4 Genetic variation for $\Delta^{13}C$ of C_4 plants 11
1.3 Objectives of this study 13
2 Methods 14
2.1 Plant material 14
2.1.1 Near isogenic lines (NILs) 14
2.1.2 Generation of crosses and recombinant lines derived from the original NILs 15
2.2 Growth conditions and experimental setup 17
2.2.1 Imbibition and pre-growth 17
2.2.2 Growth chamber experiments (Exp. 1.1 and 1.2) 18
2.2.3 Greenhouse experiments (Exp. 2.1-2.6) 19
2.2.4 Field trials 21
2.3 Leaf gas exchange measurements 23
2.3.1 Infrared gas analyzer measurements of gas exchange 23
2.3.2 Measurements of photosynthetic $\Delta^{13}C$ 24
2.4 Determination of stable isotopic compositions 25
2.4.1 Sampling and sample preparation 25
2.4.2 Carbon isotopic composition $\delta^{13}C$ 26
2.4.3 Oxygen isotopic composition $\delta^{18}O$ 26
2.5 Determination of photosynthesis-related traits 27
2.5.1 Stomatal density 27
2.5.2 Chlorophyll content 27

2.5.3 Leaf soluble sugar contents 27
2.5.4 Determination of PEPC and Rubisco activity 28
2.6 Whole plant water use efficiency and response to progressive soil drying 28
2.7 Assessment of growth- and yield-related traits 29
2.8 Data analysis 30
3 Results 32
3.1 Genetic variation in dry matter $\delta^{13}C$ and photosynthetic $\Delta^{13}C$ 32
3.1.1 $\delta^{13}C$ of leaves and kernels 32
3.1.2 Photosynthetic $\Delta^{13}C$ and the ratio of intercellular to ambient CO_2 concentration (C_i/C_a) 35
3.2 Genetic variation in gas exchange and water use efficiency under optimal conditions 39
3.2.1 Gas exchange and related traits under greenhouse conditions 40
3.2.2 Gas exchange and related traits under field conditions 45
3.2.3 Whole plant water use efficiency 48
3.3 Genetic variation in gas exchange and $\delta^{13}C$ under water deficit 50
3.3.1 Gas exchange response to progressive soil drying 50
3.3.1 Gas exchange and photosynthetic $\Delta^{13}C$ at different soil water contents 52
3.3.2 Effect of drought on dry matter $\delta^{13}C$ 54
3.4 Association of $\delta^{13}C$ with differences in agronomic traits 57
3.5 Genetic dissection of the segment on chromosome 1 60
4 Discussion 63
4.1 Connection between genotypic differences in $\delta^{13}C$ and iWUE 63
4.1.1 Genetic variation in photosynthetic $\Delta^{13}C$ and C_i/C_a 63
4.1.2 Genetic variation in leakiness 65
4.1.3 Connection between gas exchange and dry matter $\delta^{13}C$ 67
4.1.4 Divergence of leaf- and kernel-derived measures of $\Delta^{13}C$ 70
4.2 Environmental effects on gas exchange and $\Delta^{13}C$ 75
4.2.1 Effect of field conditions on genotypic differentiation in $\delta^{13}C$ 75
4.2.2 Effect of drought on genotypic differentiation in $\delta^{13}C$ 78
4.3 Conclusions 83
5 References 86
6 Supplement 93
7 Acknowledgements 101

List of figures

Figure 1.1: Pathway of carbon fixation in maize, a NADP-ME type C_4 species, with additional activity of PEPCK (Sales et al., 2021; Schlüter et al., 2019). 5

Figure 2.1: Genotyping data of NIL BY, which is homozygous for the major chromosome (chr) 1 and chr 7 introgression. 16

Figure 3.1: Carbon isotopic composition of the leaf below the uppermost ear of greenhouse-grown near isogenic lines NIL B, NIL C, NIL W, NIL X and NIL Y and recurrent parent RP. .33

Figure 3.2: Carbon isotopic composition ($\delta^{13}C$) of leaves and kernels of the near isogenic lines NIL B, NIL Y and recurrent parent RP grown under a) field or b) greenhouse conditions. 34

Figure 3.3: Relationship between photosynthetic carbon isotope discrimination ($\Delta^{13}C_{Photosynthetic}$) and the ratio of the intercellular to ambient CO_2 concentration (C_i/C_a) measured concurrently in the maize near isogenic lines NIL B and NIL Y and recurrent parent RP. 37

Figure 3.4: Stomatal conductance (g_s), assimilation rates (A) and intercellular CO_2 concentrations (C_i) in the maize near isogenic lines NIL B and NIL Y and recurrent parent RP at stage V5/6 grown in the growth chamber. 38

Figure 3.5: Gas exchange and oxygen isotopic composition ($\delta^{18}O$) of the near isogenic lines NIL B and NIL Y and recurrent parent RP under greenhouse conditions at developmental stage V5/6 and V7-9. 41

Figure 3.6: Gas exchange of near isogenic lines NIL B, NIL Y and NIL BY and recurrent parent RP in the greenhouse. 43

Figure 3.7: Assimilation rate (A) plotted against stomatal conductance (g_s) of the near isogenic lines NIL B and NIL Y and recurrent parent RP, measured around developmental stage V6 in different environments and experiments. 44

Figure 3.8: Gas exchange in the near isogenic lines NIL B, NIL Y and NIL BY and the recurrent parent (RP) at stage V6/7 grown in the field 2021. 45

Figure 3.9: Carbon isotopic composition ($\delta^{13}C$) of a) cobleaves and b) kernels of near isogenic lines NIL B, NIL Y and NIL BY and recurrent parent RP, grown in the field in 2021. 47

Figure 3.10: Consumed water and whole plant water use efficiency (WUE_{plant}) of near isogenic lines NIL B and NIL Y and recurrent parent RP in a greenhouse experiment. 49

Figure 3.11: Response of near isogenic lines NIL B and NIL Y and recurrent parent RP to progressive soil drying. 51

Figure 3.12: Stomatal conductance (g_s) and intrinsic water use efficiency (iWUE) of near isogenic lines NIL B and NIL Y and recurrent parent RP under control and drought conditions in a growth chamber experiment (Exp. 1.2). 52

Figure 3.13: Effect of water deficit on photosynthetic carbon isotope discrimination ($\Delta^{13}C_{Photosynthetic}$) in the near isogenic lines NIL B and NIL Y and recurrent parent RP. 53

Figure 3.14: Gas exchange and stable isotopic composition of near isogenic lines NIL B and NIL Y and recurrent parent RP under control and drought conditions in a greenhouse experiment (Exp. 2.4). 54

Figure 3.15: Isotopic composition of kernels of near isogenic lines NIL B and NIL Y and recurrent parent RP grown under well-watered and water-limited conditions in the field in 2019. 56

Figure 3.16: Mean carbon isotopic composition of kernels ($\delta^{13}C_{Kernel}$) plotted against the mean kernel number per plant of the respective genotype in field trials 2019 (a) and 2020 (b) under control conditions. 57

Figure 3.17: a) Kernel number per plant and b) thousand kernel weight (TKW) of near isogenic line NIL Y and recurrent parent RP in the field trials in 2019 and 2020. 58

Figure 3.18: Carbon isotopic composition ($\delta^{13}C$) of total kernels and of endosperm and embryo fractions of the kernel of near isogenic line NIL Y and recurrent parent RP grown in the field in 2018. 59

Figure 3.19: Genotyping data based on polymorphic markers in the NIL Y introgressions and kernel carbon isotopic composition ($\delta^{13}C_{Kernel}$) of recombinant lines derived from RP and NIL Y. 61

List of tables

Table 2.1: Introgressions of NIL B and NIL Y with starting and end coordinates on the respective chromosomes (chr) in bp and their size in Mb. 14

Table 2.2: KASP markers used for generating NIL BY with marker coordinates (B73 AGPv4) and nucleotide bases corresponding to the allele of the recurrent parent (RP) and the donor parent (DP).....15

Table 2.3: Temperature program for KASP genotyping reactions as given by LGC Biosearch^{TM} Technologies, UK. 16

Table 2.4: KASP markers used for generating recombinant lines derived from NIL Y with marker coordinates (B73 AGPv4) and nucleotide bases corresponding to the allele of the recurrent parent (RP) and the donor parent (DP).....17

Table 3.1: Carbon isotopic composition of kernels ($\delta^{13}C_{Kernel}$) of five near isogenic lines (NILs) and recurrent parent RP, grown in the field 2016 under well-watered and water-limited conditions. 32

Table 3.2: Photosynthesis-related traits of youngest fully developed leaves of RP, NIL B and NIL Y at stage V5/6 in the greenhouse (Exp. 2.3).....42

Table 3.3: Gas exchange - related traits in the near isogenic lines NIL B, NIL Y and NIL BY and the recurrent parent (RP), at stage V6/7 grown in the field 2021.....46

Table 3.4: Contents of sucrose, glucose and fructose of cobleaves of RP, NIL B, NIL Y and NIL BY grown in the field 2021. 48

Table 3.5: Kernel number per plant and thousand kernel weight (TKW) of RP, NIL B, NIL Y and NIL BY, grown in the field in 2021.....59

List of abbreviations

$\delta^{13}C$	carbon isotopic composition
$\Delta^{13}C$	carbon isotope discrimination
$\Delta^{13}C_{Leaf}$/ $\Delta^{13}C_{Kernel}$	carbon isotope discrimination derived from leaf or kernel $\delta^{13}C$
$\Delta^{13}C_{Photosynthetic}$	photosynthetic carbon isotope discrimination
$\delta^{18}O$	oxygen isotopic composition
φ	leakiness
A	CO_2 assimilation rate
ABA	abscisic acid
ATP	adenosine triphosphate
bp	base pairs
C_a	ambient CO_2 concentration
C_i	intercellular CO_2 concentration
Chr	Chromosome
DP	donor parent
Exp.	Experiment
FW	fresh weight
g_s	stomatal conductance to water vapor
IRGA	infrared gas analyzer
IRMS	isotope ratio mass spectrometer
iWUE	intrinsic water use efficiency
KASP	kompetitive allele specific PCR
Mb	Mega bases
NADP	nicotinamide adenine dinucleotide phosphate
NADP-ME	NADP- malic enzyme
NIL	near isogenic line
PAR	photosynthetically active radiation
PEPC	phosphoenolpyruvate carboxylase
QTL	quantitative trait locus
RH	relative humidity
RP	recurrent parent

Rubisco	Ribulose-1,5-bisphosphate carboxylase/oxygenase
SD	standard deviation
SE	standard error
SLA	specific leaf area
SPAD	single photon avalanche diode
SWC	soil water content
TKW	thousand kernel weight
VPD	vapor pressure deficit
WUE_{plant}	whole plant water use efficiency

Prior publications

Some results of this thesis have been published in advance:

Journal articles:

Blankenagel, S.*, **Eggels, S.***, Frey, M., Grill, E., Bauer, E., Dawid, C., Fernie, A. R., Haberer, G., Hammerl, R., Medeiros, D. B., Ouzunova, M., Presterl, T., Ruß, V., Schäufele, R., Schlüter, U., Tardieu, F., Urbany, C., Urzinger, S., Weber, A. P. M., Schön, C.-C., Avramova, V. (2022). Natural alleles of the abscisic acid catabolism gene *ZmAbh4* modulate water use efficiency and carbon isotope discrimination in maize. *Manuscript accepted for publication at The Plant Cell*.

*Co-first authors

Avramova, V., Meziane, A., Bauer, E., Blankenagel, S., **Eggels, S.**, Gresset, S., Grill, E., Niculaes, C., Ouzunova, M., Poppenberger, B., Presterl, T., Rozhon, W., Welcker, C., Yang, Z., Tardieu, F., & Schön, C.-C. (2019). Carbon isotope composition, water use efficiency, and drought sensitivity are controlled by a common genomic segment in maize. *Theor Appl Genet*, *132*(1), 53-63. https://doi.org/10.1007/s00122-018-3193-4

Summary

In the context of changing environmental conditions and increasing population growth more efficient plants with respect to water use are desirable for crop production. Exploring intraspecific variation in plant water use efficiency (WUE_{plant}) is thus of interest for research and breeding and requires screening of a high number of plants. In C_3 plants, the carbon isotopic composition ($\delta^{13}C$) of dry matter has been established as an easily assessable proxy trait for WUE_{plant} and has found application in many studies and in practice. $\delta^{13}C$ is shaped by the carbon isotope discrimination during photosynthetic carbon fixation ($\Delta^{13}C_{Photosynthetic}$), which depends on the ratio of CO_2 assimilation rate to stomatal conductance. This ratio is defined as intrinsic water use efficiency (iWUE) and is a main determinant of WUE_{plant}. In C_4 plants like maize, the pre-fixation of CO_2 by phosphoenolpyruvate carboxylase (PEPC) and the partitioning of carbon fixation in two cell types cause $\Delta^{13}C_{Photosynthetic}$ to be lower compared to C_3 plants and introduce leakiness as a second variable affecting $\Delta^{13}C_{Photosynthetic}$. Leakiness describes the extent of leakage of CO_2 previously fixed by PEPC from bundle sheath back to mesophyll cells and determines sign and slope of the relationship between $\Delta^{13}C_{Photosynthetic}$ and iWUE. It is not established to what extent iWUE and leakiness contribute to intraspecific variation in $\Delta^{13}C_{Photosynthetic}$ of C_4 plants and whether $\delta^{13}C$ reliably reflects differences in WUE_{plant} between genotypes.

The aim of this thesis was to characterize the relationship between leaf and kernel $\delta^{13}C$, $\Delta^{13}C_{Photosynthetic}$, different gas exchange parameters and WUE_{plant} of maize. Combined analyses of these traits for different genotypes of a C_4 species has rarely been done. Following an initial screen for kernel $\delta^{13}C$ of field-grown plants, two near isogenic lines (NILs) were selected in addition to their recurrent parent (RP) for detailed analyses under growth chamber, greenhouse and field conditions. NIL B, carrying a donor parent-introgression on chromosome 7, consistently showed increased kernel $\delta^{13}C$, whereas NIL Y, with an introgression on chromosome 1, showed consistently decreased kernel $\delta^{13}C$ in the field.

With the genetically well-defined material of this study it could be shown that lower $\Delta^{13}C_{Photosynthetic}$ was the cause for stable differences between NIL B and RP in $\delta^{13}C$ of leaves and kernels across different developmental stages and environments. Stomatal conductance was identified as the driver of the difference in $\Delta^{13}C_{Photosynthetic}$, $\delta^{13}C$ as well as WUE_{plant} in NIL B through its effect on iWUE. Additionally, leakiness was assessed and had lower values in NIL B than in RP, which most likely contributes to the low $\Delta^{13}C_{Photosynthetic}$ in NIL B without masking the link to iWUE. A direct link between the difference in $\delta^{13}C$ and WUE_{plant} was demonstrated, with a negative association between the two traits. Under drought, stomatal closure decreased $\delta^{13}C$ and minimized genotypic differences in gas exchange compared to well-watered conditions, yet under moderate or transient drought, genotypic differentiation in $\delta^{13}C$ persisted.

The analyses of NIL B ultimately led to the identification of the gene *ZmAbh4* as influencing WUE_{plant} and $\delta^{13}C$ in a flanking project.

Decreased kernel $\delta^{13}C$ of NIL Y compared to RP was not linked to a difference in WUE_{plant}. Lower assimilation rate and stomatal conductance of NIL Y detected in a subset of experiments suggested environmentally dependent differences in iWUE. Divergent patterns in variation of leaf and kernel $\delta^{13}C$ between RP and NIL Y in some experiments indicated a potential involvement of post-photosynthetic fractionations in differences in $\delta^{13}C$. Further investigations are required to elucidate whether lower kernel $\delta^{13}C$ and lower kernel number in NIL Y compared to RP share a common cause or are caused by different genetic factors within the chromosome 1 introgression. Generation of recombinant lines with segregating sub-segments of this introgression allowed to narrow down the genomic region associated with $\delta^{13}C$ to 12.7 Mb. Dissecting this region further will allow to separate interacting effects and identify the genetic cause for the $\delta^{13}C$ difference.

Analyses of this thesis demonstrated the direct link between differences in leaf and kernel $\delta^{13}C$, $\Delta^{13}C_{Photosynthetic}$, WUE_{plant} and stomatal conductance between the two maize genotypes NIL B and RP. The association of $\delta^{13}C$ and WUE_{plant} did not apply for differences between genotypes NIL Y and RP. Overall, the results highlight the potential to identify genotypes with differences in WUE_{plant} based on a kernel $\delta^{13}C$ screen in maize, but also the necessity for subsequent gas exchange and WUE_{plant} analyses to confirm the link to WUE_{plant} on selected genotypes.

Zusammenfassung

Vor dem Hintergrund sich ändernder Umweltbedingungen und steigender Bevölkerungszahlen sind Pflanzen mit einer hohen Effizienz hinsichtlich ihres Wasserverbrauches von großer Bedeutung für die landwirtschaftliche Nachhaltigkeit. Um intraspezifische Variation in der Wassernutzungseffizienz der Pflanze (WUE_{plant}) für Forschung und Züchtung zu nutzen, ist es notwendig, eine große Anzahl an Pflanzen zu screenen. Die Kohlenstoffisotopenzusammensetzung ($\delta^{13}C$) von Pflanzenmaterial wurde in C_3 Pflanzen als leicht bestimmbares Proxymerkmal für WUE_{plant} etabliert und hat in vielen Studien sowie in der Praxis Anwendung gefunden. $\delta^{13}C$ reflektiert die Diskriminierung gegen das schwere Isotop ^{13}C während der photosynthetischen Kohlenstofffixierung ($\Delta^{13}C_{Photosynthetic}$). Diese ist von der intrinsischen Wassernutzungseffizienz (iWUE) abhängig, die als Verhältnis der CO_2-Assimilationsrate zur stomatären Leitfähigkeit definiert ist. iWUE bestimmt auch zu großen Teilen die WUE_{plant}. In C_4 Pflanzen wie Mais führt die Vorfixierung von CO_2 durch die Phosphoenolpyruvatcarboxylase (PEPC) und die Aufteilung der Kohlenstofffixierung in zwei Zelltypen dazu, dass $\Delta^{13}C_{Photosynthetic}$ niedriger ist als in C_3 Pflanzen. Des Weiteren beeinflusst die sogenannte Leakiness als weitere Variable $\Delta^{13}C_{Photosynthetic}$. Leakiness beschreibt das Ausmaß an Rückdiffusion von zuvor durch die PEPC fixiertem CO_2 aus Bündelscheiden- zurück in die Mesophyllzellen. Sie bestimmt Vorzeichen und Steigung des Zusammenhangs von $\Delta^{13}C_{Photosynthetic}$ und iWUE. Es ist nicht geklärt, inwieweit iWUE und Leakiness zur intraspezifischen Variation in der $\Delta^{13}C_{Photosynthetic}$ von C_4 Pflanzen beitragen und ob $\delta^{13}C$ WUE_{plant}-Unterschiede zwischen Genotypen zuverlässig widerspiegelt.

Ziel dieser Arbeit war es, an klar definiertem genetischen Material den Zusammenhang von Blatt- und Korn-$\delta^{13}C$, $\Delta^{13}C_{Photosynthetic}$, verschiedenen Gasaustauschparametern und WUE_{plant} von Mais zu charakterisieren. Die kombinierte Analyse dieser Merkmale an verschiedenen Genotypen derselben Art wurde in C_4 Pflanzen bisher kaum durchgeführt. Ausgehend von einem Screening für Korn-$\delta^{13}C$ von Feldpflanzen wurden zwei nahezu isogene Linien (NIL) zusätzlich zum rekurrenten Elter (RP) für weiterführende Analysen in Klimakammer, Gewächshaus und Feld ausgewählt. NIL B trägt eine Introgression eines Donorelters auf Chromosom 7 und zeigt konsistent höhere Korn-$\delta^{13}C$ im Vergleich zu RP. Dagegen trägt NIL Y eine Introgression auf Chromosom 1 und weist eine niedrigere Korn-$\delta^{13}C$ im Feld auf.

Es konnte gezeigt werden, dass Unterschiede in Korn- und Blatt-$\delta^{13}C$ zwischen NIL B und RP auf einer niedrigeren $\Delta^{13}C_{Photosynthetic}$ in NIL B basieren. Die Unterschiede in $\delta^{13}C$ waren über verschiedene Entwicklungsstadien und Umweltbedingungen stabil ausgeprägt. Als Ursache der veränderten $\Delta^{13}C_{Photosynthetic}$ und $\delta^{13}C$ in NIL B wurde ein signifikanter Unterschied in der stomatären Leitfähigkeit identifiziert, der die iWUE und WUE_{plant} beeinflusst. Zudem wurde in NIL B eine niedrigere Leakiness als in RP bestimmt, die zur niedrigen $\Delta^{13}C_{Photosynthetic}$ in NIL B

beitragen könnte. Die negative Beziehung der Unterschiede in $\delta^{13}C$ und iWUE zwischen NIL B und RP wurde durch den Leakinessunterschied nicht beeinträchtigt. Unter Trockenstress führte die Stomata-Schließung zu niedrigeren $\delta^{13}C$-Werten und reduzierten Unterschieden im Gasaustausch der Genotypen im Vergleich zu Kontrollbedingungen. Die $\delta^{13}C$-Differenzierung zwischen den Genotypen blieb jedoch unter mildem oder kurzzeitigem Trockenstress bestehen. Die Untersuchungen an NIL B führten letztlich zur Identifizierung des Gens *ZmAbh4* als Einflussfaktor für WUE_{plant} und $\delta^{13}C$ in einem flankierenden Projekt.

Die niedrigeren Korn-$\delta^{13}C$ Werte von NIL Y im Vergleich zu RP waren hingegen nicht mit einem Unterschied in WUE_{plant} verbunden. Dass die niedrigere Assimilationsrate und stomatäre Leitfähigkeit von NIL Y nur in einem Teil der Experimente festgestellt werden konnten, deutete auf einen umweltabhängigen Unterschied in iWUE hin. Die Divergenz zwischen Blatt- und Korn-$\delta^{13}C$-Unterschieden zwischen NIL Y und RP in einigen Experimenten weist zudem auf post-photosynthetische Fraktionierungen hin. Es sind weitere Analysen erforderlich, um zu zeigen, ob niedrigere Korn-$\delta^{13}C$ und niedrigere Kornanzahl in NIL Y im Vergleich zu RP eine gemeinsame Ursache haben oder von verschiedenen genetischen Faktoren innerhalb der Chromosom 1-Introgression verursacht werden. Die Erzeugung rekombinanter Linien, welche für Teilsegmente dieser Introgression segregieren, ermöglichte es, die mit $\delta^{13}C$ assoziierte genomische Region auf 12.7 Mb einzugrenzen. Eine weitere Feinkartierung dieser Region könnte wechselwirkende Effekte trennen und die genetische Grundlage des $\delta^{13}C$-Unterschiedes aufklären.

Die Untersuchungen dieser Arbeit haben die genetische und physiologische Verbindung von Unterschieden in Blatt- und Korn-$\delta^{13}C$, $\Delta^{13}C_{Photosynthetic}$, WUE_{plant} und stomatärer Leitfähigkeit zwischen den Maisgenotypen NIL B und RP gezeigt. Die Beziehung zwischen Unterschieden in $\delta^{13}C$ und in WUE_{plant} im Vergleich zu RP war nicht auf den Genotypen NIL Y übertragbar. Insgesamt unterstreichen die Ergebnisse das Potenzial, Genotypen mit veränderter WUE_{plant} basierend auf einem Korn-$\delta^{13}C$ Screening zu identifizieren. Zudem wird aber auch die Notwendigkeit nachfolgender Gasaustausch- und WUE_{plant}-Analysen ersichtlich, um den Unterschied in WUE_{plant} in den selektierten Genotypen im Einzelfall zu bestätigen.

1 Introduction

Increasing the productivity of agricultural crop production has been a continuous focus in agriculture, plant breeding and plant sciences in general. The need for higher plant productivity to provide food and bioenergy is reinforced by the increasing world population, which is predicted to grow to 9.6 billion by 2050 (Sales et al., 2021). Increases in agricultural production have been accompanied by increases in water use, with the agricultural sector taking up approximately 70% of global fresh water usage today (Leakey et al., 2019; Vadez et al., 2014). Water is the major limiting factor for crop production and further increases in water usage will not be sustainable (Blankenagel et al., 2018; Leakey et al., 2019). The increases in aridity and drought periods associated with climate change make water availability for plant growth an even more critical topic (Bertolino et al., 2019). Thus, crops with high water use efficiency are highly desirable as they contribute to high plant production with reduced water use as well as secure crop production under less favorable environmental conditions (Cano et al., 2019; Leakey et al., 2019).

1.1 Carbon fixation and water use efficiency in C_4 plants

1.1.1 Water use efficiency

In the agronomic context, water use efficiency is typically defined as the amount of biomass or grain yield of a plot relative to the amount of used water (Vadez et al., 2014). It is influenced by agricultural practices as well as the water use efficiency of the plant itself. Plant water use efficiency (WUE_{plant}) describes the amount of biomass produced by a plant per liter of consumed water. If a higher WUE_{plant} is caused by increased biomass production with no increase in water use, crop growth productivity can be improved without additional water costs (Leakey et al., 2019). On the other hand, if a high WUE_{plant} is due to decreased water use with no disadvantage in biomass production, soil water might be conserved and available later in the growing season. In this case, a higher WUE_{plant} can contribute to the avoidance of drought stress (Leakey et al., 2019). A major component, which determines WUE_{plant}, is the intrinsic water use efficiency (iWUE) on the leaf level (Condon et al., 2004; Leakey et al., 2019). iWUE is defined as the ratio of CO_2 assimilation rate to stomatal conductance. Stomatal conductance describes the flux of water vapor out of the leaf for a given water vapor concentration gradient. The conductance of stomata determines how much CO_2 is taken up for assimilation and how much water is lost simultaneously through transpiration. Stomatal conductance and

assimilation rate are strongly positively correlated, yet the ratio of the two parameters, i.e. iWUE, can vary between genotypes, species and environmental conditions (Blankenagel et al., 2018; Feldman et al., 2018; Leakey et al., 2019; Vadez et al., 2021). Stomatal conductance has been found to be the main driver of genetic variation for iWUE within a species. In addition, differences in photosynthetic capacity and mesophyll conductance, which describes the conductance of CO_2 from the intercellular air space below the stomata to the site of initial carbon fixation in the mesophyll, have been identified as drivers of intraspecific iWUE variation (Barbour et al., 2016; Cano et al., 2019; Leakey et al., 2019).

Variation in iWUE that persists over an extended time period can then translate to differences in the biomass accumulation of a plant with a given amount of water, i.e. WUE_{plant} (Condon et al., 2004). WUE_{plant} can however also be affected by differences in night time transpiration and respiration and by the vapor pressure deficit (VPD), referring to the difference between water vapor concentration in atmospheric air and in the plant (Condon et al., 2004; Leakey et al., 2019; Medrano et al., 2015).

Genetically determined intraspecific variation in WUE_{plant} can be exploited for identifying or generating genotypes with superior efficiency and can also serve for investigating the mechanisms and genes, which underlie WUE_{plant} variation (Chen et al., 2011). Characterizing genotypic variation in iWUE and WUE_{plant} requires measuring the respective trait on many individuals. This screening has been one major challenge in breeding for genotypes with increased WUE_{plant}. Determining biomass production and water consumption gravimetrically is laborious, time-intensive, and often destructive and not performable in a sufficiently accurate manner in the field (Chen et al., 2011; Feldman et al., 2018; Ryan et al., 2016). Gas exchange measurements of iWUE are not destructive, but are subject to environmental and developmental variation, as they only represent a snapshot at the time point of measurement and are also time- and labor- intensive (Medrano et al., 2015). Proxy traits for iWUE and WUE_{plant} that are easy to assess could thus be of great use. For plants that perform C_3 photosynthesis, the carbon isotopic composition ($\delta^{13}C$) of plant dry matter has been established as such a proxy (Chen et al., 2011; Leakey et al., 2019; Rebetzke et al., 2002). $\delta^{13}C$ is shaped by the carbon isotope discrimination ($\Delta^{13}C$) during carbon fixation, which is influenced directly by the ratio of CO_2 assimilation rate and stomatal conductance, i.e. iWUE (Farquhar et al., 1982). There is thus a connection between $\delta^{13}C$ and iWUE. A correlation of $\delta^{13}C$ and iWUE or WUE_{plant} has been demonstrated in several C_3 plants (Adiredjo et al., 2014 for sunflower; Barbour et al., 2010 for barley; Farquhar & Richards, 1984 for wheat; Xu et al., 2008 for tomato). Due to the more complex nature of carbon fixation of C_4 plants, the relationship of C_4 $\Delta^{13}C$ and iWUE differs from that in C_3 species (Farquhar, 1983). As a consequence, the correlation of $\delta^{13}C$ with iWUE and WUE_{plant} is less certain in C_4 plants. The

relationship between differences in $\delta^{13}C$ and in iWUE and WUE_{plant} of the C_4 plant maize is the focus of this study.

1.1.2 C_4 photosynthesis

C_4 plants generally show higher iWUE, higher photosynthetic efficiency and thus higher productivity compared to C_3 plants (Sales et al., 2021). Among all crops, the C_4 crop maize (*Zea mays* L.) is the most productive and most abundantly grown food crop (Sage, 2017) with average yields of 5.75 t/ha and a worldwide production of 1.16 Mio t (FAO, 2020; www.fao.org/faostat/en/#data/QCL). Sugarcane (*Saccharum officinarum* L.) and sorghum (*Sorghum bicolor* (L.) Moench) are also important crops that perform C_4 photosynthesis (Sage, 2017).

The high photosynthetic efficiency of C_4 plants is due to the carbon concentrating mechanism that is deployed in C_4 carbon fixation. The C_4 photosynthetic pathway is characterized by the spatial separation of an initial CO_2 fixation step and the final carbon assimilation by Rubisco (Ribulose-1,5-bisphosphate carboxylase/oxygenase) in two cell types. For this partitioning, a specialized biochemistry as well as anatomy, the so-called Kranz anatomy, is the prerequisite (Furbank & Kelly, 2021). Mesophyll cells are located under the epidermis and surround the bundle sheath cells, which are arranged in a circular manner around the vascular bundles (Hatch, 1987). Mesophyll cells are the main site of photosynthetic light reactions that provide ATP and NADPH for carbon fixation, whereas bundle sheath cells are the location of the Calvin Benson cycle. The CO_2 that enters the leaf through stomata first enters mesophyll cells and after conversion to HCO_3^- by carbonic anhydrase is fixed by the enzyme phosphoenolpyruvate carboxylase (PEPC) to form the C_4 acid oxaloacetate (Hatch, 1987; von Caemmerer, 2021). This is converted further to malate or aspartate, which is transported to bundle sheath cells. There, this C_4 acid is decarboxylated to release CO_2. The resulting product is transported back to the mesophyll cell to regenerate the receptor PEP. Reactions of this pathway for pumping CO_2 into the bundle sheath cell, called the C_4 cycle, are spread not only over bundle sheath and mesophyll cells, but over different cell compartments, namely over cytosol, chloroplasts and in some species mitochondria. Activity of the C_4 cycle is higher than that of the C_3 cycle (Calvin Benson cycle). This leads to high CO_2 concentrations around Rubisco, which is only present in bundle sheath cell chloroplasts (Hatch, 1987). Additionally, since the majority or all of the photosynthetic light reactions that lead to the release of O_2 take place in mesophyll cells, O_2 concentrations are low around Rubisco. Therefore, the efficiency of Rubisco carboxylation is strongly increased in C_4 plants, as the undesirable oxygenation reaction, which leads to energetic losses during photorespiration, is suppressed (Hatch, 1987). Photosynthetic efficiency in terms of energy (ATP and NADPH) requirement per assimilated CO_2 is thus higher

in C_4 compared to C_3 plants. C_4 plants can achieve additionally high assimilation rates at relatively low CO_2 concentrations in the intercellular air space (Blankenagel et al., 2018). This allows for lower stomatal conductance per assimilated CO_2 and therefore higher iWUE compared to C_3 species. Also nitrogen use efficiency of C_4 plants is higher, as lower amounts of Rubisco, which makes up a major fraction of leaf nitrogen, are needed (Sales et al., 2021).

Despite the high efficiency of C_4 plants, there is still potential for improvement (Sales et al., 2021). Since the C_4 carbon fixation pathway evolved under lower atmospheric CO_2 concentrations, CO_2 assimilation of C_4 plants is often saturated under optimal conditions nowadays (Leakey et al., 2019). It might thus be possible to reduce stomatal conductance even further without substantial losses in CO_2 assimilation, and thereby increase iWUE. Additionally, the maximum conversion efficiency of solar energy to biomass that is expected from theoretical calculations is considerably above the one achieved by C_4 plants, demonstrating potential for improvement of photosynthetic efficiency (Sales et al., 2021). There is substantial variation for iWUE and WUE_{plant} as well as photosynthetic traits between C_4 species (Cano et al., 2019; Leakey et al., 2019; Sales et al., 2021). For example, WUE_{plant} of maize has been found to be higher than WUE_{plant} of sorghum and pearl millet (Vadez et al., 2021). Additionally, there is variation for WUE_{plant} between different genotypes of maize (Blankenagel et al., 2018; Ryan et al., 2016; Xie et al., 2021), the cause of which is worth to be explored. In this thesis, near isogenic maize lines will be studied regarding differences in iWUE between genotypes.

1.1.3 Carbon fixation in maize

The C_4 carbon fixation pathway evolved at least 61 times independently and different C_4 species can show different anatomical and biochemical characteristics (Sage, 2017). C_4 plants can be grouped into three subtypes, according to the main decarboxylating enzyme, which can be NADP-malic enzyme (NADP-ME), NAD-malic enzyme (NAD-ME) and phosphoenolpyruvate carboxykinase (PEPCK). Maize belongs to the NADP-ME type, but also shows activity of PEPCK (Figure 1.1), which has been suggested to provide photosynthetic flexibility (Arrivault et al., 2017; Furbank, 2011; Kromdijk et al., 2014).

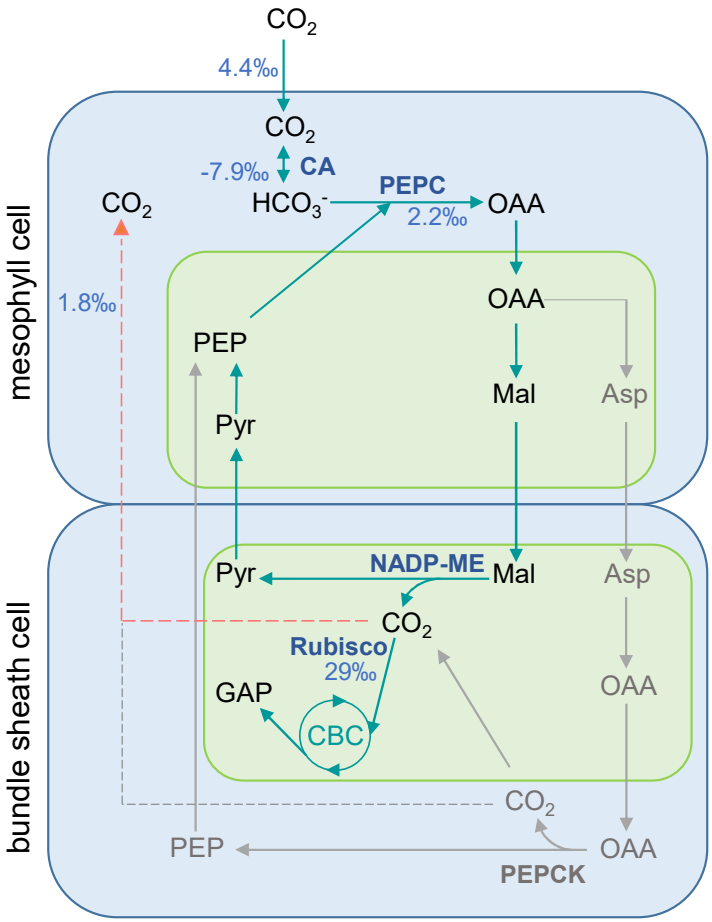

Figure 1.1: Pathway of carbon fixation in maize, a NADP-ME type C_4 species, with additional activity of PEPCK (Sales et al., 2021; Schlüter et al., 2019).
Majority of carbon fixation takes place via the NADP-ME pathway, indicated by green arrows, additional activity of the PEPCK pathway is depicted in grey. Pyruvate in bundle sheath cells can additionally be converted to alanine before being transported to the mesophyll cell, which is not shown. Leakage of CO_2 is indicated by the disrupted line; light green compartment indicates chloroplasts, major carbon isotope fractionation factors are shown at the respective reaction step in blue in ‰ (von Caemmerer et al., 2014). CBC = Calvin Benson cycle, CA = carbonic anhydrase, PEPC = phosphoenolpyruvate carboxylase, NADP-ME = NADP-malic enzyme, Rubisco = Ribulose-1,5-bisphosphate-carboxylase/oxygenase, PEPCK = phosphoenolpyruvate carboxykinase, OAA = oxaloacetate, Mal = malate, Pyr = pyruvate, PEP = phosphoenolpyruvate, Asp = aspartate, GAP = glyceraldehyde-3-phosphate.

After the initial fixation of HCO_3^- in the mesophyll cytosol, NADP-ME species convert oxaloacetate to malate in mesophyll chloroplasts (Figure 1.1, Furbank, 2011). Malate is the C_4 acid transported into bundle sheath cells and the decarboxylation of malate then takes place in bundle sheath chloroplasts by NADP-ME. In contrast, decarboxylation by PEPCK takes place in the bundle sheath cytoplasm and this decarboxylation type is connected to the transport of aspartate as the C_4 acid. Generally, the C_4 cycle requires high rates of metabolite transport between the two cells, which primarily takes place via diffusion through plasmodesmata along concentration gradients (Hatch, 1987). However, the concentration of

CO_2 in bundle sheath cells also generates a CO_2 concentration gradient, which promotes leakage of CO_2 back into mesophyll cells. This leakage is described by the term leakiness, which is defined as the fraction of CO_2 previously fixed by PEPC that subsequently leaks back to the mesophyll cell (Von Caemmerer 2003). Values for leakiness have been calculated to be mostly in the range of 0.2-0.4 (Henderson 1992, Cousins 2008, Kromdijk 2014). CO_2 leakage represents an energetic loss in the C_4 photosynthetic system, as for the repeated transport of CO_2 the acceptor PEP needs to be regenerated, which requires ATP (von Caemmerer & Furbank, 2003). Many C_4 species, including maize, thus show suberization of the cell wall separating bundle sheath from mesophyll cell in order to restrict apoplastic CO_2 diffusion (Hatch, 1987; Mertz & Brutnell, 2014). Control of minimizing leakage and ensuring efficient functioning of C_4 photosynthesis can also be attributed to the coordination of activities of the C_3 and C_4 cycle (Kromdijk et al., 2014; Sun et al., 2012). The extent of CO_2 leakage during carbon fixation can also affect $\delta^{13}C$ and will thus be explored as a potential contributing factor to $\delta^{13}C$ variation between genotypes of maize in this study.

1.2 Carbon isotope discrimination ($\Delta^{13}C$)

1.2.1 $\Delta^{13}C$ during photosynthesis

In the atmospheric air, 1.1% of CO_2 contains the isotope ^{13}C and 98.9% ^{12}C (Farquhar et al., 1989b). The ratio of ^{13}C to ^{12}C in plant material, described by $\delta^{13}C$, is even lower than that of air, because plants discriminate against ^{13}C during carbon fixation. Changes in the relative abundances of the carbon isotopes ^{12}C and ^{13}C, i.e. isotopic fractionations, occur during the different steps of CO_2 diffusion and enzymatic reactions for carbon fixation (Farquhar et al., 1989a). This can mainly be explained by the lower diffusivity of CO_2 containing the heavier isotope, but also by lower reactivity of ^{13}C in many enzymatic reactions. The isotopic fractionation during diffusion in air and during fixation by Rubisco are the main determinants of discrimination against ^{13}C ($\Delta^{13}C$) during carbon fixation of C_3 plants (Farquhar et al., 1982). The extent of this discrimination is dependent on the ratio of assimilation rate and stomatal conductance, because this determines whether diffusional or enzymatic fractionations come into effect more. As this ratio is defined as iWUE, there is a link between $\Delta^{13}C$ and iWUE. In C_3 plants, $\Delta^{13}C$ decreases with increases in iWUE. Mathematical models that describe $\Delta^{13}C$ as a function of different fractionation factors typically use the ratio of intercellular to ambient CO_2 concentration (C_i/C_a) as a variable to describe the balance of assimilation and stomatal conductance. C_i/C_a is inversely related to iWUE (iWUE = C_a (1 - C_i/C_a) / 1.6; Yang et al., 2016). In C_3 plants, $\Delta^{13}C$ thus increases with increases in C_i/C_a. During C_4 photosynthesis, there are

more steps to carbon fixation, which influence the final $\Delta^{13}C$ (Farquhar, 1983, Figure 1.1). The major fractionation steps are summarized in Equation (1), which gives a simplified model of $\Delta^{13}C$ during C_4 photosynthesis (Farquhar, 1983).

Equation (1) $\Delta^{13}C = a + (b_4 + (b_3 - s)\,\varphi - a)\,C_i/C_a$

In Equation (1), a quantifies the fractionation during diffusion of CO_2 in air of 4.4‰ that occurs after CO_2 uptake into the leaf (Figure 1.1). During the subsequent dissolution and hydration of CO_2 to HCO_3^-, an enrichment in ^{13}C takes place (von Caemmerer et al., 2014). This fractionation is dependent on temperature and has a value of -7.9‰ at 25 °C. The fixation of HCO_3^- to oxaloacetate by PEPC is associated with a fractionation against ^{13}C of 2.2‰. These two fractionation factors are summarized in b_4 with a value of -5.7‰. In the following metabolic steps there is not much potential for further fractionations until CO_2 is released in bundle sheath cells. Since discrimination requires the possibility for elimination of the rejected molecules, discrimination by Rubisco in bundle sheath cells is dependent on the extent of leakage of CO_2, i.e. leakiness φ (Farquhar et al., 1989a). The higher the leakiness, the higher $\Delta^{13}C$, because the fractionation by Rubisco (b_3, 29‰) can be realized to a larger extent (von Caemmerer et al., 2014). Additionally, some diffusional fractionations might occur during leakage, which is approximated by the fractionation during diffusion of CO_2 through the liquid phase (s, 1.8‰). As a result of the described characteristics and isotopic fractionations of C_4 carbon fixation, photosynthetic $\Delta^{13}C$ is lower in C_4 than in C_3 plants and reaches total values of approximately 2-5‰ (Cousins et al., 2008; Henderson et al., 1992) compared to 18-26‰ in C_3 plants (Farquhar et al., 1989b).

$\Delta^{13}C$ during C_4 carbon fixation is thus determined by two variables, leakiness and C_i/C_a. While in C_3 plants, the relationship of C_i/C_a and $\Delta^{13}C$ is positive, the relationship of the two parameters in C_4 plants can be positive or negative depending on leakiness (Farquhar, 1983). Based on the model and fractionation factors given in Equation (1) the relationship of C_i/C_a and $\Delta^{13}C$ is zero when leakiness is 0.37. Most studies on leakiness have determined values below 0.37, which implies a negative relationship between $\Delta^{13}C$ and C_i/C_a (Ellsworth & Cousins, 2016). In addition to the described fractionation steps that are included in the simplified $\Delta^{13}C$ model, further isotopic fractionations can occur that complicate the dependence of $\Delta^{13}C$ on C_i/C_a and might have a significant influence on the overall $\Delta^{13}C$, particularly under certain environmental conditions, like low light intensities (Kromdijk et al., 2014). The full $\Delta^{13}C$ model includes fractionations occurring during day-respiration, during photorespiration and during diffusion through the boundary layer. It also includes a ternary correction for the effect of transpiration on CO_2 uptake and considers the CO_2 concentrations in bundle sheath and mesophyll cells (Farquhar, 1983; Farquhar & Cernusak, 2012; von Caemmerer et al., 2014).

Generally, the $\Delta^{13}C$ during carbon fixation of plants determines the carbon isotopic signature of the assimilation products. Since these provide the substances for biomass accumulation, differences in photosynthetic $\Delta^{13}C$ are reflected in the carbon isotopic composition $\delta^{13}C$ of bulk leaf material. $\delta^{13}C$ of plant material may thus be used as an integrative indicator for the photosynthetic $\Delta^{13}C$ over the period of tissue synthesis (Ellsworth & Cousins, 2016; Ghashghaie & Badeck, 2014). Dry matter $\delta^{13}C$ has the advantage of reflecting a longer time period compared to photosynthetic $\Delta^{13}C$ measurements and it is also more easily assessed. Photosynthetic $\Delta^{13}C$ is often determined by coupled isotope ratio mass spectrometer (IRMS) and infrared gas analyzer (IRGA) analysis (Kubasek et al., 2007), which is time- and labor-intensive and requires a well-controlled environment for measurements on photosynthesizing plants. However, dry matter $\delta^{13}C$ is not only affected by photosynthetic $\Delta^{13}C$, but also by carbon isotopic fractionations that occur post photosynthesis. Isotopic fractionations associated with different metabolic reactions can cause differences in isotopic signatures of different substance classes or of metabolite pools of different origins. Differential export or use of these metabolites for respiration can further influence dry matter $\delta^{13}C$ (Cernusak et al., 2009; Ghashghaie & Badeck, 2014; von Caemmerer et al., 2014). Also variations in rates of day and night respiration might have a significant effect on dry matter $\delta^{13}C$. Post-photosynthetic fractionations commonly cause leaf dry matter derived estimates of $\Delta^{13}C$, which are calculated based on the difference of $\delta^{13}C$ of air and of plant dry matter (Equation (4), chapter 2.4.2), to be higher than those measured directly during photosynthesis (Henderson et al., 1992; Kubasek et al., 2007). Additionally, leaf dry matter is commonly more depleted in ^{13}C than kernel material (Cernusak et al., 2009; Eggels et al., 2021; Hobbie & Werner, 2004; Sanborn et al., 2021). Despite these deviations between dry matter-derived estimates for $\Delta^{13}C$ and photosynthetic $\Delta^{13}C$, dry matter-derived $\Delta^{13}C$ has often been used as an approximation for photosynthetic $\Delta^{13}C$ of C_3 and C_4 plants (Cernusak et al., 2013).

Because of the lower photosynthetic $\Delta^{13}C$ of C_4 compared to C_3 plants, $\delta^{13}C$ of C_4 dry matter is higher than $\delta^{13}C$ of C_3 dry matter, with values usually in the range of -15 to -11‰ compared to on average -28‰ in C_3 (Cernusak et al., 2013; Eggels et al., 2021; Farquhar et al., 1989a; von Caemmerer et al., 2014). $\delta^{13}C$ of atmospheric air is approximately -8.5‰. Because changes in C_i/C_a cause less pronounced changes in $\Delta^{13}C$ in C_4 compared to C_3 plants, intraspecific differences in $\delta^{13}C$ are typically lower in C_4 plants (Cernusak et al., 2013; Eggels et al., 2021). For example, among a set of diverse, commonly used maize lines, including the founders of the nested association mapping (NAM) panel (Yu et al., 2008), differences in leaf $\delta^{13}C$ of 1.3-1.4‰ were found (Kolbe et al., 2018; Twohey et al., 2019). These values are similar to the range within a maize introgression library used for kernel $\delta^{13}C$ QTL mapping (Gresset et al., 2014). In contrast, in C_3 mapping populations genotypic differences go up to 3-4‰ in barley (Chen et al., 2012).

Given intraspecific variation for both $\delta^{13}C$ and WUE_{plant} in C_4 plants, there is high interest in understanding, which factors are underlying this variation and whether they are linked between both traits (Eggels et al., 2021; von Caemmerer et al., 2014). These questions are the focus of this thesis.

1.2.2 Connection of carbon isotopic composition ($\delta^{13}C$) and water use efficiency

In C_3 plants, $\delta^{13}C$ is positively correlated with iWUE and WUE_{plant} (Farquhar et al., 1982). As a result, $\delta^{13}C$ has often been used as a surrogate for WUE_{plant} in mapping populations to identify QTL for WUE_{plant}, e.g. in tomato (Xu et al., 2008), barley (Chen et al., 2012) and soybean (Bazzer et al., 2020). Additionally, $\delta^{13}C$ has found direct application as a proxy for WUE_{plant} in a wheat breeding program, where the selection for higher leaf $\delta^{13}C$ led to the selection of more water use efficient wheat varieties with higher yield under drought (Rebetzke et al., 2002).

While in C_4 plants, the relationship of $\delta^{13}C$ and iWUE could theoretically be positive, negative or zero depending on leakiness, a negative correlation of $\delta^{13}C$ and iWUE has often been observed (Eggels et al., 2021; Ellsworth & Cousins, 2016). For testing the correlation of iWUE and $\delta^{13}C$, one approach has been to study variation in both traits over different watering regimes and a second approach has been to study variation over different genotypes. Using the first approach, a negative relationship has been demonstrated in different species. Increases in iWUE under water deficit were connected to decreases in $\delta^{13}C$ in maize (Cabrera-Bosquet et al., 2009a; Dercon et al., 2006; Twohey et al., 2019), sorghum (Sonawane & Cousins, 2020; Williams et al., 2001), *Setaria* (Ellsworth et al., 2017), pearl millet (Brück et al., 2000) and different Australian C_4 grasses (Ghannoum et al., 2002). While these changes in $\delta^{13}C$ are likely caused by the higher iWUE because of stomatal closure, additional effects of leakiness cannot be excluded, as leakiness was often not directly assessed. Only in the study by Sonawane and Cousins (2020), leakiness was determined by on-line measurements of $\Delta^{13}C$ and was found to be ≤0.2 with no effect of the water treatment.

The second approach tests, whether intraspecific genotypic variation in $\delta^{13}C$ and in WUE_{plant} are correlated in C_4 plants. To address this question, Monneveux et al. (2007) and Cabrera-Bosquet et al. (2009a) studied associations of $\delta^{13}C$ and yield under drought in different maize genotypes. Monneveux et al. (2007) found drought tolerant maize hybrids and inbred lines to have lower leaf $\delta^{13}C$ and higher yield under drought than susceptible inbreds. Additionally, in their study a negative correlation was found between $\delta^{13}C$ and ear dry weight at female flowering under drought conditions among inbred lines differing in drought tolerance. These findings could be indicative of a negative correlation of $\delta^{13}C$ and WUE_{plant} between genotypes.

Within drought-tolerant hybrids, no correlation of yield and $\delta^{13}C$ was observed (Cabrera-Bosquet et al., 2009a; Monneveux et al., 2007). For sorghum, negative correlations of leaf $\delta^{13}C$ and WUE_{plant} were demonstrated over 30 lines (Henderson et al., 1998). Gas exchange measurements on selected lines of that study revealed significant variation for iWUE, but not for leakiness. In different sorghum lines studied by Hammer et al. (1997), no correlation of leaf $\delta^{13}C$ and WUE_{plant} was found. A recent study on an interspecific *Setaria* population demonstrated a negative correlation of leaf $\delta^{13}C$ and WUE_{plant} at the phenotypic as well as at the genetic level (Ellsworth et al., 2020). In addition to the phenotypic correlation of $\delta^{13}C$ and WUE_{plant} (r= -0.51), the three QTL identified for leaf $\delta^{13}C$ in their study overlapped with QTL for WUE_{plant} and/or transpiration.

In summary, there are multiple studies that point towards a negative connection of $\delta^{13}C$ and iWUE in C_4 plants, yet there are still several uncertainties in how robust and universal this connection is. It is also not yet established, whether $\delta^{13}C$ of leaves and kernels reliably reflect differences in photosynthetic $\Delta^{13}C$ of C_4 plants. These questions will be explored on selected maize genotypes in this study.

1.2.3 Leakiness

The main uncertainty in the relationship of $\delta^{13}C$ and iWUE in C_4 plants stems from its dependence on leakiness as an additional variable, which is not easily assessable (Sonawane & Cousins, 2020). Leakiness is determined by two major factors, the concentration gradient for CO_2 between bundle sheath and mesophyll cells as well as the conductance for CO_2 leakage (Kromdijk et al., 2014). The CO_2 gradient primarily depends on how well the C_4 and C_3 cycle are coordinated. Higher activity of the C_4 compared to the C_3 cycle is required for achieving high CO_2 concentrations in bundle sheath cells, yet a disproportionate excess of PEPC activity compared to the capacity for Rubisco carboxylation will promote energetic losses through leakage (Ubierna et al., 2011). Bundle sheath conductance can be influenced by several components, like suberization as well as area size of the bundle sheath-mesophyll interface, cell wall thickness, plasmodesmata density and also the pathway of diffusion (Retta et al., 2016).

While for different C_4 species most studies have obtained leakiness values below 0.37, leading to a negative relationship of $\Delta^{13}C$ and C_i/C_a (Cousins et al., 2008; Henderson et al., 1992; Sonawane & Cousins, 2020; Ubierna et al., 2011), there are also examples of higher values, from which an opposite relationship would be expected (Cousins et al., 2008; Gong et al., 2017). Leakiness is commonly determined from simultaneous measurements of photosynthetic $\Delta^{13}C$ and C_i/C_a and subsequent calculation based on the above-mentioned

model (Equation 1). These calculations are often associated with strong simplifying assumptions, mainly regarding diffusional conductances (Kromdijk et al., 2014), so absolute values are not certain. Several studies have determined leakiness for one genotype of a single species or for different species, yet intraspecific variation for leakiness has rarely been explored. Saliendra et al. (1996) based their analysis of intraspecific differences in leakiness on dry matter $\delta^{13}C$-derived estimates for leakiness. However, it is difficult to draw conclusions on leakiness from dry matter $\delta^{13}C$, because of the difference in time-integration compared to gas exchange measurements and because of post-photosynthetic fractionations (Sonawane & Cousins, 2020). In sorghum, concurrent measurements of photosynthetic $\Delta^{13}C$ and C_i/C_a were used to investigate intraspecific variation in leakiness, and no significant differences were found between eight lines (Henderson et al., 1998).

Since leakiness influences the efficiency of carbon fixation, it has been a focus of $\Delta^{13}C$ studies independently of WUE_{plant} (Kromdijk et al., 2014). A main point of interest has been, how environmental fluctuations affect leakiness and photosynthetic efficiency. It was found that leakiness is fairly stable over environmental conditions like temperature (Henderson et al., 1992), salinity (Sharwood et al., 2014), water deficit (Sonawane & Cousins, 2020) and a wide range of irradiances (Henderson et al., 1992). On the other hand, some studies have observed significant changes in leakiness in response to high VPD (Gong et al., 2017) and low light (Bellasio & Griffiths, 2014; Henderson et al., 1992; Kromdijk et al., 2008). Overall, there seems to be a high metabolic flexibility and tight coordination of the C_3 and C_4 cycle capacities in C_4 plants for ensuring leakiness is sufficiently restricted (Bellasio & Griffiths, 2014; Kromdijk et al., 2014; Ubierna et al., 2013). Leakiness will be estimated in this study in different genotypes and under different environmental conditions.

1.2.4 Genetic variation for $\Delta^{13}C$ of C_4 plants

As the previous sections point out, both WUE_{plant} and $\delta^{13}C$ are complex traits, which are influenced by many processes that in turn can be controlled by many genes (Chen et al., 2011; Feldman et al., 2018). Unravelling the genetic control of these two traits can help to identify the main physiological drivers of WUE_{plant} and $\delta^{13}C$ and uncover to what extent their control is shared. $\delta^{13}C$ QTL analyses of C_3 species often had the aim of identifying QTL for WUE_{plant} (Bazzer et al., 2020; Chen et al., 2012; Xu et al., 2008).

The number of genetic studies of $\delta^{13}C$ in C_4 species is limited, although it increased in recent years. One of the first studies of C_4 $\delta^{13}C$ genetics was presented by Gresset et al. (2014), who used an introgression library derived from two elite maize lines to characterize the genetic control of kernel $\delta^{13}C$. A dent line from southeastern Europe served as the recurrent parent (RP) and a European flint line as the donor parent (DP). In total, 77 introgression lines were

analyzed for kernel $\delta^{13}C$ under field and greenhouse conditions and used to calculate kernel dry matter-derived $\Delta^{13}C$ ($\Delta^{13}C_{Kernel}$). Significant and highly heritable (h^2=0.69) variation for $\Delta^{13}C_{Kernel}$ was found with maximum genotypic differences of 1.6‰. 22 out of 164 tested genomic target regions were significantly associated with $\Delta^{13}C_{Kernel}$, in line with the expected polygenic, quantitative nature of the trait. Four introgression lines, with one to four introgressions each, were found to differ significantly in $\Delta^{13}C_{Kernel}$ from RP in greenhouse and field. One region on chromosome 7 explained the highest percentage of phenotypic variance (15%) and was associated with a difference in $\Delta^{13}C_{Kernel}$ of 0.26‰.

Twohey et al. (2019) also studied $\delta^{13}C$ in maize using 31 diverse inbred lines. Their study revealed a slightly lower heritability for $\delta^{13}C$ in leaves of 0.57 and a similar span of values of 1.4‰ compared to the values determined for kernels by Gresset et al. (2014). Sorgini et al. (2021) recently analyzed the genetic control of leaf $\delta^{13}C$ using four recombinant inbred line (RIL) families of maize and identified five QTL for $\delta^{13}C$, out of which three overlapped with the QTL for kernel $\delta^{13}C$ found by Gresset et al. (2014). The identification of genomic regions or ultimately genes controlling $\delta^{13}C$ might be of use for marker assisted selection in breeding, if a connection to WUE_{plant} can be established (Ellsworth et al., 2020).

The analysis of leaf $\delta^{13}C$ and WUE_{plant} QTL in an interspecific *Setaria* RIL population by Ellsworth et al. (2020) pointed to the difficulty of detecting QTL for $\delta^{13}C$ under water deficit. A similar analysis of WUE_{plant} of the same genetic material emphasized the relevance of genotype-by-environment interactions with respect to control and drought conditions (Feldman et al., 2018), which can complicate analyses of $\delta^{13}C$ and WUE_{plant}. Also regarding the different environments greenhouse and field, genotype-by-environment interactions might play a role in genetic studies of $\delta^{13}C$ and WUE_{plant}. Although Gresset et al. (2014) did not observe considerable genotype-by-environment interactions for greenhouse and field experiments with maize, Twohey et al. (2019) and Henderson et al. (1998) did find some environmental interaction for $\delta^{13}C$ of maize and sorghum genotypes, when comparing field and greenhouse data. This highlights the importance of analyses under field conditions, particularly if the conclusions have relevance for breeding in the field. Analyses in this thesis will comprise growth chamber, greenhouse and field environments to gain comprehensive and representative results on $\delta^{13}C$ and its connection to gas exchange.

1.3 Objectives of this study

The previous sections have pointed out the relevance as well as knowledge gaps of research on $\delta^{13}C$ of C_4 species, particularly in the context of WUE_{plant}. Variation in photosynthetic $\Delta^{13}C$ in response to changes in iWUE is smaller in C_4 compared to C_3 plants and there is no sufficient knowledge of intraspecific variation in leakiness and post-photosynthetic fractionations. Thus, more studies are needed to improve the understanding of the connection between C_4-$\delta^{13}C$ and -WUE_{plant}. Gresset et al. (2014) generated a maize introgression library and characterized the genetic variation for kernel $\delta^{13}C$. The recurrent parent and two near isogenic lines (NILs) that are derived from this introgression library were selected in this study for investigating the connection of differences in their kernel $\delta^{13}C$ with WUE_{plant}. The use of NILs allows to separate different interacting factors influencing $\delta^{13}C$ and limits genetic background variation. The aim of this thesis was to characterize the relationship between genotypic differences in photosynthetic $\Delta^{13}C$, dry matter $\delta^{13}C$, gas exchange parameters and WUE_{plant} in the C_4 plant maize.

The objectives were:

1) Examine, whether $\delta^{13}C$ of leaf and $\delta^{13}C$ of kernel dry matter reflect genotypic differences in photosynthetic $\Delta^{13}C$.

2) Investigate the role of stomatal conductance, assimilation rate, iWUE and leakiness as potential drivers for genetic variation in photosynthetic $\Delta^{13}C$ and the $\delta^{13}C$ of dry matter.

3) Examine the effect of water deficit on the relationship between photosynthetic $\Delta^{13}C$ and iWUE and on genotypic differentiation in $\delta^{13}C$.

4) Investigate an association of dry matter $\delta^{13}C$ with agronomically relevant traits under field conditions.

5) Fine-map a genomic region on chromosome 1 underlying the changed kernel $\delta^{13}C$ of one NIL.

2 Methods

2.1 Plant material

2.1.1 Near isogenic lines (NILs)

Analyses in this study focused on a set of near isogenic maize lines and their recurrent parent, RP. The lines NIL B, NIL C, NIL W, NIL X and NIL Y carry introgressions from a drought-sensitive European flint donor parent in the genetic background of the more drought-tolerant dent RP from southeastern Europe (Tables 2.1, S1). The lines were derived from an introgression library described by Gresset et al. (2014). Positions and sizes of donor introgressions were determined for all NILs based on data obtained using the 600k Axiom™ Maize Genotyping Array (Affymetrix, USA; Unterseer et al., 2014) and B73 AGPv4 (www.maizegdb.org; Jiao et al., 2017).

Based on their leaf and kernel $\delta^{13}C$ ($\delta^{13}C_{Leaf}$, $\delta^{13}C_{Kernel}$), NIL B and NIL Y were selected in addition to RP for the main experiments, because they showed differences compared to RP in opposite directions (chapter 3.1.1). NIL B was derived from the cross of the introgression lines IL059 and IL027 and NIL Y from the cross of IL003 and IL077, described by Gresset et al. (2014). NIL B carries a 55 Mb introgression on chromosome 7 (including the QTL increasing $\delta^{13}C_{Kernel}$ identified by Gresset et al., 2014) and smaller introgressions on chromosomes 3 and 7 (Table 2.1). NIL Y carries a 27 Mb introgression on chromosome 1 and smaller introgressions on chromosomes 7 and 8. RP and NIL B are also described in Avramova et al. (2019).

Table 2.1: Introgressions of NIL B and NIL Y with starting and end coordinates on the respective chromosomes (chr) in bp and their size in Mb.
Coordinates are based on B73 AGPv4.

	NIL B		NIL Y	
	coordinates [bp]	size [Mb]	coordinates [bp]	size [Mb]
chr 1	-	-	8,048,178 - 34,709,915	26.7
chr 3	212,550,017 - 218,246,085	5.7	-	-
chr 7	4,096,879 - 5,232,852	1.1	140,311,696 - 141,952,684	1.6
	110,757,334 - 166,102,662	55.3	-	-
	172,544,488 - 173,500,795	1.0	-	-
chr 8	-	-	181,189 - 683,453	0.5

2.1.2 Generation of crosses and recombinant lines derived from the original NILs

NIL BY

To generate NIL BY, which carries both the major chromosome 1 and chromosome 7 introgression of NIL Y and NIL B, respectively, NIL Y and NIL B were crossed. The progeny was self-pollinated to obtain the F_2 generation. Seedlings of the F_2 generation were genotyped with 15 KASP (Kompetitive allele specific PCR) markers (LGC Biosearch™ Technologies, UK), spread over the introgressions on chromosomes 1, 3 and 7 (Table 2.2). The design of KASP markers was based on the 600k Axiom™ Maize Genotyping Array (Affymetrix, USA; Unterseer et al., 2014).

Table 2.2: KASP markers used for generating NIL BY with marker coordinates (B73 AGPv4) and nucleotide bases corresponding to the allele of the recurrent parent (RP) and the donor parent (DP).
For primer sequences see Table S2.

ID	chromosome	position [bp]	RP	DP
AX-90528544	1	9,638,977	A	G
AX-90564732	1	12,146,599	A	G
AX-90570846	1	20,022,709	C	T
AX-90528796	1	26,609,865	A	G
AX-90528942	1	34,592,871	G	T
AX-91393015	3	212,550,017	C	G
AX-90607846	3	215,865,146	C	T
AX-91355356	7	4,233,140	C	T
AX-90570605	7	5,052,968	A	G
AX-91356933	7	118,512,477	C	A
AX-90552118	7	124,341,628	T	C
AX-90527158	7	132,117,607	A	G
AX-90552405	7	141,161,954	G	A
AX-90572351	7	155,419,484	A	G
AX-90552866	7	173,286,556	G	A

For genotyping, DNA was extracted from leaf samples of young plants around vegetative developmental stage V2 following the protocol described by Saghai-Maroof et al. (1984) using CTAB (cetyltrimethylammonium bromide). DNA concentrations were adjusted to 10 ng μL^{-1} with the Epoch Microplate Spectrophotometer (BioTek, USA). The PCR reaction mix was prepared in 96 well plates as described by the manufacturer (www.biosearchtech.com), but using a total reaction volume of 8 µL. The PCR reaction solution consisted of 4 µL DNA, 4 µL 2X KASP-TF Master Mix and 0.12 µL KASP Assay Mix, containing the respective KASP primers. The reaction was run using the temperature program given by the KASP manufacturer (Table 2.3) and results read using the QuantStudio 3 Real-Time-PCR System (Thermo Fisher

Scientific, USA). Data was analyzed with the Software KlusterCaller™ (LGC Biosearch™ Technologies, UK).

Table 2.3: Temperature program for KASP genotyping reactions as given by LGC Biosearch™ Technologies, UK.

Step	Description	Temperature	Time	Number of cycles
1	Activation	94 °C	15 min	1
2	Denaturation Annealing/ Elongation	94 °C 61-55 °C (drop 0.6 °C per cycle)	20 s 60 s	10
3	Denaturation Annealing/ Elongation	94 °C 55°C	20 s 60 s	26

Out of 195 seedlings, two plants were homozygous for both the chromosome 1 and chromosome 7 introgression. One of these plants was heterozygous for all minor introgressions (Figure 2.1). This plant was named NIL BY, grown to maturity and self-pollinated to produce seeds for subsequent experiments. Assuming that the small segregating introgressions do not influence trait expression, the resulting NIL BY progeny (generation F_3) was analyzed for gas exchange and $\delta^{13}C$ to examine the effect of combining the major chromosome 1 and chromosome 7 introgression (Experiment 2.5). The F_4 plants were included in the field trial 2021.

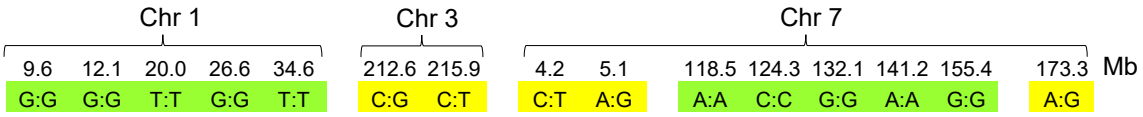

Figure 2.1: Genotyping data of NIL BY, which is homozygous for the major chromosome (chr) 1 and chr 7 introgression.
Shown are marker data of a plant in the F_2 generation of the cross of NIL B and NIL Y. This plant was self-pollinated and all derived plants are named NIL BY. Marker positions (B73 AGPv4) are given at the top in Mega bases (Mb). Marker results corresponding to the genotype of the donor parent are marked in green, marker positions marked in yellow are heterozygous.

NIL Y- derived recombinant lines

NIL Y was backcrossed to RP to generate recombinant lines with smaller introgressions within the region of the chromosome 1 introgression carried by NIL Y. After self-pollination of the F_1, seeds were germinated for genotyping of the F_2 generation. Out of 77 seedlings, seven plants with different genotypes were selected to be grown to maturity and self-pollinated based on the results of five KASP markers spread over the chromosome 1 introgression. These eight

genotypes, as well as their derived progeny were named Yb, Yc, Yd, Ye, Yf, Yh and Yi. Plants of the F_3 and F_4 generation were analyzed with 16 markers, 14 markers within the chromosome 1 introgression and one each in the chromosome 7 and chromosome 8 introgression (Table 2.4). Ten progeny plants of each of these recombinant lines were grown in the greenhouse in winter to analyze $\delta^{13}C_{Kernel}$. $\delta^{13}C_{Kernel}$ was unusually low, with values of -15.1 to -14.3‰. Seeds of the plants were used to repeat the analysis of $\delta^{13}C_{Kernel}$ in the F_4 generation in the greenhouse in summer in Experiment 2.6. The F_5 generation was planted in the field trial 2021.

Table 2.4: KASP markers used for generating recombinant lines derived from NIL Y with marker coordinates (B73 AGPv4) and nucleotide bases corresponding to the allele of the recurrent parent (RP) and the donor parent (DP).
For primer sequences see Table S2.

ID	chromosome	position [bp]	RP	DP
AX-90528533	1	8,048,178	A	T
AX-90528544	1	9,638,977	A	G
AX-90564732	1	12,146,599	A	G
AX-90598853	1	14,082,518	A	C
AX-91456390	1	16,129,251	C	T
AX-91456763	1	18,001,999	G	C
AX-90570846	1	20,022,709	C	T
AX-91457497	1	22,006,632	T	C
AX-90656493	1	24,417,904	T	C
AX-90528796	1	26,609,865	A	G
AX-90526031	1	28,638,770	G	A
AX-90528864	1	30,554,699	A	C
AX-90528910	1	32,474,714	C	T
AX-90528942	1	34,592,871	G	T
AX-90552405	7	141,161,954	G	A
AX-90553010	8	494,673	G	A

2.2 Growth conditions and experimental setup

2.2.1 Imbibition and pre-growth

For growth chamber and greenhouse experiments, seeds were pre-germinated in filter paper rolls (Type 751, Macherey-Nagel GmbH & Co. KG, Germany). Kernels were placed with approximately 1.5 cm distance at the top of wet filter paper with the tipcap directed to the bottom of the filter paper. The paper was rolled up, placed in a covered beaker and kept at 28 °C in the dark for three days. Germinated kernels were then planted into 585 mL pots, filled with a mixture of soil (CL ED73, Einheitserde, Germany) and sand (SAKRET Trockenbaustoff

Europa GmbH & Co. KG, Germany) in the ratio 6:1, for pre-growth in the growth chamber (PlantMaster, CLF Plant Climatics GmbH, Germany) for two to three weeks. Growth conditions in this growth chamber were set to 16/8 h day/night (d/n), 25/20 °C d/n, 75/70% relative humidity (RH) d/n, with a maximum light intensity of 650 µmol m^{-2} s^{-1}. At the end of the second week, plants were fertilized with Guano-Fertilizer (Rubin, Germany, ½ cap per 2 L, 2 L per 24 plants).

2.2.2 Growth chamber experiments (Exp. 1.1 and 1.2)

Growth chamber Experiments 1.1 and 1.2 were conducted to simultaneously assess photosynthetic carbon isotope discrimination ($\Delta^{13}C_{Photosynthetic}$) and gas exchange of RP, NIL B and NIL Y under controlled conditions at stage V5/6. Plants were transferred from the growth chamber used for pre-growth to growth chambers (PGR15, Conviron, Canada) at the Technical University of Munich (TUM) Plant Technology Center two weeks after planting. There, plants were grown at a light intensity of 800 µmol $m^{-2}s^{-1}$ at plant height and 16/8 h d/n, 25/20 °C d/n, 60/60% RH d/n. The chamber was supplied with air mixed from CO_2-free dry air and tank CO_2 with known isotopic composition and CO_2 concentrations were maintained at 400 ppm. Plants were grown in completely randomized designs in two batches per experiment, planted one week apart. At least one week after transfer, when plants reached developmental stage V5/6, simultaneous measurements of $\Delta^{13}C_{Photosynthetic}$ and gas exchange (chapter 2.3.2) took place on five to six consecutive days.

In the first experiment (Experiment 1.1), 32 replicates of RP, NIL B and NIL Y, respectively, were grown under well-watered conditions, achieved by regular manual watering. Measurements were taken on 13-14 replicates per genotype, selected to have similar developmental stage and plant height. In addition to analysis of $\Delta^{13}C_{Photosynthetic}$, five plants per genotype of Experiment 1.1 were used for recording of A/C_i curves (chapter 2.3.1).

In the second experiment (Experiment 1.2), $\Delta^{13}C_{Photosynthetic}$ and gas exchange were assessed additionally in plants grown under water deficit. Fifteen to sixteen replicates of RP, NIL B and NIL Y were included in batch 1 and 13-14 in batch 2 and all plants were well-watered until five to six days before measurements. For five to six days before measurements, half of the plants received a limited amount of water to a volumetric soil water content (SWC) of 30% (total volume of 500 mL, the weight of the dried soil was 145 g) each day in the evening. The rest of the plants (control plants) were watered to a SWC of 50% per day. Measurements were performed on a total of 13-15 replicates per genotype and treatment.

In both experiments, after measurements of $\Delta^{13}C_{Photosynthetic}$, the leaf part, which was clipped in the leaf cuvette, was sampled for determination of specific leaf area (SLA; see chapter 2.7).

2.2.3 Greenhouse experiments (Exp. 2.1-2.6)

Greenhouse experiments were conducted in the greenhouse of the TUM Plant Technology Center, Freising, Germany. After pre-growth in the growth chamber of two to three weeks, plants were transferred to 10 L pots, filled with soil (Stender Topfsubstrat, C700). All experiments were arranged as randomized complete block designs. Water was provided by drip irrigation and mixed with fertilizer Universol Blue (EC value 2.8, approximately 2 g fertilizer per liter of water). Growth conditions were set to 25-35 °C /18-20°C d/n and 40% RH. Light with an intensity of 300-400 µmol $m^{-2}s^{-1}$ was supplied, when sunlight was not sufficient.

Experiment 2.1

In Experiment 2.1, $\delta^{13}C$ of the cobleaf (leaf below the uppermost ear) of RP and five NILs was determined and used to select genotypes for subsequent analyses. Ten replicates of seven genotypes, RP, NIL B, NIL C, NIL W, NIL X, NIL Y and the commonly used maize inbred line B73, were included in this experiment. Average temperature and RH in the greenhouse were 24.1 °C and 51.4%. During flowering, the leaf below the uppermost ear was harvested for RP and the five NILs and sampled for subsequent analysis of $\delta^{13}C$ as described in chapter 2.4.

Experiment 2.2

In Experiment 2.2, gas exchange of RP, NIL B and NIL Y was investigated at developmental stage V7-9. RP, NIL B and NIL Y were part of a larger experiment comprising a total of six genotypes, each replicated 10 times. Gas exchange was measured on the youngest fully developed leaf (see chapter 2.3.1), when plants were at developmental stage V7-9 for three days. During the period from transfer to the greenhouse to the final gas exchange measurements, average temperature in the greenhouse was 22.8 °C and average RH 38.3%.

Experiment 2.3

Experiment 2.3 comprised 20 replicates of RP, NIL B and NIL Y, respectively, for measurements of gas exchange, stomatal density, chlorophyll content, enzyme activities and stable isotopic compositions ($\delta^{13}C$ and oxygen isotopic composition $\delta^{18}O$) at stage V5/6. $\delta^{18}O$ was assessed as a potential integrative measure for transpiration (Barbour et al., 2000). Average temperature and relative humidity in the greenhouse were 25.9 °C and 52.6%, respectively. Gas exchange measurements were performed on the last developed leaf at developmental stage V5/6 on 17-20 replicates per genotype on three days. One day after gas

exchange measurement, leaves were sampled for analysis of stomatal density, stable isotopic compositions, chlorophyll content and enzyme activities (see chapter 2.4 and 2.5).

Experiment 2.4

The main purpose of Experiment 2.4 was to analyze the effect of a temporary drought treatment around developmental stage V10 on gas exchange and stable isotopic compositions of leaves and kernels of RP, NIL B and NIL Y. Pots were filled with 3.9 kg of sifted soil to enable a uniform and controlled drought treatment at stage V10. Twenty plants per genotype of RP, NIL B and NIL Y were grown until seed production at an average temperature of 25.0 °C and an average RH of 51.3%. Initially, plants were automatically watered as in other experiments. At developmental stage V5/6, gas exchange was measured on the youngest fully developed leaf on 16-20 replicates on four days. When plants were at stage V7-8, volumetric SWC was determined and had an average value of 61.5% (calculated with a volume of 8 L, weight of the dried soil was 1860 g). Subsequently, automatic watering was stopped to attain drought stress for half of the plants at approximately stage V10. For half of the plants watering was stopped completely until a SWC of 23% was reached. Then, plants were manually watered to maintain this SWC until gas exchange measurements took place six days after beginning of the drought treatment of the respective plants. The other half of the plants (well-watered plants) were watered manually to maintain the SWC of 61.5% until gas exchange measurements took place. Gas exchange measurements were performed on the youngest fully developed leaf on eight to ten replicates of well-watered and eight to ten replicates of drought-treated plants. This resulted in measurements taken on leaves 9-12 over five days. On the same day of gas exchange measurements, leaves were harvested for analysis of stable isotopic compositions. After sampling, all plants were rewatered to a SWC of 61.5% and maintained at that SWC until automatic watering was resumed, when all plants had been sampled. Plants were grown until maturity and one ear per plant was manually self-pollinated. When seeds were fully matured, kernels were harvested for subsequent analysis of $\delta^{13}C$.

Experiment 2.5

In Experiment 2.5, the individual and joint effect of the chromosome 1 introgression of NIL Y and the chromosome 7 introgression of NIL B on gas exchange, stomatal density and stable isotopic compositions of cobleaves and kernels was assessed. The experiment comprised twenty-seven replicates of the genotypes RP, NIL B, NIL Y and NIL BY. All individuals of NIL BY were genotyped with KASP markers listed in Table 2.2 as described in chapter 2.1.2 (together with 5 replicates of RP, NIL B and NIL Y as controls). Plants were grown in the

greenhouse at an average temperature and RH of 26.0 °C and 57.0%, respectively. At stage V5/6, gas exchange of 14-15 replicates per genotype was measured on the youngest fully developed leaf over four days. Subsequently, samples of the measured leaves were taken to determine stomatal density. When plants were in reproductive stage R1, the leaf below the uppermost ear was harvested for nine replicates. Ears had been covered with paper bags before, so no pollination could have occurred before cobleaf harvest. For all other plants, one ear per plant was manually self-pollinated and when seeds were fully matured, kernels were harvested for subsequent analysis of $\delta^{13}C$ and $\delta^{18}O$.

Experiment 2.6

Experiment 2.6 served to analyze $\delta^{13}C_{Kernel}$ in NIL Y-derived recombinant lines, which carry overlapping sub-segments of the chromosome 1 introgression carried by NIL Y. The aim was to narrow down the genetic region associated with $\delta^{13}C_{Kernel}$. The NIL Y-derived recombinants Yb, Yc, Yd, Ye, Yf, Yh, Yi, as well as NIL Y, RP and NIL B were included in the experiment. Genotyping of the NIL Y-derived recombinant lines was carried out as described in chapter 2.1.2. Plants were grown in the greenhouse at an average temperature and RH of 26.0 °C and 58.9%, respectively, until maturity. RP was included as duplicate entry and 10 replicates were included per entry, leading to 20 replicates of RP and 10 of all other genotypes. Pollination was performed manually on one ear per plant. When kernels had fully matured, cobs were harvested and used for determination of $\delta^{13}C_{Kernel}$, kernel number and thousand kernel weight. NIL B was not included in the statistical analysis.

2.2.4 Field trials

The main field trials took place in 2019 to 2021. The purpose of these field trials was to link the results obtained under controlled growth chamber and greenhouse conditions to the phenotype of RP, NIL B and NIL Y in the field, particularly with respect to $\delta^{13}C_{Kernel}$. Additionally, different growth- and yield-related traits were assessed (see chapter 2.7) in field trials under well-watered and water-limited conditions to test a link with $\delta^{13}C_{Kernel}$. Field trials included a control field (48°24′12.2″N, 11°43′22.3″E), in which plants grew under rain-fed conditions supplemented by irrigation, and a drought-field (48°24′40.9″N, 11°43′22.4″E), where plants grew under a movable rain-out shelter, both located in Freising, Germany. Sowing took place in the second half of April. The genotypes RP, NIL B and NIL Y were included in a larger experiment comprising 91 entries, grown as a randomized complete block design in the control

field and in the drought field with three replications, respectively. In these trials, RP, NIL B and NIL Y were included as duplicate entries, resulting in six replicates per genotype. In the control field, each plot consisted of a 3 m row with 20 plants. In the drought field, a plot consisted of a 1.2 m row with 10 plants. Herbicides and fertilizer were applied following good agricultural practice. In the control field, plants were irrigated when needed to avoid water deficit. In the rain-out shelter watering was reduced between stage V9 and R1 to achieve water stress around flowering. In both fields, plants were grown until maturity. All cobs per row were manually harvested at maturity for determination of $\delta^{13}C_{Kernel}$, TKW and kernel number. Throughout the development, measurements of plant height and SPAD (Single photon avalanche diode) were taken and flowering dates were recorded.

In 2019, average temperature between May and September was 16.3 °C and a total precipitation of 431 L m^{-2} was supplemented by irrigation. Watering in the rain-out-shelter reached a total of 193 L m^{-2}. In addition to measurements of the above-mentioned traits, kernels of RP, NIL B and NIL Y of this trial were analyzed for $\delta^{18}O$.

In 2020, average temperature between May and September at the location of the field trials was 15.9 °C. In the control field, a total precipitation of 436 L m^{-2} was supplemented by irrigation. Plants in the rainout shelter received 219 L m^{-2} water. In addition to measurements of the above-mentioned traits, cobleaves (leaf below the uppermost ear) of RP, NIL B and NIL Y in the control field 2020 were sampled for $\delta^{13}C$ analysis right before flowering. Sampling took place, when ears were visible, but no pollen and silks were developed, so no pollination had occurred yet. Twenty to thirty 0.2 cm^2 leaf punches were taken on three plants per plot and combined to one sample per plot for $\delta^{13}C_{Leaf}$ analysis. Plants of which cobleaves were sampled were excluded from analysis of $\delta^{13}C_{Kernel}$.

After assessing $\delta^{13}C_{Kernel}$ and agronomic traits under well-watered and water limited conditions in the field in 2019 and 2020, the focus of the field trial in 2021 was to connect measurements of gas exchange taken under well-watered field conditions with $\delta^{13}C$. A second objective was to connect $\delta^{13}C_{Kernel}$ of the NIL Y-derived recombinants analyzed in the greenhouse with $\delta^{13}C_{Kernel}$ in the field. In addition to RP, NIL B and NIL Y, NIL BY and the NIL Y-derived recombinant lines Yb, Yc, Yd, Ye, Yf, Yh and Yi were included in this field trial. These genotypes were included as duplicate entries, except for Ye. No data from the drought trial is included from this year. Average temperature between May and September was 15.6 °C and precipitation in the control field was 578 L m^{-2}, which was supplemented by irrigation. To link the results on stable isotopic compositions in the field to stomatal conductance, assimilation rate and iWUE under field conditions, gas exchange and -related traits were measured on RP, NIL B, NIL Y and NIL BY at stage V6/7. Gas exchange measurements were performed on the youngest fully expanded leaf of two to three plants per plot over five days. Subsequently, the

leaf part, which was clipped in the leaf cuvette, was sampled for determination of SLA. The rest of the measured leaf, excluding tip, base and midvein, was sampled for determination of $\delta^{13}C$ and chlorophyll content. Leaf 5 was sampled for stomatal density. At a later developmental stage, cobleaves (leaf below the uppermost ear) of RP, NIL B, NIL Y and NIL BY in the control field were sampled, when ears were visible, but no pollen and silks were developed yet. For this, a leaf piece of 20 cm was taken from the cobleaf excluding the tip of the leaf and the midvein, and frozen in liquid nitrogen. Samples were taken on two plants per plot. These samples were analyzed for $\delta^{13}C_{Leaf}$ and contents of sucrose, glucose and fructose and the average value over the plants of a plot was taken. Plants of which cobleaves were sampled were excluded from analysis of $\delta^{13}C_{Kernel}$.

An additional field experiment was performed at the location of the control field (48°24′12.2″N, 11°43′22.3″E) in 2018, which provided kernels for separate analysis of embryo and endosperm $\delta^{13}C$. Average temperature and total precipitation during growth were 17.6 °C and 425 L m^{-2}, respectively. RP, NIL B and NIL Y were part of a larger experiment comprising six genotypes, arranged in a randomized complete block design with two replicates. Each plot consisted of a 1.5 m row of 10 plants. Kernels of two to three plants per plot were used for kernel dissection and $\delta^{13}C$ analysis (chapter 2.4).

2.3 Leaf gas exchange measurements

2.3.1 Infrared gas analyzer measurements of gas exchange

CO_2 uptake and water release by leaves was measured by infrared gas analyzers (IRGA) using the portable photosynthesis systems LI-6800 and LI-6400 (LI-COR Inc., USA) to assess relevant parameters of gas exchange. The LI-6800 was used for measurements of steady-state gas exchange, including assimilation rate, stomatal conductance and intercellular CO_2 concentrations (C_i), of greenhouse- and field-grown plants. A leaf piece close to the tip of the youngest fully expanded leaf was clipped into the leaf cuvette. After equilibration of the measurement values approximately 30 min after clipping, the average over 10 measurement values obtained every 30 s was taken for each plant. Measurement conditions in the leaf cuvette were set to photosynthetically active radiation (PAR) of 1500 µmol $m^{-2}s^{-1}$, leaf temperature of 25 to 26°C, RH of 50%, and ambient CO_2 concentration of 400 ppm.

A/C_i curves were recorded with the portable photosynthesis system LI-6400 on five replicates per genotype of growth-chamber-grown plants used for measurements of $\Delta^{13}C_{Photosynthetic}$ (Experiment 1.1). The youngest fully developed leaf was clipped into the leaf cuvette.

Measurements were recorded at ambient CO_2 concentrations of 635 ppm, 405 ppm, 210 ppm, 125 ppm, 90 ppm, 60 ppm, 35 ppm and 25 ppm, PAR of 1500 µmol $m^{-2}s^{-1}$, leaf temperature of 25 °C and RH of approximately 60%. After stabilization, a minimum of seven values were recorded at each CO_2 concentration spread over 1 min.

2.3.2 Measurements of photosynthetic $\Delta^{13}C$

Simultaneous measurements of $\Delta^{13}C_{Photosynthetic}$ and gas exchange were performed at the TUM Chair of Grassland sciences. The deployed growth chambers are part of a gas exchange mesocosm system described by Baca Cabrera et al. (2020). Gas exchange measurements were performed on the youngest fully developed leaf at stage V5/6 with the portable photosynthesis system LI-6400 (LI-COR Inc., USA). For simultaneous measurements of $\Delta^{13}C_{Photosynthetic}$, the leaf cuvette of the LI-6400 was coupled to a continuous-flow isotope ratio mass spectrometer (IRMS; Deltaplus Advantage equipped with GasBench II, ThermoFinnigan, Germany). A detailed description of the technical details of the LI-6400-coupled IRMS measurements is given in Gong et al. (2015). Measurements were recorded after approximately 30 min of equilibration.

$\Delta^{13}C_{Photosynthetic}$ was calculated as:

Equation (2) $$\Delta^{13}C_{Photosynthetic} = \frac{\xi(\delta_{out}-\delta_{in})}{1+\delta_{out}-\xi(\delta_{out}-\delta_{in})},$$

with $\xi = C_{in}/(C_{in}-C_a)$, $C_{in}=CO_2$ concentration and δ_{in} = carbon isotopic composition of the air supplied to the leaf cuvette, respectively; and $C_a=CO_2$ concentration and δ_{out} = carbon isotopic composition of the air exiting the leaf cuvette, respectively. The gas exchange measurement system was supplied with CO_2 of the same isotopic composition as the growth chambers. In each measurement, four values for δ_{out} and three values for δ_{in} were recorded. Average precision (SD) of the IRMS was 0.11‰. ξ was kept below 7 during measurements. For each LI-6400 measurement, 20 values were recorded every 15 s.

In Experiment 1.1 and Experiment 1.2, each plant was measured under standard conditions in the leaf cuvette, set to a light intensity of 1500 µmol $m^{-2}s^{-1}$, temperature of 25 °C, RH of 60% and CO_2 concentration of 400 ppm. In Experiment 1.1, plants were additionally measured at a light intensity of 800 µmol $m^{-2}s^{-1}$, which was the light intensity in the growth chamber, where plants were grown. In Experiment 1.2, 10 plants were additionally measured at a RH of 35%.

From the simultaneous measurements of $\Delta^{13}C_{Photosynthetic}$ and C_i/C_a, leakiness (φ) was calculated by rearranging the simplified model given in Equation (1) as:

Equation (3) $$\varphi = \frac{(\Delta^{13}\mathrm{C}-\mathrm{a})\, C_a/C_i - b_4 + a}{b_3 - s},$$

with a=4.4‰, b_3=29‰, b_4=-5.7‰ and s=1.8‰ based on von Caemmerer et al. (2014).

2.4 Determination of stable isotopic compositions

2.4.1 Sampling and sample preparation

For analysis of stable isotopic compositions ($\delta^{13}C$ and $\delta^{18}O$) of leaves, leaf blades excluding the tip, base and midveins were harvested in greenhouse experiments. For sampling of the cobleaf in field trials, leaves were sampled differently to ensure kernel production. In the field trial 2020, 20-30 leaf punches of approximately 0.2 cm² were taken spread over the leaf blade; in the field trial in 2021, a leaf piece of 20 cm was taken from the cobleaf excluding the tip of the leaf and the midvein. Sampled leaves were snapfrozen in liquid nitrogen, and frozen leaves were ground with mortar and pestle. If this did not result in sufficiently fine leaf powder, subsamples were milled with 3 mm metal balls in 2 mL Eppendorf tubes using the Tissue Lyser II (Retsch, Qiagen, Netherlands). Drying of ground leaf samples in Eppendorf tubes was achieved either by lyophilization (Christ Alpha 1-4, Martin Christ Gefriertrocknungsanlagen GmbH, Germany) or in a speedvac vacuum concentrator (SA Speed Concentrator, H. Saur Laborbedarf, Germany). Leaf punches from the field trial 2020 were dried at 60 °C and ground with metal balls in Eppendorf tubes using the Tissue Lyser II (Retsch, Qiagen, Netherlands).

For analysis of stable isotopic compositions of kernels of greenhouse-grown plants, cobs with less than 30 kernels were excluded. For the remaining samples, five kernels per cob were milled in a Tissue Lyser II (Retsch, Qiagen, Netherlands) using 10 mm metal balls.

For kernels of field-grown plants, all kernels per plot were pooled with exception of the plants sampled for cobleaf $\delta^{13}C$. A subsample of approximately 250 kernels was milled in a rotor beater mill (model SR300, Retsch, Germany) to about 0.5 mm particle size. A subsample of the ground kernel material was transferred to an Eppendorf tube and ground further with Tissue Lyser II (Retsch, Qiagen, Netherlands).

For separate analysis of $\delta^{13}C$ of embryo and endosperm, five kernels per plant were imbibed in demineralized water for 3 h. Subsequently, kernels were cut in half and the pericarp removed with forceps. Then, the embryo was separated from the endosperm with forceps. All embryos and all endosperms of one plant were combined and dried at 60 °C, respectively. Samples were ground with 10 mm metal balls in a Tissue Lyser II (Retsch, Qiagen, Netherlands).

2.4.2 Carbon isotopic composition $\delta^{13}C$

For $\delta^{13}C$ analysis, 3 ± 0.1 mg of ground and dried leaf or kernel material was weighed into tin capsules (5x8 mm IVA Analysentechnik e.K., Germany) with three to four technical replicates per biological sample. $\delta^{13}C$ was determined by coupled elemental analyzer and IRMS analysis carried out by Isolab GmbH (Schweitenkirchen, Germany). The method is described in detail by Werner and Rossmann (2015). Values for $\delta^{13}C$ are expressed relative to the international standard Vienna Pee Dee Belemnite (V-PDB).

Dry matter-derived $\Delta^{13}C$ was calculated as described by Farquhar, et al. (1989a):

Equation (4) $$\Delta^{13}C = \frac{\delta^{13}C_{air} - \delta^{13}C_p}{1+\delta^{13}C_p},$$

with $\delta^{13}C_{air}$ as $\delta^{13}C$ of air, taken as -8‰, and $\delta^{13}C_p$ as $\delta^{13}C$ of the plant sample.

2.4.3 Oxygen isotopic composition $\delta^{18}O$

Analyses of oxygen isotopic compositions ($\delta^{18}O$) of plant dry matter and of irrigation water were carried out by the group of Ecophysiology of Plants (Prof. Thorsten Grams) at TUM by isotope ratio mass spectrometry.

For $\delta^{18}O$ analysis of leaf and kernel dry matter, 0.8 ± 0.05 mg of ground and dried plant material was weighed into silver capsules (3.3x5mm IVA Analysentechnik e.K., Germany). The Isoprime Precision mass spectrometer (Elementar Analysensysteme GmbH, Germany), coupled to the elemental analyzer Vario PyroCube (Elementar Analysensysteme GmbH, Germany) was used for the analysis with a temperature for pyrolysis of 1450 °C. Isotopic compositions were calculated relative to the international standard V-PDB.

A water sample of the irrigation water in the greenhouse Experiments 2.3 and 2.4 was also analyzed for its $\delta^{18}O$. The IsoPrime 100 mass spectrometer (Isoprime, UK) was coupled to the IsoPrime Multiflow (Isoprime, UK) for the analysis. Isotopic composition was calculated relative to the international standard Vienna Standard Mean Ocean Water (V-SMOW).

2.5 Determination of photosynthesis-related traits

2.5.1 Stomatal density

To determine stomatal density, three leaf pieces of approximately 0.5 cm² were cut within approximately 12 cm from the leaf tip. The abaxial side of these leaf pieces was coated with clear nail polish. Once dried, nail polish imprints were removed from the leaf pieces and transferred to a microscopic slide with transparent tape. Pictures of the imprints were taken under the microscope (BX61, Olympus K.K., Japan) at the Center of Advanced Light Microscopy (CALM, TUM) with 10x magnification at three different spots. The number of stomata per picture was counted using the software ImageJ (imagej.nih.gov/ij/; Schneider et al., 2012). For each biological sample, the average over nine pictures (three per leaf piece) was taken and was related to the respective leaf area covered by the picture.

2.5.2 Chlorophyll content

For analysis of chlorophyll content, 25-40 mg of finely ground and frozen leaf tissue was weighed into 2 mL Eppendorf tubes. Photosynthetic pigments were extracted with 1 mL 95 % Ethanol, containing traces of $CaCO_3$, in a Tissue Lyser II (Retsch, Qiagen, Netherlands). After centrifugation and transfer of the supernatant, extraction was repeated and supernatants combined. Absorptions of the 1:5-diluted supernatant were determined in 96-well plates in an Epoch Microplate Spectrophotometer (BioTek Instruments, USA) at wavelengths of 470, 649 and 664 nm. Concentrations of chlorophyll a and b were calculated as described by Lichtenthaler (1987):

Equation (5) $\text{Chl.a } [\mu g\ mL^{-1}] = 13.36\ A_{664} - 5.19\ A_{649}$

Equation (6) $\text{Chl.b } [\mu g\ mL^{-1}] = 27.43\ A_{649} - 8.12\ A_{664}$,

with Chl.a = chlorophyll a concentration and Chl.b = chlorophyll b concentration and A_{649} and A_{664} as the absorptions at the respective wavelengths of 649 and 664 nm.

Amounts of chlorophyll were then related to the fresh weight of the analyzed leaf material.

2.5.3 Leaf soluble sugar contents

For determination of sucrose, glucose and fructose content of cobleaves, 100 ± 10 mg of finely ground and frozen leaf material was used. Sugars were extracted and quantified based on the protocol described by Leach and Braun (2016) and using the sucrose, D-fructose and D-

glucose kit by Megazyme Ltd. (Ireland). Plant material was extracted with 1 mL methanol-chloroform-water (12:5:3) buffer in screw cap tubes using the Tissue Lyser II (Retsch, Qiagen, Netherlands) and 3 mm metal balls. Samples were vortexed and incubated in a water bath at 50 °C for 30 min. After centrifugation and transfer of the supernatant to a 15 mL tube, extraction of the pellet was repeated twice and the supernatants combined. The volume of the combined supernatant was determined and 0.6 volumes of water added. The resulting solution was vortexed and centrifuged. The volume of the aqueous upper phase was recorded and a subsample was used for determination of soluble sugar contents. Quantification of sucrose, glucose and fructose content followed the protocol of the sucrose, D-fructose and D-glucose kit by Megazyme. Volumes of 30 µL for the sugar sample, 80 µL for solution 6, 800 µL for water, 40 µL for solutions 1 and 2 and 8 µL for suspensions 3 and 4 were used. Reactions and absorbance measurements at 340 nm were performed in semi-micro UV cuvettes (VWR International, USA) and using the spectrophotometer U-1800 (Hitachi High-Technologies Corporation, Japan). Absorbance differences (ΔA) that could be attributed to sucrose, glucose and fructose, respectively, were calculated and used for calculating the concentration of the respective substances as instructed by the Megazyme kit. For this, the equation $c = (V \times MW) / (\varepsilon \times d \times v) \times \Delta A$ was used, with c= concentration, V= reaction volume, MW= molecular weight, ε= extinction coefficient of NADPH at 340 nm, d= light path and v= volume of sugar sample. Sugar levels were expressed relative to the fresh weight of the leaf material.

2.5.4 Determination of PEPC and Rubisco activity

PEPC and Rubisco activities in leaf samples of greenhouse-grown plants (Experiment 2.3) were measured by the group of Central Metabolism (Prof. Alisdair Fernie) at the Max Planck Institute for Molecular Plant Physiology (Golm, Germany). Initial and total Rubisco activities were measured based on the protocol by Sulpice et al. (2007), PEPC activity based on the protocol by Gibon et al. (2004). Initial activity of Rubisco reflects the activity state at time of harvest, total activity was measured after incubation with an activation solution to reach a fully activated state of Rubisco. Activities are expressed relative to the fresh weight of the analyzed leaf material.

2.6 Whole plant water use efficiency and response to progressive soil drying

Whole plant water use efficiency (WUE_{plant}) was determined in a progressive drought experiment in the greenhouse based on a protocol described in Avramova et al. (2019) and

adapted from Yang et al. (2016). Fifteen replicates of RP, NIL B and NIL Y were arranged in a randomized complete block design. Two-week-old plants were transferred to leak-proof 10 L pots, which were filled to 3.9 kg with sifted soil (CL ED73, Einheitserde, Germany) and watered to achieve field capacity at an equal weight of 8.6 kg. Pots were covered with plastic foil to avoid evaporation of water from the soil. Five additional plants of RP were planted in pots left uncovered to observe combined water loss through transpiration and evaporation. Additionally, in two pots a stick was placed instead of a plant to monitor potential soil evaporation despite covering. After the start of the experiment, plants were not watered again. Every three to four days, plant height, developmental stage and plant weight was monitored throughout the whole experiment. Based on the weight loss, volumetric SWC was calculated (based on a volume of 8 L, weight of the dried soil was 1740 g). Seven weeks after the start of the experiment, plants stopped growing and did not consume any additional water. At that time point, above-ground biomass was harvested, weighed and dried at 60 °C. After two weeks of drying, biomass dry weight was determined. WUE_{plant} was calculated by dividing the dry weight of the aboveground biomass by the consumed water.

In the period between 16 and 34 days after beginning of the experiment, gas exchange of six replicates was tracked by LI-6800 (LI-COR Inc., USA) measurements. Measurements were performed on the youngest fully developed leaf as described in chapter 2.3.1, with a leaf temperature of 25 °C, light intensity of 1500 µmol $m^{-2}s^{-1}$, RH of 50% and ambient CO_2 concentration of 400 ppm. Gas exchange was measured on day 16 and every one to two days in the period of 22 to 34 days after beginning of the experiment.

2.7 Assessment of growth- and yield-related traits

Specific leaf area

Specific leaf area (SLA) was determined on growth chamber- and field-grown plants on the leaves, on which gas exchange measurements were performed. For this, a leaf piece of approximately 3 cm length was cut at the position, where the leaf cuvette had been clipped. Area was determined based on measurement of length and width of the leaf piece. The sample was dried at 60 °C and dry weight was determined. SLA was calculated as leaf area divided by dry weight.

Thousand kernel weight of greenhouse-grown plants

Thousand kernel weight (TKW) of greenhouse-grown plants was determined on individual plants with cobs carrying a minimum of 30 kernels. For Experiments 2.4 and 2.6, a subsample of 50 kernels (or if kernel numbers were below 50, all kernels) of the cob was weighed. For Experiment 2.5, subsamples of 20 kernels were weighed. The weight of 1000 kernels was calculated from the weight of the subsample.

Growth- and yield-related traits of field-grown plants

In the field trials 2019 and 2020, SPAD (Single photon avalanche diode) values and final plant height were measured in the control field and in the rain-out shelter. Final plant height was measured on three plants per plot as height from soil to the base of the flag leaf. SPAD values were measured as a proxy for chlorophyll content using the chlorophyll meter SPAD 502 (Konica Minolta, Japan) on the youngest developed leaf at developmental stages V6, V9 and the cobleaf at stage R1 on three plants per plot. In all field trials, kernel numbers per plant were determined by dividing the total number of kernels produced by a plot by the number of plants in the plot. Thousand kernel weight was assessed by weighing four subsamples of 100 kernels per plot and multiplying the mean by 10.

2.8 Data analysis

Data analysis and visualization was performed in R Studio (RStudio Team, 2021). Values, which deviated more than three interquartile ranges from the first and third quartile were regarded as extreme outliers and excluded from the dataset. Analyses of variance (ANOVA) were performed using the function anova (R Core Team, 2019) to test for treatment effects in addition to the genotype effect. For significance testing between genotypes within a treatment, a Dunnett's test was used (R package "DescTools ", Signorell et mult. al., 2020), when comparing NILs to the common reference genotype RP. For comparison between all genotypes, two-sided Student's t-tests were conducted using the function pairwise.t.test with multiple testing correction by the method "holm" (R Core Team, 2019). For data obtained in field trials, means were adjusted for the block effect of the experimental design using the R package "emmeans" (Lenth, 2022) and subsequently significance testing was done by a Dunnett's test for comparison to the common reference RP or by a Tukey test for comparisons among all genotypes. Analogously to adjustment of means for the block effect, means of

stomatal density were adjusted for the effect of the developmental stage using the R package “emmeans” and significance testing was done as described for the field data. Correlations were calculated using the function lm (R Core Team, 2019). Smoothed conditional means of stomatal conductance per genotype in response to decreasing soil water content were obtained using the function geom_smooth in the package “ggplot2” (Wickham, 2016). Data was visualized using the R package “ggplot2”.

3 Results

3.1 Genetic variation in dry matter $\delta^{13}C$ and photosynthetic $\Delta^{13}C$

3.1.1 $\delta^{13}C$ of leaves and kernels

Five near isogenic maize lines that were derived from introgression lines used for $\delta^{13}C_{Kernel}$ mapping by Gresset et al. (2014), were preselected for investigation of genotypic differences in $\delta^{13}C_{Kernel}$. Data for $\delta^{13}C_{Kernel}$ was available for these lines grown under well-watered and semi-controlled drought conditions in field trials in 2016 (Table 3.1), described by Avramova et al. (2019). In the field trial 2016, increased $\delta^{13}C_{Kernel}$ was observed in lines NIL B (Table 3.1; Avramova et al., 2019) and NIL C and decreased $\delta^{13}C_{Kernel}$ in NIL W, NIL X and NIL Y (Table 3.1). In the present study, these lines were grown in the greenhouse and also analyzed for $\delta^{13}C$ of the leaf beneath the uppermost ear during flowering. Based on this $\delta^{13}C_{Leaf}$ and the previous $\delta^{13}C_{Kernel}$ analyses under field conditions, two genotypes were selected in addition to RP for in depth analyses of the connection between dry matter $\delta^{13}C$, photosynthetic $\Delta^{13}C$ and gas exchange.

Table 3.1: Carbon isotopic composition of kernels ($\delta^{13}C_{Kernel}$) of five near isogenic lines (NILs) and recurrent parent RP, grown in the field 2016 under well-watered and water-limited conditions. For description of the experiment and statistical analysis, see Avramova et al. (2019). The control treatment comprised two replications, the drought treatment three replications. RP was included as a duplicate entry, the other genotypes as single entries. Listed are means ± SE. Significant differences compared to RP are indicated as *:p<0.05, **:p<0.01, ***:p<0.001. ns, not significant. Values for RP and NIL B given in Avramova et al. (2019).

Genotype	$\delta^{13}C_{Kernel}$ [‰], well-watered	$\delta^{13}C_{Kernel}$ [‰], water-limited
RP	-12.92 ± 0.06	-13.43 ± 0.07
NIL B	-12.66 ± 0.08**	-13.25 ± 0.10 ns
NIL C	-12.63	-13.41 ± 0.10 ns
NIL W	-13.12 ± 0.08*	-13.52 ± 0.10 ns
NIL X	-13.16	-13.57 ± 0.10 ns
NIL Y	-13.42 ± 0.08***	-13.75 ± 0.10*

In the greenhouse experiment, NIL B was the only line differing significantly from RP in $\delta^{13}C_{Leaf}$ (Figure 3.1). $\delta^{13}C_{Leaf}$ of NIL B was 0.18‰ higher than $\delta^{13}C_{Leaf}$ of RP, which is consistent with the difference of 0.26‰ higher $\delta^{13}C_{Kernel}$ in NIL B under well-watered conditions in the field

2016 (Table 3.1; Avramova et al., 2019). The observation of increased $\delta^{13}C$ of NIL B compared to RP is in line with the localization of a QTL increasing $\delta^{13}C_{Kernel}$ within the chromosome 7 introgression of NIL B that was identified by Gresset et al. (2014). NIL Y showed the most pronounced difference in $\delta^{13}C_{Kernel}$ in the field in 2016 and was the only line of the five NILs differing significantly from RP under drought conditions (Table 3.1). $\delta^{13}C_{Kernel}$ in the field was 0.50‰ and 0.32‰ lower in NIL Y than in RP under well-watered and water limited conditions, respectively. NIL Y followed a similar trend in $\delta^{13}C_{Leaf}$ in the greenhouse as in $\delta^{13}C_{Kernel}$ in the field (Figure 3.1). The decrease in $\delta^{13}C_{Leaf}$ in the greenhouse in NIL Y compared to RP was 0.11‰ and just below the significance threshold (p=0.067). The other three lines, NIL C, NIL W and NIL X, did not differ from RP for $\delta^{13}C_{Leaf}$. NIL B and NIL Y were thus selected for subsequent experiments based on the differences in $\delta^{13}C$ compared to RP, which go in opposite directions. The analyses of $\delta^{13}C_{Kernel}$ under control and drought conditions in the field and $\delta^{13}C_{Leaf}$ under control conditions in the greenhouse indicated that differences in $\delta^{13}C$ of these lines in comparison to RP might be stably expressed, with stronger differences for $\delta^{13}C_{Leaf}$ in NIL B and for $\delta^{13}C_{Kernel}$ in NIL Y.

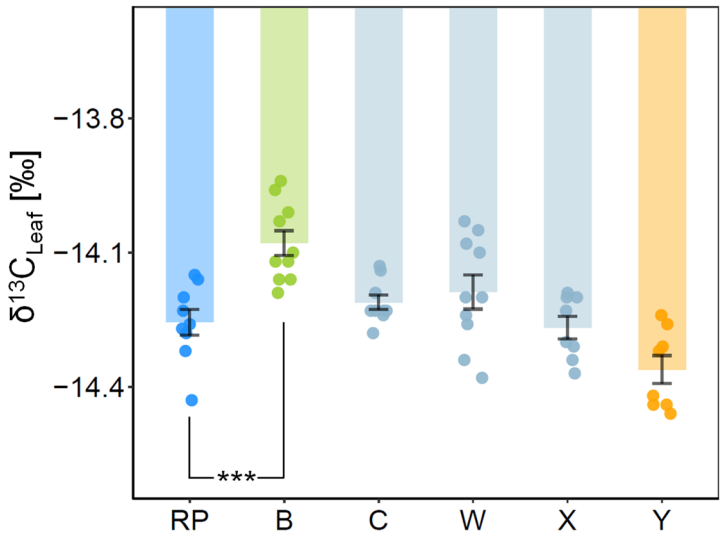

Figure 3.1: Carbon isotopic composition of the leaf below the uppermost ear of greenhouse-grown near isogenic lines NIL B, NIL C, NIL W, NIL X and NIL Y and recurrent parent RP.
Bars show means ± SE, n=8-10. Significant differences compared to RP based on a Dunnett's test are indicated as ***:p<0.001.

Building on the differences in $\delta^{13}C$ of NIL B and NIL Y compared to RP, $\delta^{13}C$ of leaves and kernels of these lines were assessed in multiple experiments. These analyses served to uncover, whether the differentiation in $\delta^{13}C_{Kernel}$ originates in the leaves, which is the prerequisite for a connection to gas exchange and WUE_{plant}. Additionally, the environmental stability of the $\delta^{13}C_{Kernel}$ and $\delta^{13}C_{Leaf}$ differences was tested by these analyses.

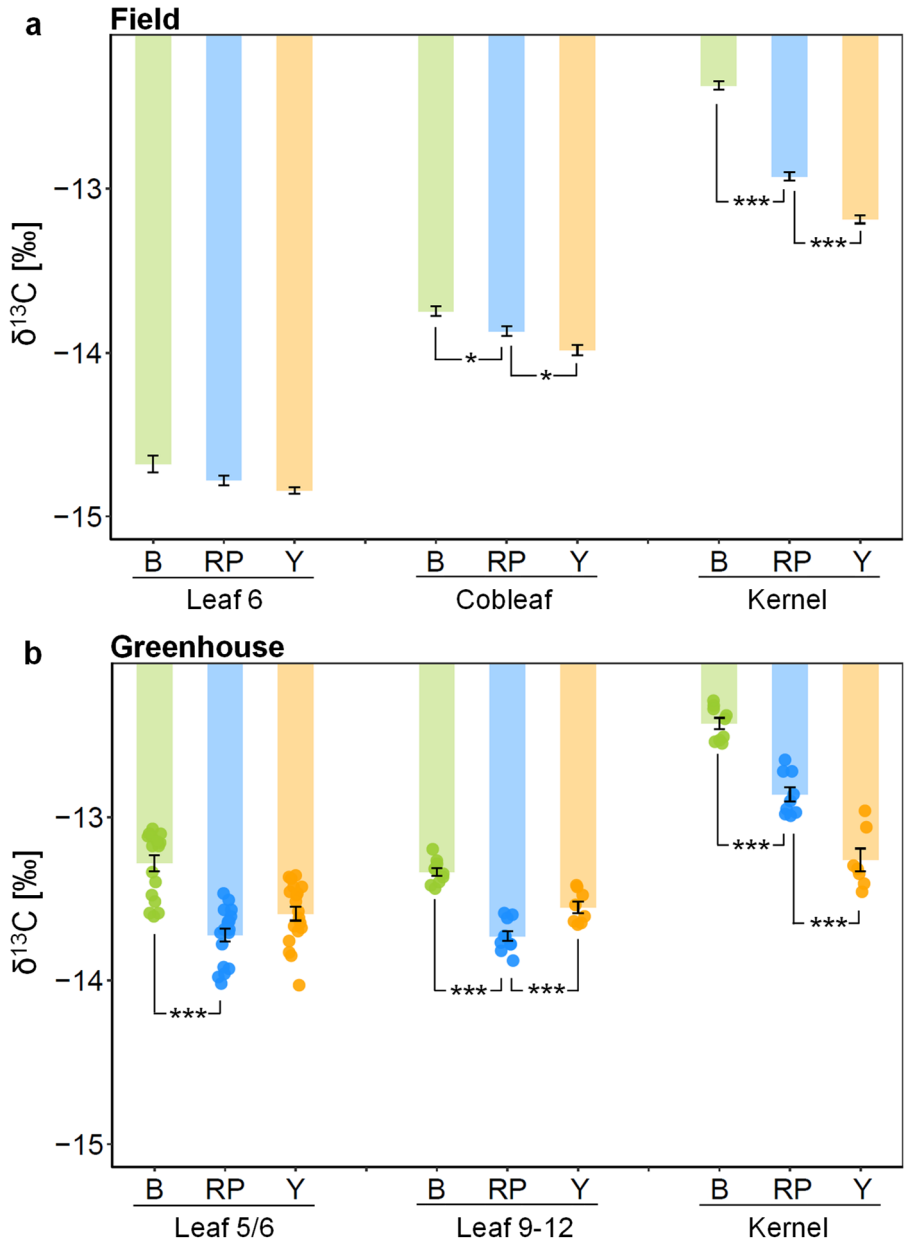

Figure 3.2: Carbon isotopic composition ($\delta^{13}C$) of leaves and kernels of the near isogenic lines NIL B, NIL Y and recurrent parent RP grown under a) field or b) greenhouse conditions.
Leaves 5/6 and 9-12 were sampled as the youngest fully developed leaf at the respective developmental stage. Cobleaf refers to the leaf below the uppermost ear. For a) n=6, leaf 6 data from 2021, cobleaf data from 2020, kernel data from 2019. For b) leaf 5/6 data from Exp. 2.3 (n=17-19), leaf 9-12 and kernel data from Exp. 2.4 (n=8-10 and 7-9, respectively). Bars show means ± SE, for b) individual values are shown by round symbols. Significant differences compared to RP based on a Dunnett's test are indicated as *:p<0.05, ***:p<0.001. Data partially published in Blankenagel et al. (2022).

Significantly higher $\delta^{13}C_{Kernel}$ of NIL B and lower $\delta^{13}C_{Kernel}$ of NIL Y compared to their RP were consistently found across years under well-watered conditions in the field (Figure 3.2a, Table S3, Figure 3.9, Avramova et al., 2019; Blankenagel et al., 2022). NIL B additionally showed consistently higher $\delta^{13}C_{Kernel}$ than RP in the greenhouse as well as higher $\delta^{13}C_{Leaf}$ in most greenhouse and field experiments (Figure 3.2, Table S4, Blankenagel et al., 2022). While under field conditions, differences between NIL B and RP in $\delta^{13}C_{Leaf}$ were often small or not

significant, in the greenhouse they were more pronounced. Under greenhouse conditions, $\delta^{13}C$ of NIL B was approximately 0.4‰ more positive than of RP in all sampled tissues, leaf 5/6, leaves 9-12 and kernels, suggesting a connection between differences in $\delta^{13}C$ of leaves and of kernels between these lines.

For NIL Y, the decrease in $\delta^{13}C_{Kernel}$ compared to RP was similarly pronounced in a greenhouse experiment as it was in the field the same year, with a difference of 0.4‰ (Figure 3.2). The $\delta^{13}C_{Kernel}$ difference was however less consistent in greenhouse-grown NIL Y plants than it was in the field, with a significant but less pronounced (0.18‰) difference in a second greenhouse experiment (Figure 3.19) and no difference in a third experiment (Table S4). Leaves of greenhouse-grown NIL Y plants, including those differing in $\delta^{13}C_{Kernel}$, showed no $\delta^{13}C$ decrease (or in some cases even an increase) compared to RP (Figure 3.2). Only the cobleaf of NIL Y sampled in the field had significantly lower $\delta^{13}C$ values compared to RP.

For all genotypes and experiments, kernels had higher $\delta^{13}C$ than leaves (Figure 3.2, Figure 3.9, Table S4).

Overall, consistently higher $\delta^{13}C$ of leaves and kernels of NIL B compared to RP suggest that the $\delta^{13}C_{Kernel}$ difference originates in leaves in NIL B and is stable across environments. While $\delta^{13}C_{Kernel}$ of NIL Y was consistently lower compared to RP in the field, patterns for $\delta^{13}C_{Leaf}$ of this line were variable and demonstrated an environmental dependence. This suggests that different mechanisms are involved in causing the $\delta^{13}C_{Kernel}$ difference in comparison to RP in NIL B and in NIL Y.

3.1.2 Photosynthetic $\Delta^{13}C$ and the ratio of intercellular to ambient CO_2 concentration (C_i/C_a)

The $\delta^{13}C$ of plant dry matter can be used to quantify dry matter $\Delta^{13}C$ ($\Delta^{13}C_{Leaf}$, $\Delta^{13}C_{Kernel}$) using Equation (4). The equation accounts for the difference between $\delta^{13}C$ of plant dry matter and $\delta^{13}C$ of air, with more negative plant $\delta^{13}C$ values yielding higher $\Delta^{13}C$. Differences in $\Delta^{13}C$ of plant dry matter can be an indication for differences in $\Delta^{13}C$ during photosynthesis ($\Delta^{13}C_{Photosynthetic}$). To connect $\delta^{13}C$ of the maize lines with measures of gas exchange assessed at stage V5/6, $\Delta^{13}C_{Leaf}$ was calculated from $\delta^{13}C$ of leaf 5/6. Based on the $\delta^{13}C$ of leaf 5/6 in the greenhouse-grown plants (Figure 3.2b, Exp. 2.3) and assuming $\delta^{13}C$ of air being -8‰, NIL B has significantly lower $\Delta^{13}C_{Leaf}$ than RP with a mean value of 5.36‰ compared to 5.80‰. Since NIL Y did not differ significantly in $\delta^{13}C$ of leaves 5/6, there was also no significant difference in the $\Delta^{13}C$ derived from the leaf dry matter.

While $\Delta^{13}C_{Leaf}$ provides a time-integrated approximation for differences in $\Delta^{13}C_{Photosynthetic}$, values can deviate not only due to time integration, but also due to post-photosynthetic fractionations (Badeck et al. 2005). $\Delta^{13}C_{Photosynthetic}$ was thus measured directly and concurrently with gas exchange on the three genotypes on the last developed leaf at stage V5/6 of growth chamber-grown plants. Measurements were based on the change in $\delta^{13}C$ of the air entering and exiting the leaf during photosynthetic gas exchange by combined IRGA and IRMS measurements. A light intensity of 1500 µmol $m^{-2}s^{-1}$ and a relative humidity (RH) of 60% were used as standard measurement conditions in the leaf cuvette. Under these conditions, $\Delta^{13}C_{Photosynthetic}$ of all lines was in the range of 3-5‰ and thus lower than the $\delta^{13}C_{Leaf}$-derived values (Figure 3.3). Measurements were performed in two experiments (Exp. 1.1 and 1.2) and in both, $\Delta^{13}C_{Photosynthetic}$ of NIL B was significantly lower than that of RP, differing by almost 1‰ (0.85 and 0.99‰, Figure 3.3b,d). This compares to a difference in $\Delta^{13}C_{Leaf}$ of 0.44‰. NIL Y and RP did not differ significantly from each other in $\Delta^{13}C_{Photosynthetic}$ (Figure 3.3).

Simultaneously to $\Delta^{13}C_{Photosynthetic}$, the ratio of the intercellular to ambient CO_2 concentration (C_i/C_a) was assessed as one potential driver of $\Delta^{13}C$ variation. C_i/C_a of NIL B was significantly higher than that of RP with a mean of 0.44 compared to 0.35 in Exp. 1.2 (Figure 3.3a; Blankenagel et al., 2022). Thus, C_i/C_a was 25% higher and $\Delta^{13}C_{Photosynthetic}$ 21% lower in NIL B compared to RP. NIL Y did not differ from RP in $\Delta^{13}C_{Photosynthetic}$ or C_i/C_a. Based on the simultaneously obtained values of $\Delta^{13}C_{Photosynthetic}$ and C_i/C_a, leakiness, the extent of leakage of CO_2 from bundle sheath back into mesophyll cells, was calculated (Equation 3). Under standard measurement conditions in Exp. 1.2, mean values of leakiness of 0.27 for NIL B, 0.32 for RP and 0.34 for NIL Y were obtained (Figure 3.3b, Table S5), predicting a negative relationship between C_i/C_a and $\Delta^{13}C_{Photosynthetic}$ (Farquhar, 1983). With significantly lower leakiness in NIL B compared to RP and NIL Y, the slope of the relationship between C_i/C_a and $\Delta^{13}C_{Photosynthetic}$ is steeper in NIL B (Figure 3.3). Exp. 1.1 confirmed the results of Exp. 1.2: Higher C_i/C_a, lower $\Delta^{13}C_{Photosynthetic}$ and lower leakiness were found in NIL B compared to RP, whereas NIL Y did not differ from RP in these parameters (Figure 3.3d). Values of $\Delta^{13}C_{Photosynthetic}$ and leakiness were overall higher in Exp. 1.1 compared to Exp. 1.2, with mean leakiness of 0.30 in NIL B, 0.38 in RP and 0.39 in NIL Y.

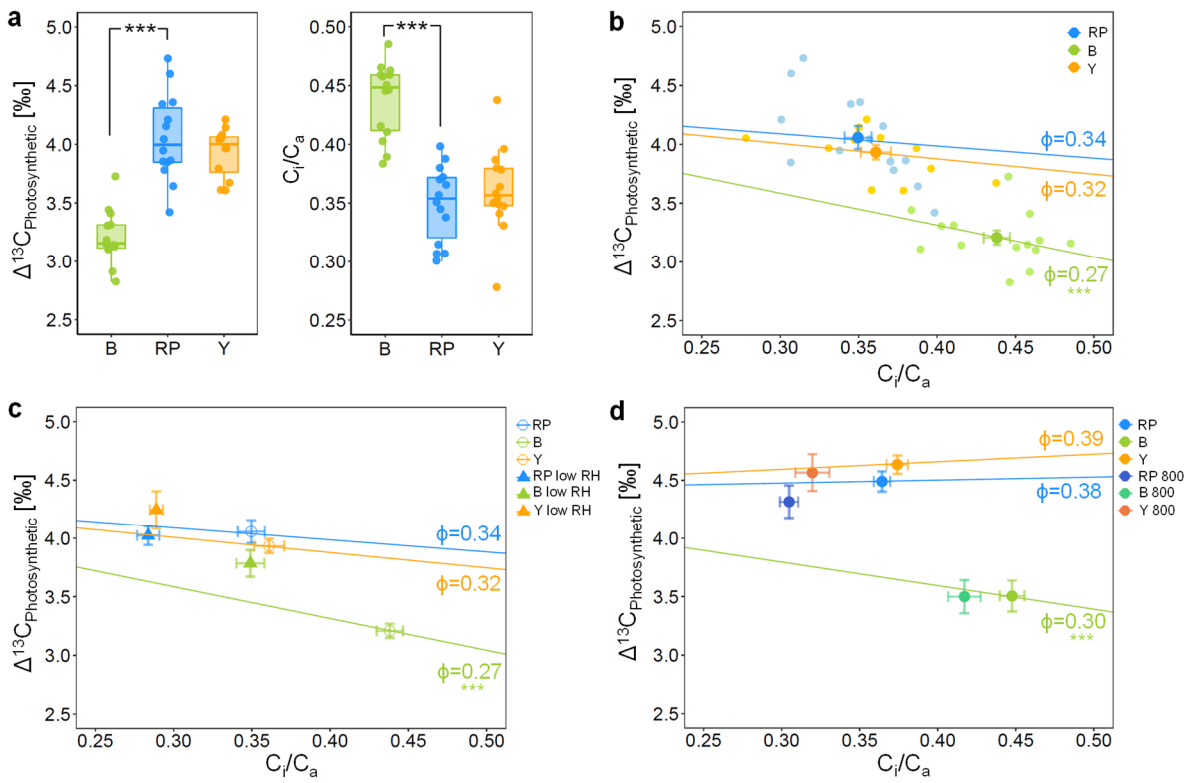

Figure 3.3: Relationship between photosynthetic carbon isotope discrimination ($\Delta^{13}C_{Photosynthetic}$) and the ratio of the intercellular to ambient CO_2 concentration (C_i/C_a) measured concurrently in the maize near isogenic lines NIL B and NIL Y and recurrent parent RP.
$\Delta^{13}C_{Photosynthetic}$ and C_i/C_a were determined on the last developed leaf at stage V5/6 of growth-chamber grown plants. a) $\Delta^{13}C_{Photosynthetic}$ and C_i/C_a obtained at standard measurement conditions at a light intensity of 1500 µmol $m^{-2}s^{-1}$ and relative humidity (RH) of 60% in Exp. 1.2 (n=12-14). Center line of boxplot shows median. b) Individual measurements of $\Delta^{13}C_{Photosynthetic}$ plotted against the corresponding C_i/C_a. Larger symbols show means ± SE. Mean leakiness (φ) per genotype calculated with the simplified $\Delta^{13}C$ model (Equation 3) is indicated. Colored lines show the predicted relationship of $\Delta^{13}C_{Photosynthetic}$ and C_i/C_a based on the respective φ. c) Triangles show means of measurements of $\Delta^{13}C_{Photosynthetic}$ vs. C_i/C_a at a RH of 35% in the leaf cuvette (n=9-10), open circles show measurements at standard conditions in Exp.1.2. φ is shown for standard conditions. d) Means of measurements of $\Delta^{13}C_{Photosynthetic}$ vs. C_i/C_a in Exp. 1.1 (n=12-14). Lighter colors show measurements at standard conditions, darker colors at a light intensity of 800 µmol $m^{-2}s^{-1}$ in the leaf cuvette. φ is shown for standard conditions. Error bars indicate SE. Significant differences compared to RP based on a Dunnett's test are indicated by ***: p<0.001 in a) and for φ in b-d). Data of RP and NIL B in a) are also published in Blankenagel et al. (2022).

When RH inside the leaf cuvette was reduced in Exp. 1.2, C_i/C_a significantly decreased compared to standard conditions for all genotypes (Figure 3.3c, Table S5, p<0.001). A strong decrease in C_i/C_a in NIL B was accompanied by an increase in $\Delta^{13}C_{Photosynthetic}$ at reduced RH. This supports a negative dependence of the two parameters in NIL B. Since the measurements deviate from the values predicted from the simplified $\Delta^{13}C$ model based on a leakiness value of 0.27 (Figure 3.3c), higher leakiness values were calculated for NIL B at 35% RH compared to values at 60% RH (Table S5). In RP and NIL Y, $\Delta^{13}C_{Photosynthetic}$ and leakiness at 35% RH did not differ significantly from values under standard conditions (Figure 3.3c, Table S5). The effect

of a reduction in light intensity in the leaf cuvette from 1500 µmol $m^{-2}s^{-1}$, which was used for gas exchange measurements under standard conditions, to 800 µmol $m^{-2}s^{-1}$, which is the light intensity in the growth chamber, in which the plants were grown, was tested in Exp. 1.1. The decrease in light intensity caused decreased C_i/C_a for all genotypes, but did not significantly change $\Delta^{13}C_{Photosynthetic}$ (Figure 3.3d).

Therefore, in these experiments it was shown that NIL B has consistently and significantly lower $\Delta^{13}C_{Photosynthetic}$ compared to RP, with a clear connection to higher C_i/C_a in NIL B. Additionally, lower leakiness was determined in NIL B than in RP. The results provide strong evidence that higher kernel and leaf $\delta^{13}C$ of NIL B compared to RP are caused by lower $\Delta^{13}C_{Photosynthetic}$. In NIL Y, lower $\delta^{13}C_{Kernel}$ compared to RP could not be linked to differences in $\Delta^{13}C_{Photosynthetic}$ or C_i/C_a in the on-line measurements at stage V5/6. This indicates that different factors contribute to the $\delta^{13}C_{Kernel}$ differences in NIL B and in NIL Y.

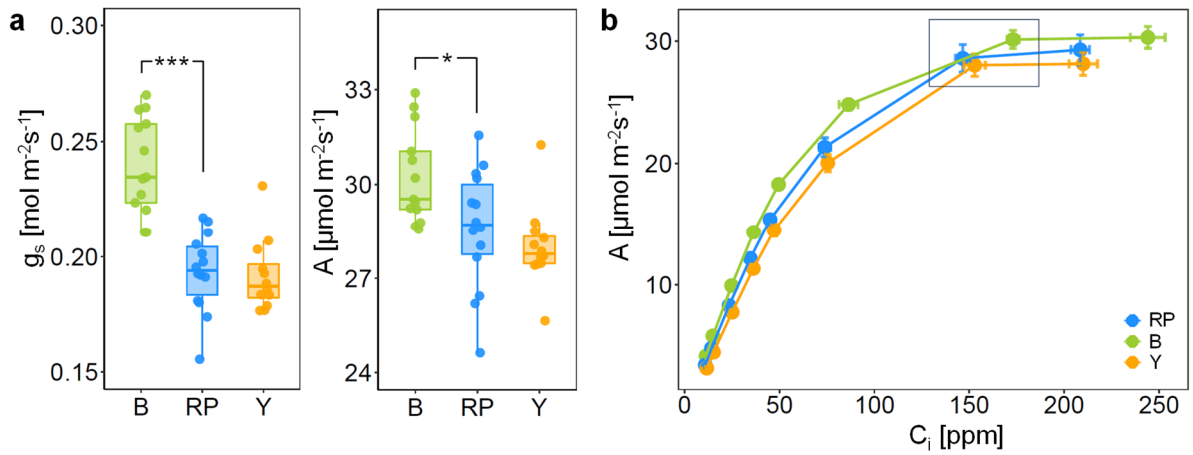

Figure 3.4: Stomatal conductance (g_s), assimilation rates (A) and intercellular CO_2 concentrations (C_i) in the maize near isogenic lines NIL B and NIL Y and recurrent parent RP at stage V5/6 grown in the growth chamber.
a) g_s and A measured at a light intensity of 1500 µmol $m^{-2}s^{-1}$ and ambient CO_2 concentration (C_a) of 400 ppm during measurements of photosynthetic carbon isotope discrimination in Exp. 1.1 (n=12-14). Center line of boxplot shows median. Significant differences compared to RP based on a Dunnett's test are marked as *: p<0.05, ***: p<0.001. b) A plotted against different values of C_i, obtained by varying C_a. Measurements were performed at a light intensity of 1500 µmol $m^{-2}s^{-1}$, measurements at a C_a of 400 ppm are framed by a grey box. Shown are means ± SE; n=5. Data of RP and NIL B in b) are published in Blankenagel et al. (2022).

Differences in C_i/C_a can result from changes in assimilation rates (A) and in stomatal conductance (g_s). Significantly higher g_s and A were identified in NIL B compared to RP at stage V5/6 in the growth chamber (Figure 3.4a). The difference in g_s was more pronounced than the difference in A, resulting in increased C_i/C_a in NIL B (Figure 3.3). NIL Y did not differ in A or g_s from RP in this experiment (Figure 3.4a).

To acquire a more complete picture of gas exchange in the three genotypes, A was measured over a range of intercellular CO_2 concentrations (C_i) that were obtained by varying the ambient CO_2 concentration C_a (Figure 3.4b). Assimilation rates of the maize lines were nearly saturated at a C_i of 150 ppm. At a C_a of 400 ppm, which is close to the atmospheric CO_2 concentration, mean C_i was 173 ppm in NIL B, 147 ppm in RP and 153 ppm in NIL Y (Figure 3.4b; Blankenagel et al., 2022). Thus, despite higher g_s and C_i, A of NIL B was only slightly increased compared to RP at 400 ppm. Contrastingly, at low C_is of 50 and 80 ppm, A was strongly dependent on C_i and higher in NIL B compared to RP. C_i of NIL Y was not different from RP at any C_a. Assimilation rates of NIL Y were slightly lower than in RP, but did not differ significantly at 400 ppm.

Since differences in gas exchange can result from differences in specific leaf area (SLA), SLA was assessed at the measured leaf sections. No differences in SLA were observed between NIL B or NIL Y in comparison to RP in either experiment. In Exp. 1.1, mean SLA were in the range of 305 to 325 $cm^2\ g^{-1}$, in Exp. 1.2 mean SLA were between 345 and 365 $cm^2\ g^{-1}$ (Table S5).

In summary, g_s was identified as the driver for higher C_i/C_a in NIL B compared to RP, that is linked to decreased $\Delta^{13}C_{Photosynthetic}$. NIL Y did not differ from RP in any gas exchange parameter in these measurements at stage V5/6 in the growth chamber. Thus, while in NIL B higher $\delta^{13}C_{Leaf}$ and $\delta^{13}C_{Kernel}$ compared to RP are connected to differences in gas exchange, in NIL Y no connection of $\delta^{13}C_{Kernel}$ and gas exchange was detected.

3.2 Genetic variation in gas exchange and water use efficiency under optimal conditions

Gas exchange measurements of growth chamber-grown plants had revealed that in NIL B the difference in $\Delta^{13}C_{Photosynthetic}$ compared to RP is linked to an increased C_i/C_a. Additionally, these measurements showed that the high C_i/C_a is caused by a higher g_s compared to RP. These genetic differences of NIL B and RP in gas exchange are thus a likely cause for the difference in dry matter $\delta^{13}C$ observed in field and greenhouse. NIL Y showed a decreased $\delta^{13}C_{Kernel}$ compared to RP in field and greenhouse and in some experiments also a decreased $\delta^{13}C_{Leaf}$. No difference in $\Delta^{13}C_{Photosynthetic}$ or other gas exchange parameters were found between NIL Y and RP in the growth chamber experiments (Figures 3.3-3.4). Since gas exchange can be influenced by growth conditions and plant development, A and g_s were analyzed in additional experiments at different developmental stages in the greenhouse as well as in the field. These analyses served to test whether the differences between RP and NIL B are expressed stably and whether there are differences in gas exchange characteristics of NIL Y linked to the

$\delta^{13}C_{Kernel}$ difference that were not caught in the short-term measurements in the growth chamber. To describe the ratio of A to g_s, iWUE is used in this chapter as a parameter that can be easily linked to WUE_{plant}. The increased C_i/C_a detected for NIL B compared to RP is equivalent to a low iWUE ($iWUE = C_a (1 - C_i/C_a) / 1.6$; Yang et al., 2016).

3.2.1 Gas exchange and related traits under greenhouse conditions

Gas exchange of the three maize lines was analyzed in the greenhouse at developmental stage V5/6 and in a separate experiment at V7-9. Similar to the measurements in the growth chamber, NIL B had consistently higher g_s than RP at both developmental stages (Figure 3.5a). At V5/6, mean g_s of NIL B was 0.28 mol $m^{-2}s^{-1}$ compared to a g_s of RP of 0.22 mol $m^{-2}s^{-1}$, at stage V7-9 g_s was on average 0.29 mol $m^{-2}s^{-1}$ in NIL B and 0.24 mol $m^{-2}s^{-1}$ in RP (Figure 3.5; Avramova et al., 2019; Blankenagel et al., 2022). Assimilation rate was slightly increased in NIL B compared to RP, but the difference was less pronounced than the difference in g_s and not significant for the later developmental stage. Accordingly, iWUE was significantly lower in NIL B than RP at both developmental stages with mean values of 125-130 µmol CO_2 / mol H_2O in NIL B and approximately 150 µmol CO_2 / mol H_2O in RP.

NIL Y had significantly lower g_s than RP at stage V5/6 in the greenhouse (Figure 3.5a). The difference of 0.03 mol $m^{-2}s^{-1}$ was smaller than the difference in NIL B. Since NIL Y also showed a pronounced decrease in A compared to RP, iWUE was not significantly altered (Figure 3.5b,d). At stage V7-9, there were no differences in gas exchange between RP and NIL Y.

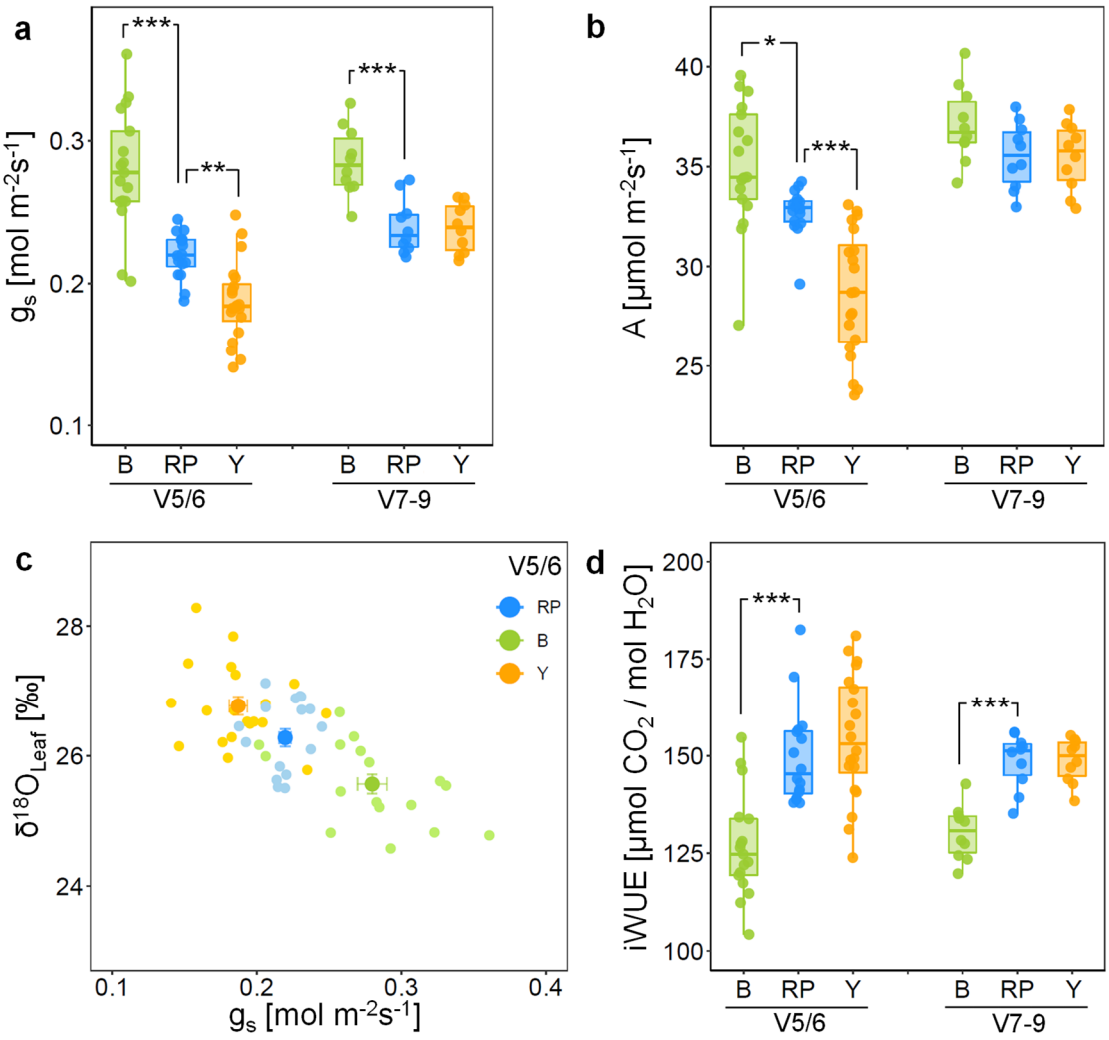

Figure 3.5: Gas exchange and oxygen isotopic composition ($\delta^{18}O$) of the near isogenic lines NIL B and NIL Y and recurrent parent RP under greenhouse conditions at developmental stage V5/6 and V7-9.
Gas exchange was measured on the last fully developed leaf at a light intensity in the leaf cuvette of 1500 µmol $m^{-2}s^{-1}$. Data for V5/6 from Exp. 2.3 (n=16-20), data for V7-9 from Exp. 2.2 (n=10). a) Stomatal conductance (g_s), b) assimilation rate (A), c) $\delta^{18}O$ of leaves ($\delta^{18}O_{Leaf}$) plotted against g_s measured on the same leaf, and d) intrinsic water use efficiency (iWUE). Larger symbols in c) indicate means ± SE, smaller symbols show individual measurements. In a), b) and d) significant differences compared to RP based on a Dunnett's test are indicated as *: p<0.05, **: p<0.01, ***: p<0.001. Center line of boxplot shows median. Gas exchange data for RP and NIL B in V5/6 published in Blankenagel et al. (2022) and for V7-9 in Avramova et al. (2019).

Subsequent to the gas exchange measurements in the greenhouse at V5/6, additional photosynthesis- and stomata-related traits were analyzed on the measured leaves after harvest. These included activities of the carbon fixing enzymes, chlorophyll content, stomatal density and oxygen isotopic composition ($\delta^{18}O$) of the leaves.

No significant differences were found neither for PEPC or Rubisco activity nor chlorophyll content of the leaves between the three genotypes (Table 3.2; Blankenagel et al., 2022). Stomatal density was by tendency higher in NIL B compared to RP (p=0.091, Table 3.2) and

did not differ between RP and NIL Y. As an additional trait linked to g_s, the $\delta^{18}O$ of bulk leaf material ($\delta^{18}O_{Leaf}$) was determined. During evaporation of water, including transpiration, the remaining liquid water is enriched in ^{18}O relative to ^{16}O (Barbour et al. 2000). Leaf temperature and transpiration rates are two of the main factors that influence the oxygen isotopic enrichment and thus $\delta^{18}O$ of leaf water, which is reflected in $\delta^{18}O$ of bulk leaf material. Plant $\delta^{18}O$ has thus been proposed as an integrative measure for transpiration rates. Values for $\delta^{18}O_{Leaf}$ of the maize lines were mainly in the range of 25-28‰ (Figure 3.5c); $\delta^{18}O$ of the irrigation water was -10‰. A negative relationship between $\delta^{18}O_{Leaf}$ and g_s measured on the same leaves was found, with a significantly lower $\delta^{18}O_{Leaf}$ in NIL B compared to RP ($p<0.01$) and significantly higher $\delta^{18}O_{Leaf}$ in NIL Y compared to RP ($p<0.05$). This could indicate that the higher g_s in NIL B and lower g_s in NIL Y detected in the short-term gas exchange measurements at stage V5/6 were expressed over an extended time period in this experiment.

Table 3.2: Photosynthesis-related traits of youngest fully developed leaves of RP, NIL B and NIL Y at stage V5/6 in the greenhouse (Exp. 2.3).
Enzymatic activity of PEPC, initial and total Rubisco activity (n=15-20) and chlorophyll a and b content (n=17-20) are expressed relative to the fresh weight (FW). Enzyme activities and chlorophyll content for RP and NIL B published in Blankenagel et al. 2022. For stomatal density, n=17-20. Listed are means ± SE, for stomatal density means are adjusted for the developmental stage. No significant differences were found in comparison to RP based on a Dunnett's test for any trait.

Genotype	PEPC [nmol g^{-1} FW min^{-1}]	$Rubisco_{initial}$ [nmol g^{-1} FW min^{-1}]	$Rubisco_{total}$ [nmol g^{-1} FW min^{-1}]	Chlorophyll a+b [µg mg^{-1} FW]	Stomatal density [mm^{-2}]
RP	12967 ± 623	450 ± 34	813 ±54	1.152 ± 0.034	77 ± 2
NIL B	13789 ± 738	508 ± 48	843 ± 53	1.143 ± 0.036	82 ± 2
NIL Y	13363 ± 482	449 ± 45	826 ± 75	1.133 ± 0.033	74 ± 2

NIL B and NIL Y both differed in g_s and $\delta^{13}C_{Kernel}$ from RP, but varied with respect to direction and robustness. The major introgression in NIL B has a size of 55 Mb and is located on chromosome 7, the major introgression in NIL Y has a size of 27 Mb and is located on chromosome 1. In order to examine the effect of a combination of both introgressions on $\delta^{13}C$ and gas exchange, NIL B and NIL Y were crossed to combine both of the major introgressions in NIL BY (see chapter 2.1.2). A plant in the F_2 generation, which was homozygous for the chromosome 1 and chromosome 7 introgression, was selected for propagation. All individuals of the F_3 generation of the NIL B and NIL Y cross were named NIL BY, as they all carry the chromosome 1 and 7 introgression homozygously.

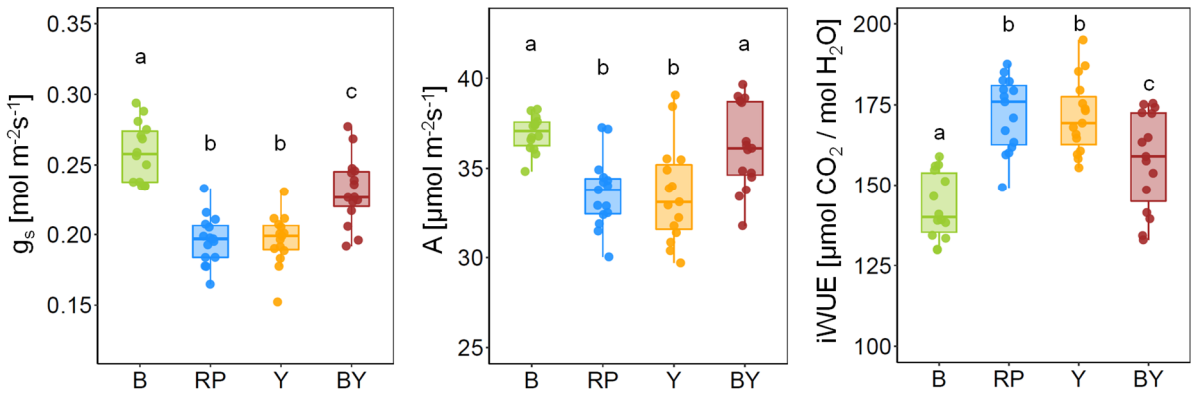

Figure 3.6: Gas exchange of near isogenic lines NIL B, NIL Y and NIL BY and recurrent parent RP in the greenhouse.
NIL B carries a 55 Mb introgression on chromosome 7 in the genetic background of RP, NIL Y carries a 27 Mb introgression on chromosome 1 and NIL BY carries both the chromosome 7 and chromosome 1 introgression. Stomatal conductance (g_s), assimilation rate (A) and intrinsic water use efficiency (iWUE) were measured on the last developed leaf at stage V5/6 (Exp. 2.5; n=14-15). Center line of boxplot shows median. Different letters indicate significant differences based on a pairwise t-test with Holm correction ($p<0.05$).

Gas exchange was analyzed in NIL BY in parallel with RP, NIL B and NIL Y. As in previous experiments, g_s and A of NIL B at stage V5/6 were significantly higher compared to RP and iWUE of NIL B was significantly lower (Figure 3.6). NIL Y did not differ from RP in this experiment in any gas exchange parameter. While NIL BY differed from RP and NIL Y in all gas exchange parameters in the same direction as NIL B, g_s and iWUE of NIL BY were also significantly different from NIL B, showing an intermediate value between NIL B and NIL Y. Differences in g_s were 0.027 mol $m^{-2}s^{-1}$ between NIL BY and NIL B and 0.035 mol $m^{-2}s^{-1}$ between NIL BY and NIL Y. Differences in iWUE were 14.2 µmol CO_2/mol H_2O between NIL BY and NIL B and 13.8 µmol CO_2/mol H_2O between NIL BY and NIL Y. Assimilation rates did not differ between NIL BY and NIL B.

Stomatal density was not different between RP, NIL B and NIL BY, whereas NIL Y had a significantly lower density compared to all other genotypes (Table S4).

$\delta^{13}C$ was determined later in the development, on the cobleaf and on the kernels (Table S4). $\delta^{13}C_{Kernel}$ was significantly higher in the genotypes carrying the chromosome 7 introgression than in RP and NIL Y. $\delta^{13}C$ of the cobleaves was also higher in NIL B and NIL BY compared to RP and NIL Y, although the difference between NIL B and NIL Y was not significant. While NIL B and NIL BY differed in iWUE in the short-term measurements at stage V5/6, these lines did not differ in $\delta^{13}C$ of cobleaves or kernels. This indicates that gas exchange did not differ between NIL B and NIL BY for a sufficiently long time period to influence $\delta^{13}C$. RP and NIL Y did not differ from each other in $\delta^{13}C$ of cobleaves or kernels. Thus, the effect of the chromosome 7 introgression of increasing $\delta^{13}C_{Leaf}$ and $\delta^{13}C_{Kernel}$ supported previous results,

yet no effect of the chromosome 1 introgression on $\delta^{13}C_{Leaf}$ or $\delta^{13}C_{Kernel}$ was observed in this greenhouse experiment.

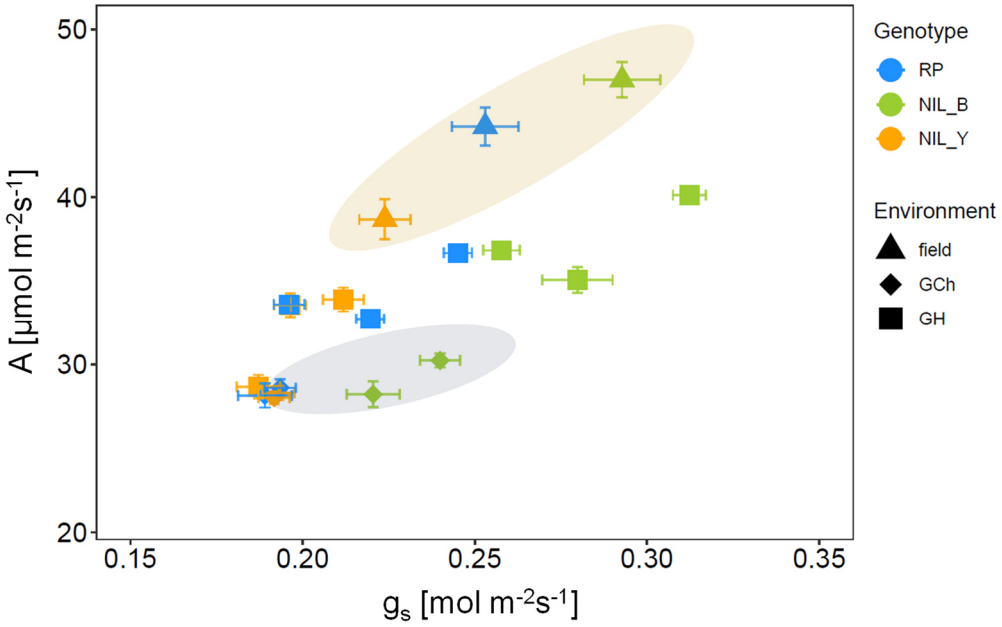

Figure 3.7: Assimilation rate (A) plotted against stomatal conductance (g_s) of the near isogenic lines NIL B and NIL Y and recurrent parent RP, measured around developmental stage V6 in different environments and experiments.
Measurements were taken at a light intensity of 1500 µmol $m^{-2}s^{-1}$ in the leaf cuvette. Data from the field 2021 shown by triangles and shaded in brown, measurements in the greenhouse (GH; Exp. 2.3, 2.4, 2.5) shown by squares and data from growth chamber experiments (GCh; Exp. 1.1, 1.2) as diamond shapes and shaded in gray. Shown are means ± SE. For values and significance of differences, see Table S6.

As described in the previous chapters, gas exchange of the NILs at stage V5/6 was analyzed in several experiments and environments. Absolute values of A, g_s and iWUE were influenced by the environment, with lowest values obtained in the growth chamber experiments, intermediate values in the greenhouse and highest values under field conditions (Figure 3.7). NIL B had consistently higher g_s and lower iWUE compared to RP in all experiments at stage V5/6, demonstrating environmental stability of the NIL B phenotype. Contrastingly, the effect of the chromosome 1 introgression of NIL Y on gas exchange and $\delta^{13}C$ varied between environments and experiments. Regarding gas exchange at stage V5/6, NIL Y did not differ from RP in the growth chamber experiments, and neither in one of the greenhouse experiments. In the two other greenhouse experiments as well as in the field experiment, g_s and A of NIL Y were reduced compared to RP (although the decrease in g_s in the field was not significant with p=0.058). Only in one experiment in the greenhouse, NIL Y showed significantly higher iWUE than RP (Table S6). These results indicate that specific

environmental conditions are required for the differences in gas exchange between NIL Y and RP to occur.

3.2.2 Gas exchange and related traits under field conditions

Since stable $\delta^{13}C_{Kernel}$ differences between the NILs and the RP were identified under field conditions and an environmental dependence of their gas exchange (and $\delta^{13}C$) was observed in growth chamber and greenhouse experiments, gas exchange was investigated under field conditions. Gas exchange and the gas exchange-related traits stomatal density, chlorophyll content and SLA, were examined in the four genotypes RP, NIL B, NIL Y and NIL BY at stage V6/7 on the last developed leaf in the field in 2021. In general, values of g_s, A, iWUE, chlorophyll content and stomatal density were higher in the field (Figure 3.8, Table 3.3) than under greenhouse conditions. Variation within each genotype for the respective traits was also increased. These results reflect the plant growth under less controlled conditions with higher light intensity in the field.

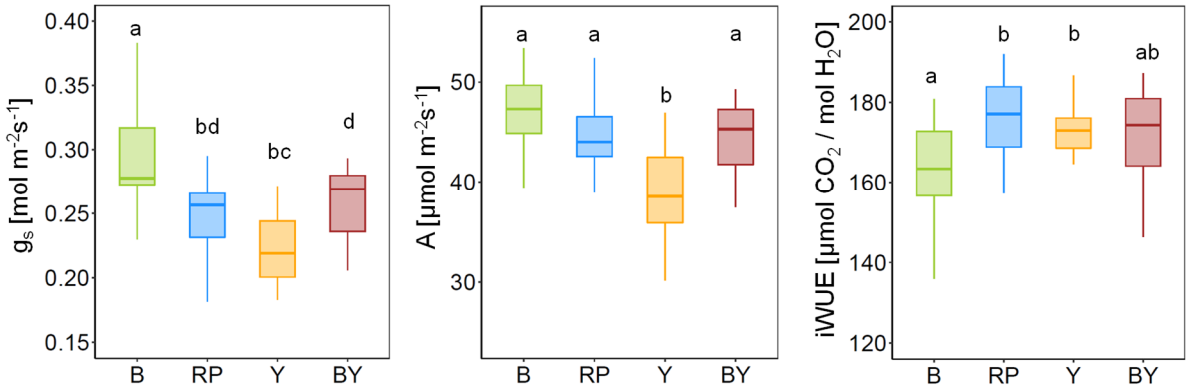

Figure 3.8: Gas exchange in the near isogenic lines NIL B, NIL Y and NIL BY and the recurrent parent (RP) at stage V6/7 grown in the field 2021.
Stomatal conductance (g_s), assimilation rate (A) and intrinsic water use efficiency (iWUE) were measured at a light intensity of 1500 µmol $m^{-2}s^{-1}$ on the last developed leaf (n=14-15). Center line of boxplot shows median. Different letters indicate significant differences based on a pairwise t-test with Holm correction ($p<0.05$).

Higher g_s and lower iWUE of NIL B compared to RP and NIL Y were detected under field conditions (Figure 3.8). In addition to the higher g_s also stomatal density was increased in NIL B compared to RP (Table 3.3). NIL Y on the other hand did not differ from RP in stomatal density, yet g_s tended to be lower ($p=0.057$; Table 3.3, Figure 3.8). Additionally, assimilation rate A, expressed on a leaf area basis, was significantly reduced in NIL Y compared to all other genotypes (Figure 3.8). Since SLA of NIL Y was significantly higher than of RP (Table 3.3), NIL Y and RP did not differ in A per leaf dry weight (1.17 ± 0.04 µmol g^{-1} DW s^{-1} in RP, 1.13 ±

0.04 µmol g^{-1} DW s^{-1} in NIL Y). Nevertheless, the chlorophyll content of NIL Y leaves, expressed on a weight basis (FW), was also significantly lower than of RP (Table 3.3). iWUE did not differ between NIL Y and RP as both A and g_s were lower in NIL Y (Figure 3.8). NIL BY showed an intermediate phenotype between NIL B and NIL Y for most traits (Figure 3.8, Table 3.3). For g_s, NIL BY differed significantly from both NIL B and NIL Y with an intermediate mean value between the two lines. Mean A and stomatal density of NIL BY were more similar to values of NIL B and differed significantly only from NIL Y. For all other parameters, NIL BY did not differ from either of the two NILs it was derived from.

Table 3.3: Gas exchange - related traits in the near isogenic lines NIL B, NIL Y and NIL BY and the recurrent parent (RP), at stage V6/7 grown in the field 2021.
Stomatal density was measured on leaf 5. Content of chlorophyll a and b per fresh weight (FW) and specific leaf area (SLA) were determined on the youngest fully expanded leaf. Listed are means ± SE (n=13-15). Different letters indicate significant differences based on a pairwise t-test with Holm correction ($p<0.05$).

Genotype	Stomatal density [mm^{-2}]	Chlorophyll content [µg mg^{-1} FW]	SLA [cm^2 g^{-1}]
RP	82 ± 3 ab	1.95 ± 0.06 a	265 ± 5 a
NIL B	94 ± 3 c	1.93 ± 0.06 a	264 ± 5 a
NIL Y	76 ± 3 a	1.71 ± 0.05 b	294 ± 6 b
NIL BY	90 ± 2 bc	1.78 ± 0.05 ab	281 ± 6 ab

Leaf 6, cobleaf and kernels of these plants were additionally analyzed for $\delta^{13}C$. While no difference was found between the four genotypes in leaf $\delta^{13}C$ at stage V6 (Figure 3.2a for RP, NIL B, NIL Y), cobleaf $\delta^{13}C$ was significantly lower in NIL Y compared to the other three genotypes (Figure 3.9a). NIL BY showed an intermediate value between NIL B and NIL Y, but differed significantly only from NIL Y.

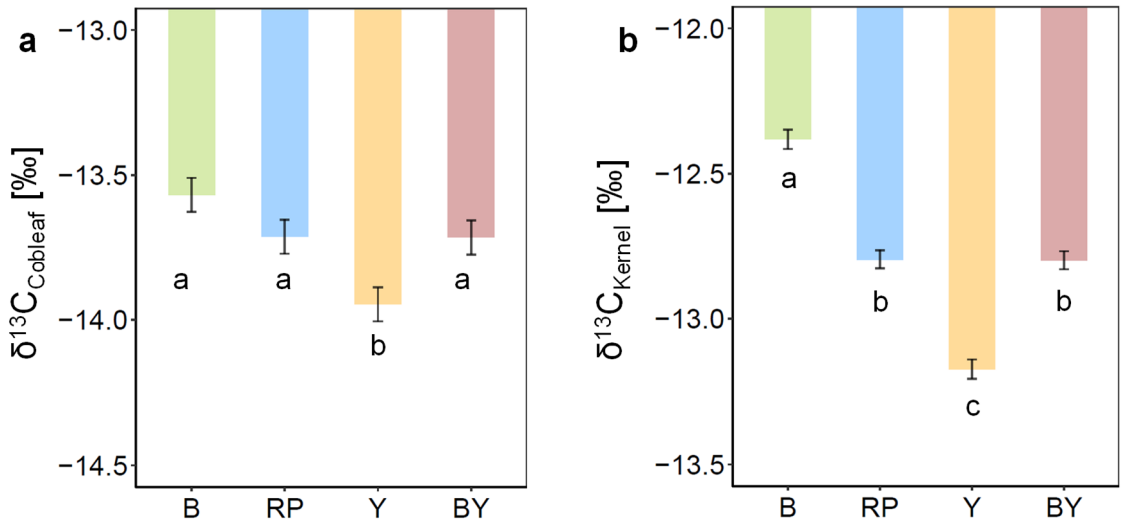

Figure 3.9: Carbon isotopic composition ($\delta^{13}C$) of a) cobleaves and b) kernels of near isogenic lines NIL B, NIL Y and NIL BY and recurrent parent RP, grown in the field in 2021.
Shown are means ± SE. n=6. Significant differences based on a Tukey test are indicated by different letters ($p<0.05$).

To test, whether differences in carbon status in the leaf closest to the ear exist around flowering, cobleaves of these plants grown in the field in 2021 were analyzed for their soluble sugars contents. Differences in sugar content may be linked to differences in A and may have an effect on $\delta^{13}C_{Kernel}$ by affecting the source of carbon used for grain filling (Condon et al., 2004; Westgate & Boyer, 1985). No differences were detected in soluble sugar contents between genotypes, aside from a higher fructose content in NIL B compared to RP (Table 3.4). In 2021, $\delta^{13}C_{Kernel}$ was significantly higher in NIL B and significantly lower in NIL Y compared to RP (Figure 3.9b), as in previous years in the field (Figure 3.2, Tables 3.1, S3). NIL BY differed from both NIL B and NIL Y by approximately 0.4‰ with an intermediate mean $\delta^{13}C_{Kernel}$ of -12.80‰, comparable to RP. These $\delta^{13}C_{Kernel}$ results suggested that under field conditions the chromosome 1 and chromosome 7 introgressions have opposite effects on $\delta^{13}C_{Kernel}$ with similar effect size and thus differences to RP cancel out. This is contrasting to the observations in the greenhouse experiment for analysis of NIL BY, where no effect of the chromosome 1 introgression on $\delta^{13}C_{Kernel}$ was found in NIL Y or NIL BY (Table S4). This discrepancy might be the result of the effect of environmental conditions in the field on gas exchange.

Table 3.4: Contents of sucrose, glucose and fructose of cobleaves of RP, NIL B, NIL Y and NIL BY grown in the field 2021.
Shown are means ± SE of six plots adjusted for the block effect of the experimental design. Significant differences based on a Tukey test are indicated by different letters ($p<0.05$).

Genotype	Sucrose [µg mg^{-1} FW]	Glucose [µg mg^{-1} FW]	Fructose [µg mg^{-1} FW]
RP	7.66 ± 0.49 a	0.28 ± 0.03 a	0.27 ± 0.04 a
NIL B	8.55 ± 0.49 a	0.32 ± 0.03 a	0.47 ± 0.04 b
NIL Y	8.10 ± 0.49 a	0.29 ± 0.03 a	0.31 ± 0.05 ab
NIL BY	9.06 ± 0.49 a	0.29 ± 0.03 a	0.34 ± 0.04 ab

Analysis of gas exchange in different greenhouse experiments and in the field demonstrated a high environmental stability of the higher g_s and lower iWUE caused by the chromosome 7 introgression in NIL B compared to RP. These results further support a causal role of higher g_s for the stably higher $\delta^{13}C_{Leaf}$ and $\delta^{13}C_{Kernel}$ of NIL B compared to RP. Despite the lack of differences in gas exchange between NIL Y and RP in the growth chamber, lower g_s and A were observed in NIL Y compared to RP in some greenhouse experiments and in the field. These environmentally dependent differences in gas exchange likely contribute to the environmentally dependent differences in $\delta^{13}C_{Leaf}$ and $\delta^{13}C_{Kernel}$ of NILY.

3.2.3 Whole plant water use efficiency

A main interest in the investigation of $\delta^{13}C$ lies in its connection to WUE_{plant}. The short-term gas exchange measurements revealed that iWUE of NIL B is significantly lower than iWUE of RP, whereas between NIL Y and RP no consistent difference was found for iWUE. Differences in iWUE that are expressed over an extended time period can cause a measurable differentiation in the amount of biomass that plants produce with a given amount of water, i.e. WUE_{plant}. To investigate, whether the lower iWUE of NIL B translates into a lower WUE_{plant} and whether over a longer time period there are differences in gas exchange of NIL Y that would affect its WUE_{plant}, a greenhouse experiment was conducted to assess WUE_{plant}.

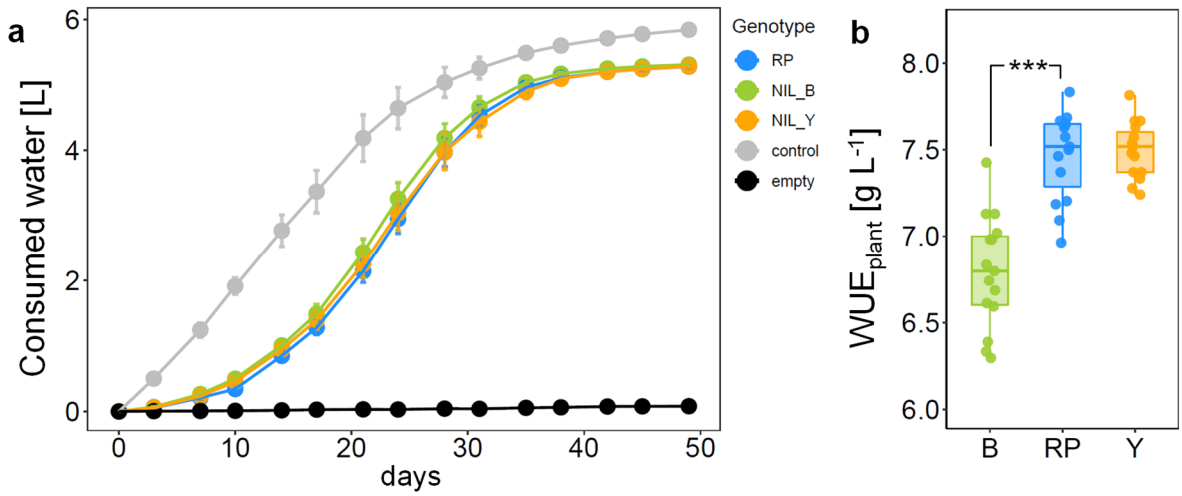

Figure 3.10: Consumed water and whole plant water use efficiency (WUE_{plant}) of near isogenic lines NIL B and NIL Y and recurrent parent RP in a greenhouse experiment.
Two-week old plants were planted in 10 L pots, watered to field capacity and covered with plastic foil on day 0. a) Consumed water was assessed gravimetrically every three to four days. Pots of "control" plants were not covered with foil, "empty" pots were covered, but contained no plant. Shown are means ± SE. b) After seven weeks, plants had stopped growing and above-ground biomass was harvested. WUE_{plant} was calculated as dry weight of above-ground biomass at the end of the experiment divided by consumed water. Center line of boxplot shows median. Significant differences compared to RP based on a Dunnett's test are indicated as ***: p<0.001. n=15 (control n=5). Data of RP and NIL B in b) also published in Blankenagel et al. (2022).

Two-week old plants of RP, NIL B and NIL Y were planted in 10 L pots, watered to field capacity and covered with plastic foil to avoid evaporation from the soil. Subsequently, plants were left to grow until they had consumed all available water. Between day 20 and day 30 after beginning of the experiment, plants consumed most water per day (Figure 3.10a). During this time, NIL B had consumed slightly more water than the other genotypes, however, differences in the amount of consumed water were not significant at any time point. After seven weeks, plants had reached developmental stages V10-15 and stopped growing. At that point, all genotypes had consumed on average 5.4 L of water and above-ground biomass was harvested. The produced biomass of NIL B was significantly less than that of RP. Thus, NIL B has lower WUE_{plant} with a mean of 6.8 g L^{-1} compared to 7.5 g L^{-1} in RP (Figure 3.10b; Blankenagel et al., 2022). NIL Y on the other hand produced a similar amount of above-ground dry biomass as RP, resulting in a WUE_{plant} of NIL Y of 7.5 g L^{-1} comparable to RP.

To make sure measurements of WUE_{plant} were not confounded by plant height, differences between RP, NIL B and NIL Y were recorded throughout the experiment. NIL Y tended to have higher height than RP throughout the experiment, but did not differ in final dry biomass (Figures S1a, 3.10b). NIL B initially tended towards higher values for height compared to RP, but this tendency was reversed towards the end of the experiment, likely due to the lower water availability for NIL B because of higher water consumption earlier in the experiment. Even

though at the beginning of the experiment all plants were in developmental stage V3, RP was between half a developmental stage and a full developmental stage further developed than the other genotypes for most of the experiment (Figure S1b). This tendency was also observed in other experiments, yet at the earlier stages at which most measurements were taken in other experiments (V5/6) developmental differences were not pronounced.

The experiment demonstrated that the low iWUE of NIL B translates to lower WUE_{plant} compared to RP. Consequently, there is a negative connection between differences in $\delta^{13}C$ and WUE_{plant} in NIL B compared to RP, which is driven by g_s and iWUE. NIL Y on the other hand did not differ from RP in WUE_{plant}, demonstrating that there are no robust differences in iWUE between NIL Y and RP over an extended time period in the greenhouse.

3.3 Genetic variation in gas exchange and $\delta^{13}C$ under water deficit

In the previous chapters, gas exchange, $\Delta^{13}C_{Photosynthetic}$ and $\delta^{13}C$ of the maize genotypes were investigated under well-watered conditions. A link between g_s, iWUE, $\Delta^{13}C_{Photosynthetic}$ and $\delta^{13}C$ was shown for differences between NIL B and RP, but these traits could not clearly be connected in NIL Y. The following experiments were conducted to analyze the effect of water deficit on the relationship between iWUE, $\Delta^{13}C_{Photosynthetic}$ and $\delta^{13}C$. The intention was to understand, how drought conditions affect the possibility of detecting iWUE differences between genotypes based on $\delta^{13}C$ and additionally to gain a better understanding on the relationship of $\Delta^{13}C_{Photosynthetic}$, $\delta^{13}C$ and iWUE by expanding the range of iWUE values.

3.3.1 Gas exchange response to progressive soil drying

Since the three maize lines RP, NIL B and NIL Y showed differences in g_s and iWUE under control conditions and in WUE_{plant}, it was analyzed whether their response to progressive soil drying differed with respect to gas exchange. Gas exchange of six plants per genotype was tracked in the experiment conducted for determining WUE_{plant}, starting 16 days after beginning of the experiment, when plants had a mean SWC of 60% (NIL B) to 64% (RP; Figure 3.11a).

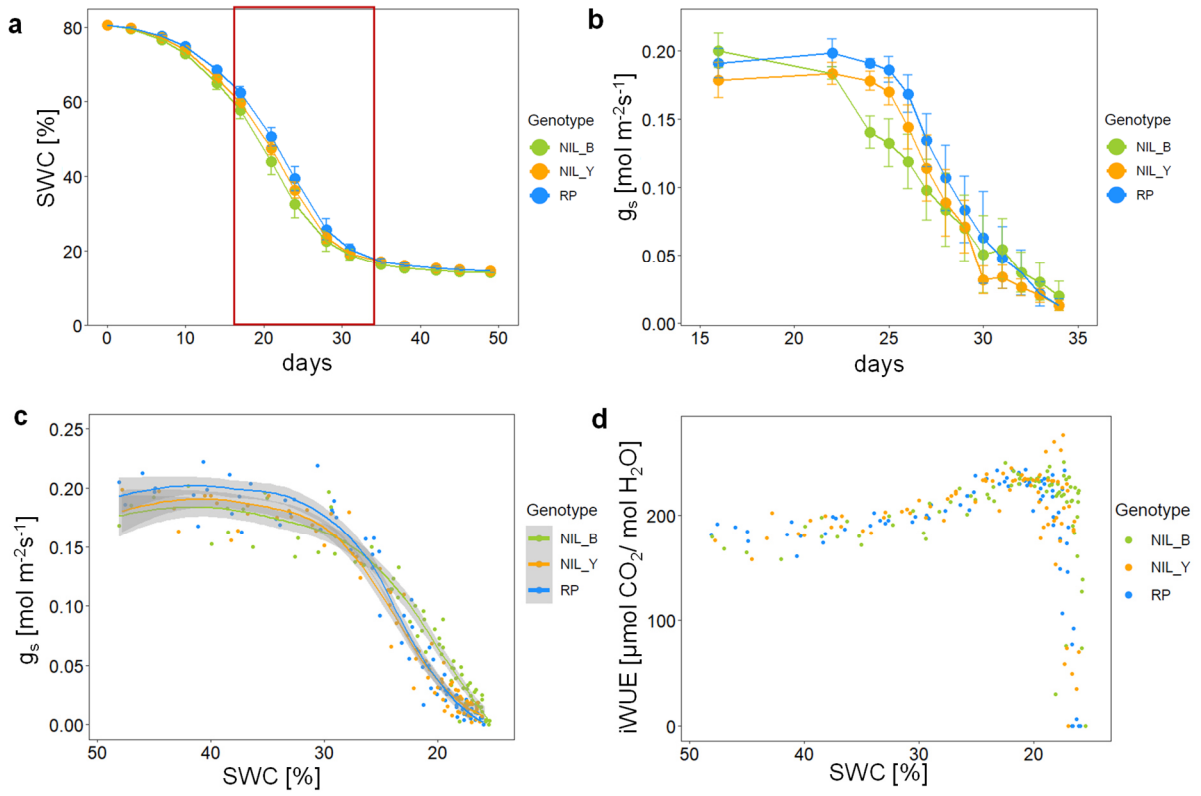

Figure 3.11: Response of near isogenic lines NIL B and NIL Y and recurrent parent RP to progressive soil drying.
a) Volumetric soil water content (SWC) throughout the experiment. At day 0, two-week-old plants were watered to field capacity, covered with foil and not watered further until the end of the experiment. Red box highlights the time period of gas exchange measurements. b) Stomatal conductance (g_s) measured between days 16 and 34 of progressive soil drying on the last developed leaf at a light intensity of 1500 µmol $m^{-2}s^{-1}$. Data in a) and b) are means ± SE. The same six plants per genotype were measured at every time point. c) Individual measurements of g_s plotted against the respective SWC of the plant. Lines show smoothed conditional means with grey area depicting the 95% confidence interval. d) Individual measurements of intrinsic water use efficiency (iWUE) plotted against the respective SWC of the plant.

Initially, all plants selected for gas exchange measurements were at stage V8 and mean g_s per genotype were 0.18-0.20 mol $m^{-2}s^{-1}$, with no significant differences between genotypes (Figure 3.11b). Starting from day 22, gas exchange was measured every one to two days until stomata were closed on day 34. In that period, g_s progressively decreased in all genotypes. The drop in g_s occurred earlier and faster in NIL B compared to RP, leading to significantly lower g_s in NIL B on days 24 and 25. Also the SWC of NIL B pots was lower in the measurement period, although not significantly, indicating that NIL B had transpired more water earlier in the experiment (Figure 3.11a). Thus, when individual measurements of g_s are plotted against the respective SWC, g_s decreases at a similar SWC of approximately 30% in all genotypes (Figure 3.11c). Stomatal conductance of NIL B was slightly lower than that of RP between 50 and 30% SWC, whereas at low SWC of 20-25% g_s was significantly higher in NIL B than in the other genotypes. The response of g_s to the decreasing SWC of NIL Y was parallel to that of RP, both relative to days and to SWC, with slightly, but not significantly, lower values in NIL Y, except

at very low SWC (Figure 3.11b,c). For all genotypes, the decrease of A was slightly delayed compared to the decrease in g_s, leading to an increase in iWUE between SWC of 40 to 20% to approximately 230-240 µmol CO_2/mol H_2O before it dropped drastically at 20-15% SWC in all genotypes (Figure 3.11d). By the end of the experiment, the measured plants reached developmental stage V10-13. In the main measurement period, between day 22 and 34, RP was slightly more advanced in development than NIL B and NIL Y.

The stomatal response to progressive soil drying indicated that NIL B experienced water limitation earlier due to its higher water consumption in young developmental stages. RP and NIL Y seem to restrict water loss through stomata more strongly at low SWC.

3.3.1 Gas exchange and photosynthetic $\Delta^{13}C$ at different soil water contents

To study the effect of water deficit on the relationship between $\Delta^{13}C_{Photosynthetic}$ and iWUE, and on genotypic differences in both traits, gas exchange and $\Delta^{13}C_{Photosynthetic}$ were analyzed in parallel under well-watered and water-limited conditions. In the previously described growth chamber experiment designed for simultaneous measurements of gas exchange and $\Delta^{13}C_{Photosynthetic}$ in RP, NIL B and NIL Y at stage V5/6 (Exp. 1.2), one set of plants received limited watering to a volumetric SWC of 30% for five to six days to induce partial stomatal closure.

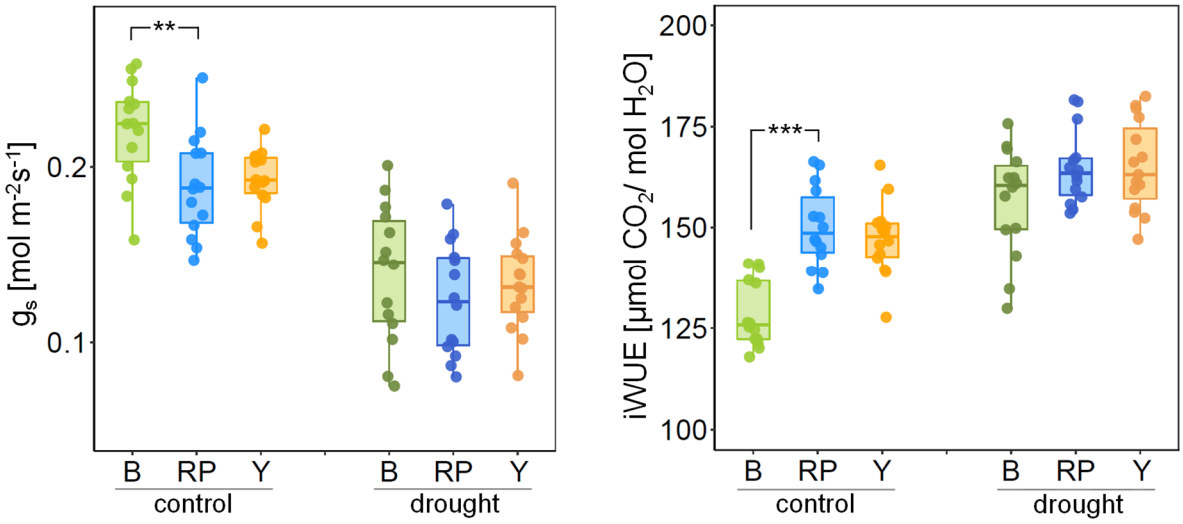

Figure 3.12: Stomatal conductance (g_s) and intrinsic water use efficiency (iWUE) of near isogenic lines NIL B and NIL Y and recurrent parent RP under control and drought conditions in a growth chamber experiment (Exp. 1.2).
Measurements were performed on the last developed leaf at stage V5/6. For control conditions, plants were watered to a volumetric soil water content (SWC) of 50%. For drought conditions, plants received limited watering to a SWC of 30% for five to six days. Center line of boxplot shows median. Significant differences compared to RP based on a Dunnett's test within each treatment are indicated as **:p<0.01, ***: p<0.001. n=13-15.

Growth under water limitation reduced g_s to approximately 0.13 mol $m^{-2}s^{-1}$ and increased iWUE by 10-20% in all genotypes (Figure 3.12). Contrary to control conditions, where NIL B had significantly higher g_s and lower iWUE than RP, no differences were detected among the three genotypes RP, NIL B and NIL Y under drought conditions in any gas exchange parameter.

For viewing the effect of water deficit on $\Delta^{13}C_{Photosynthetic}$ and leakiness, $\Delta^{13}C_{Photosynthetic}$ is plotted against C_i/C_a analogously to the visualization under control conditions. The described increase in iWUE under water limitation corresponds to a decrease in C_i/C_a (Figure 3.13).

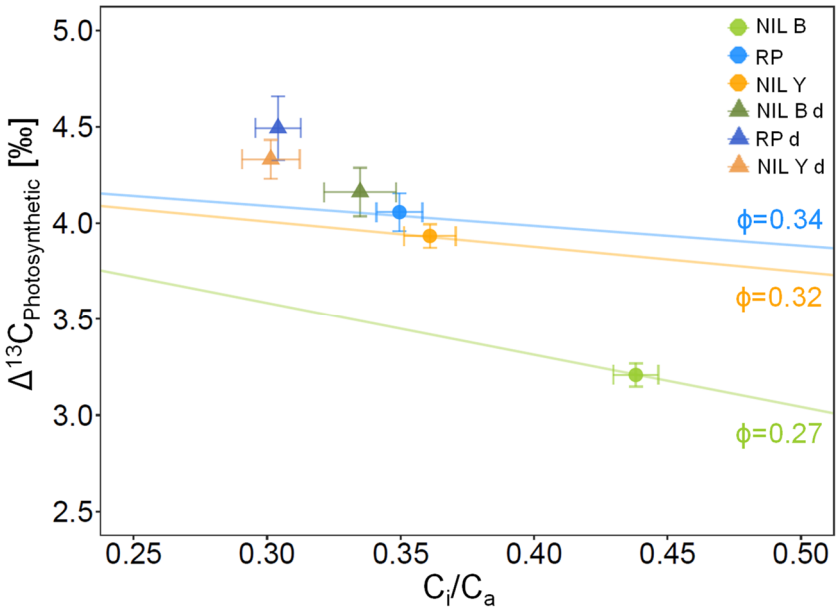

Figure 3.13: Effect of water deficit on photosynthetic carbon isotope discrimination ($\Delta^{13}C_{Photosynthetic}$) in the near isogenic lines NIL B and NIL Y and recurrent parent RP.
Means of $\Delta^{13}C_{Photosynthetic}$ plotted against means of the intercellular relative to ambient CO_2 concentration (C_i/C_a) under control (round symbols) and drought (d, triangles) conditions. Colored lines show the predicted relationship of $\Delta^{13}C_{Photosynthetic}$ and C_i/C_a from the respective leakiness (φ) based on the simplified $\Delta^{13}C$ model (von Caemmerer et al., 2014) under control conditions. Shown are means ± SE. Control plants were watered to a SWC of 50%, drought-treated plants were watered to a SWC of 30% for five to six days before measurements. n=12-15.

Simultaneous to the 15-25% decrease in C_i/C_a, water limitation led to 10-30% increased $\Delta^{13}C_{Photosynthetic}$ in all genotypes, supporting a negative relationship between the two parameters in all lines (Figure 3.13). The reduction in C_i/C_a was strongest in NIL B, which had the highest C_i/C_a under control conditions. NIL B also showed the strongest increase in $\Delta^{13}C_{Photosynthetic}$, resulting in a loss of genotypic differentiation in $\Delta^{13}C_{Photosynthetic}$ under drought. Values under drought deviated from the relationship of C_i/C_a and $\Delta^{13}C_{Photosynthetic}$ that is predicted from the leakiness determined under control conditions. This indicates an increase in leakiness under drought, assuming the model to be valid under both conditions. Under water limitations, mean

leakiness was between 0.35 and 0.39 with no significant differences between genotypes (Table S5). The experiment thus showed that a reduction in soil water availability removes differences between the genotypes in g_s, C_i/C_a, $\Delta^{13}C_{Photosynthetic}$ and leakiness, most likely due to stomatal closure.

3.3.2 Effect of drought on dry matter $\delta^{13}C$

In addition to studying the effect of water deficit on $\Delta^{13}C_{Photosynthetic}$ in young plants, the influence of stomatal closure on leaf and kernel dry matter $\delta^{13}C$ at a later developmental stage was analyzed.

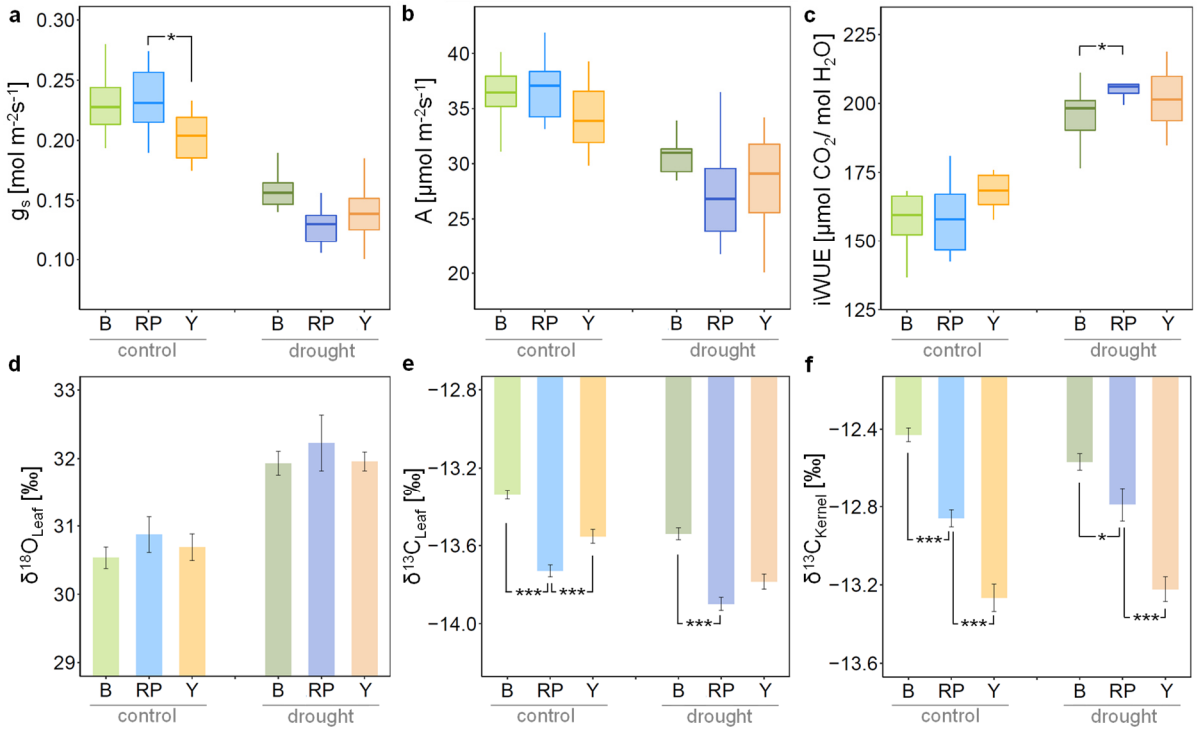

Figure 3.14: Gas exchange and stable isotopic composition of near isogenic lines NIL B and NIL Y and recurrent parent RP under control and drought conditions in a greenhouse experiment (Exp. 2.4).
Control plants were well-watered, drought plants received limited watering to a volumetric soil water content of 23% for six days before gas exchange measurements and leaf harvest. a) Stomatal conductance (g_s), b) assimilation rate (A) and c) intrinsic water use efficiency (iWUE) were measured on the last developed leaf at stage V9-12. Center line of boxplot shows median. d) Oxygen isotopic composition ($\delta^{18}O$) and e) carbon isotopic composition ($\delta^{13}C$) of bulk leaf material were determined on the measured leaves. For a)-e), n=8-10. f) $\delta^{13}C$ of kernels (n=6-10). Significant differences compared to RP based on a Dunnett's test within each treatment are indicated as *:p<0.05, ***: p<0.001.

A greenhouse experiment was conducted with RP, NIL B and NIL Y to study the effect of mild drought stress before flowering on the genotypic differences in $\delta^{13}C$ of leaves and kernels. Thus, watering was restricted to achieve a SWC of 23% for half of the plants. Six days after

the beginning of the drought treatment, gas exchange was measured on the last developed leaves of well-watered control and of drought-stressed plants and the measured leaves were harvested. At this time point, plants had reached stage V9-12 with plants of RP on average one developmental stage further developed than plants of NIL B and NIL Y. Surprisingly, no differences in gas exchange were found between RP and NIL B under control conditions (Figure 3.14a-c), whereas NIL Y had significantly lower g_s than RP. Water limitation reduced g_s of all genotypes to similar levels as in the growth chamber experiment with mean values of 0.13-0.16 mol $m^{-2}s^{-1}$. By tendency, g_s of NIL B was higher under drought than g_s of RP ($p=0.066$, Figure 3.14a). iWUE was increased in all genotypes by 20-30% by the drought treatment (Figure 3.14c). Under drought conditions, iWUE was significantly lower in NIL B than in RP and did not differ between NIL Y and RP.

As a consequence of the reduction in transpiration, $\delta^{18}O_{Leaf}$ increased under drought (Figure 3.14d, $p<0.001$). Differences between the lines in $\delta^{18}O_{Leaf}$ were observed neither under control, nor under drought conditions. As shown in chapter 3.1.1, under control conditions, $\delta^{13}C_{Leaf}$ was significantly higher in both NIL B and NIL Y compared to RP in this greenhouse experiment, with the difference between NIL B and RP being more pronounced (Figure 3.14e). $\delta^{13}C_{Kernel}$ matched the observations from the field with significantly higher values in NIL B compared to RP and significantly lower values in NIL Y (Figure 3.14f). In line with the observation of an increase in $\Delta^{13}C_{Photosynthetic}$ under water deficit in the growth chamber experiment 1.2, the drought treatment caused a significant decrease in $\delta^{13}C_{Leaf}$ values for all genotypes (Figure 3.14e, $p<0.001$). NIL B had significantly more positive $\delta^{13}C_{Leaf}$ than RP also in plants that experienced drought. Absolute values for $\delta^{13}C_{Kernel}$ were less affected by the six-day drought treatment than $\delta^{13}C_{Leaf}$ values (Figure 3.14f). The difference in $\delta^{13}C_{Kernel}$ between NIL B and RP was reduced, but still significant in the plants that were subjected to water limitation. As $\delta^{13}C_{Kernel}$ of RP and NIL Y were unaffected by the drought treatment, NIL Y showed significantly lower $\delta^{13}C_{Kernel}$ than RP also in this set of plants.

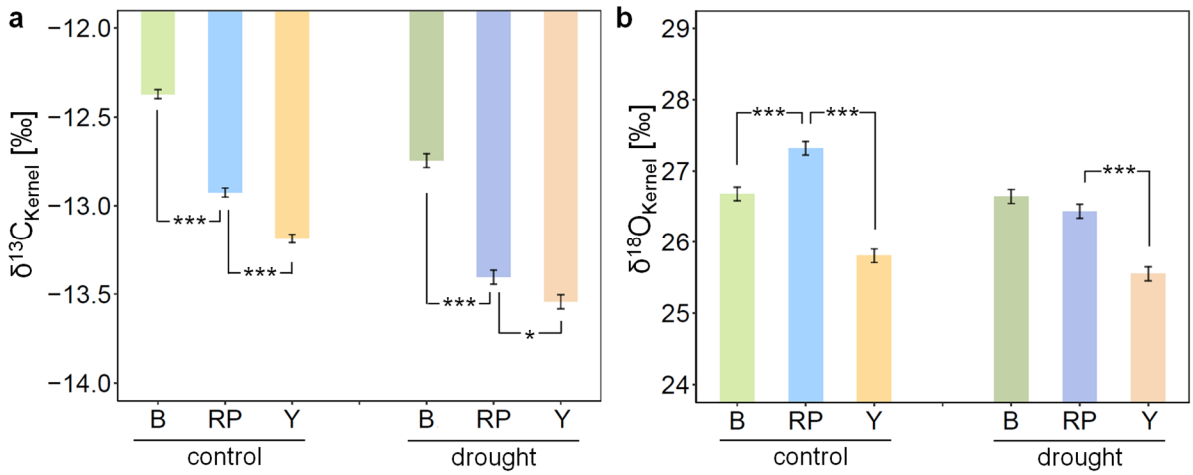

Figure 3.15: Isotopic composition of kernels of near isogenic lines NIL B and NIL Y and recurrent parent RP grown under well-watered and water-limited conditions in the field in 2019.
a) Carbon isotopic composition of kernels ($\delta^{13}C_{Kernel}$), b) oxygen isotopic composition of kernels ($\delta^{18}O_{Kernel}$). For the drought-treated plants, irrigation was restricted between developmental stage V9 and R1. Shown are means ± SE over six replicates. Significant differences compared to RP based on a Dunnett's test within each treatment are indicated as *:p<0.05, ***: p<0.001.

The effect of reduced watering before flowering on genotypic differentiation in $\delta^{13}C_{Kernel}$ was analyzed in 2019 and 2020 on field-grown plants. In the control treatment, plants were well-watered, whereas in a second treatment, drought was induced in a rain-out shelter by restriction of watering between developmental stages V9 and R1. Under water limitation, $\delta^{13}C_{Kernel}$ of RP, NIL B and NIL Y was decreased (Figure 3.15a). A higher $\delta^{13}C_{Kernel}$ of NIL B and lower $\delta^{13}C$ of NIL Y compared to RP, detected under control conditions in several years of field trials, was also found in drought stressed plants in the field trial 2019 (Figure 3.15a). However, the difference between RP and NIL Y was less pronounced under drought than under control conditions. In 2020, a difference in $\delta^{13}C_{Kernel}$ was found for both NIL B and NIL Y under control, but only for NIL B under drought conditions in comparison to RP (Table S3).

Greenhouse and field experiments showed that stomatal closure under water deficit decreases $\delta^{13}C$ of leaves and kernels of all maize lines. Genotypic differences in $\delta^{13}C$ of leaves and kernels mostly persisted under drought, as the drought treatment was of limited severity and duration.

$\delta^{18}O$ of kernels ($\delta^{18}O_{Kernel}$) did not differ consistently for all genotypes, when comparing the control and drought treatment (Figure 3.15b). No genotype showed higher values for $\delta^{18}O_{Kernel}$ under water limitation compared to well-watered conditions, as it was observed in the greenhouse for $\delta^{18}O_{Leaf}$ (Figure 3.14). In the control treatment, $\delta^{18}O_{Kernel}$ of both NIL B and NIL Y were lower than $\delta^{18}O_{Kernel}$ of RP, with a larger difference in NIL Y. In greenhouse-grown plants, both NIL B and NIL Y had lower $\delta^{18}O_{Kernel}$ than RP (Table S4), confirming the results from this field experiment under control treatment. Under drought in the rain-out shelter, only NIL Y showed lower $\delta^{18}O_{Kernel}$ compared to RP (Figure 3.15b). Thus, results of $\delta^{18}O_{Kernel}$

obtained in the field differed from the patterns regarding the effect of drought (Figure 3.14) and genotypic differences (Figure 3.5) observed for $\delta^{18}O_{Leaf}$ in the greenhouse.

Differences in $\delta^{18}O_{Kernel}$ therefore could not be connected with differences in g_s. $\delta^{18}O_{Leaf}$ on the other hand showed a negative correlation with g_s over different watering regimes and at a younger developmental stage over different genotypes. This indicates that $\delta^{18}O_{Leaf}$ may be useful as an integrated measure of g_s, given differences in g_s are sufficiently pronounced.

3.4 Association of $\delta^{13}C$ with differences in agronomic traits

The connection of iWUE and $\delta^{13}C_{Kernel}$ can cause associations between $\delta^{13}C_{Kernel}$ and plant development or yield. However, associations between $\delta^{13}C_{Kernel}$ and agronomic traits can also be the consequence of secondary effects of changed plant development on $\delta^{13}C$ (Condon et al., 2002).

To test the connection to altered $\delta^{13}C_{Kernel}$ in the material studied in this thesis, several agronomic traits were assessed on the maize lines under well-watered control and semi-controlled drought conditions. The three maize lines RP, NIL B and NIL Y were part of larger trials with 69 additional genotypes in 2019 and 72 in 2020. In addition to the RP and DP, 25 lines in 2019 and 27 lines in 2020 were derived from the same dent/flint introgression library (Gresset et al., 2014) that NIL B and NIL Y were developed from.

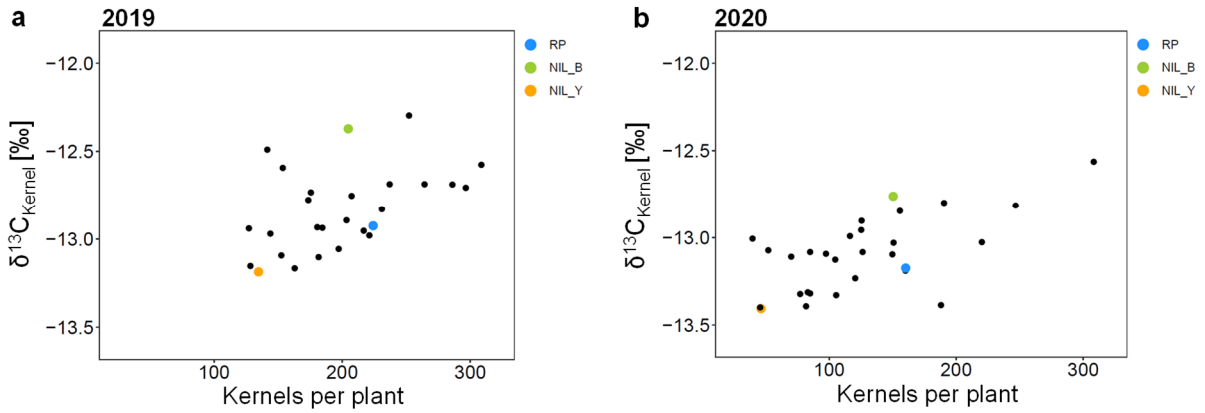

Figure 3.16: Mean carbon isotopic composition of kernels ($\delta^{13}C_{Kernel}$) plotted against the mean kernel number per plant of the respective genotype in field trials 2019 (a) and 2020 (b) under control conditions.
Shown are data of 25 and 27 introgression lines, in 2019 and 2020 respectively, and their common recurrent parent (RP) and donor parent. Data for RP, NIL B and NIL Y are highlighted by colored symbols. Data are means over three replicates, with a subset of lines included as duplicate entries. For values of means ± SE, see Table S8.

In both field trials, positive correlations were found between $\delta^{13}C_{Kernel}$ and the number of kernels per plant under control conditions (2019 r^2=0.20, p=0.012; 2020 r^2=0.37, p<0.001, Figure 3.16). Under drought conditions, kernel numbers were reduced and the correlation of $\delta^{13}C_{Kernel}$ and kernel number was weaker (2019) or not significant (2020; Figure S2). RP and NIL B both had an intermediate number of kernels, when considering all lines derived from the introgression library, and did not differ significantly from each other under control conditions (Figure 3.16, Table S3). NIL Y had lower kernel numbers compared to RP and NIL B and also compared to most other introgression lines and showed the most negative $\delta^{13}C_{Kernel}$ in both years (Figure 3.16).

No consistent patterns were observed between NIL B, NIL Y and RP regarding differences in flowering time, plant height or approximations for chlorophyll content by SPAD-measurements (Table S3).

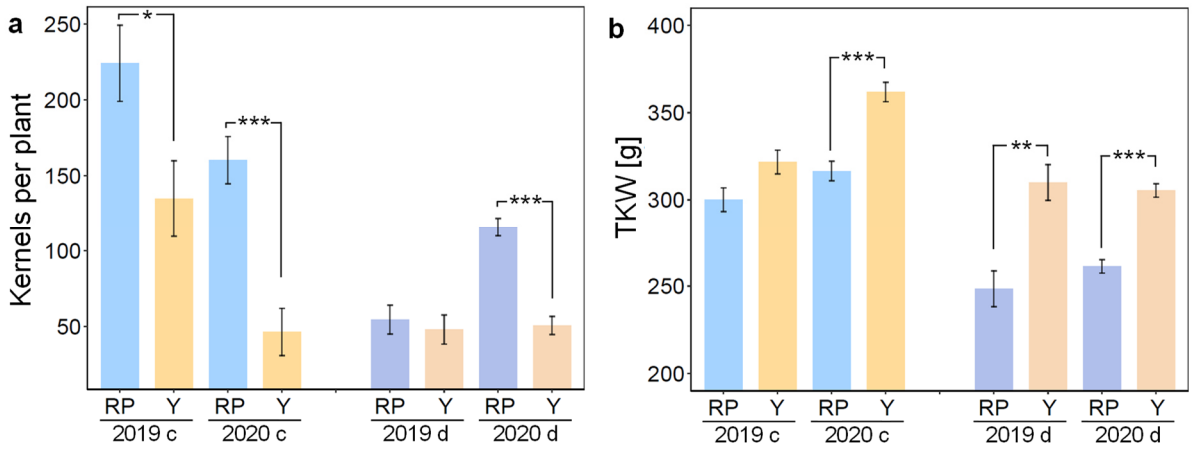

Figure 3.17: a) Kernel number per plant and b) thousand kernel weight (TKW) of near isogenic line NIL Y and recurrent parent RP in the field trials in 2019 and 2020.
Shown are data from plants in a well-watered control field ("c") and from plants grown under semi-controlled drought conditions in a rain-out shelter ("d"). Data are means over six plots. Within each year and treatment, significant differences compared to RP based on a Dunnett's test (including NIL B) are indicated as *: p<0.05, **: p<0.01, ***: p<0.001.

The reduction in kernel number in NIL Y compared to RP in the field was significant under control conditions in 2019 and 2020 and also under drought conditions in 2020 (Figure 3.17a). As commonly observed (Chen et al., 2016), differences were reverse for thousand kernel weight (TKW). NIL Y frequently had higher TKW than RP under control and drought conditions, although in 2019 the difference was not significant under control conditions (Figure 3.17b). NIL B did not show consistent differences compared to RP in kernel number nor TKW in 2019-2021 (Tables 3.5, S3). NIL BY, carrying both the chromosome 1 and 7 introgression of NIL Y and NIL B, respectively, showed a reduced kernel number compared to RP and NIL B in the field trial 2021, but still produced more kernels than NIL Y (Table 3.5).

Contrasting to observations under field conditions, there was no difference in kernel numbers between RP and NIL Y in the greenhouse, where plants were pollinated by hand (Table S7). Still, kernels of NIL Y still frequently showed higher TKW in the greenhouse. In summary, in addition to lower $\delta^{13}C$ of kernels, NIL Y often showed higher TKW and in the field lower kernel number than RP. As these three traits did not consistently differ in combination in the same experiments, the connection between traits requires further investigation.

Table 3.5: Kernel number per plant and thousand kernel weight (TKW) of RP, NIL B, NIL Y and NIL BY, grown in the field in 2021.
Values are means over six plots. Significant differences based on a Tukey test are indicated by different letters ($p<0.05$).

Genotype	Kernels per plant	TKW [g]
RP	259 ± 21 a	276 ± 9 a
NIL B	337 ± 21 a	283 ± 9 a
NIL Y	82 ± 21 b	347 ± 9 b
NIL BY	170 ± 21 c	324 ± 9 b

Kernels of plants grown in the field in 2018, which differed in $\delta^{13}C_{Kernel}$ (Figure 3.18), were used to investigate the differences in kernel traits between RP and NIL Y in more depth. Pericarp and tip cap were removed and the rest of the kernel was separated into the endosperm fraction and the embryo fraction for analysis of $\delta^{13}C$. Both fractions of the kernel had lower $\delta^{13}C$ in NIL Y than in RP, with differences similarly pronounced as the differences in total kernel $\delta^{13}C$ (Figure 3.18). $\delta^{13}C$ of the embryo were distinctly lower than those of the endosperm with values of -14.5 and -14.9‰ compared to -13.1 and -13.5‰. NIL Y and RP did not differ in their relative percentages of the two fractions; in NIL Y and RP the embryo accounted for approximately 8% of the total weight of embryo plus endosperm.

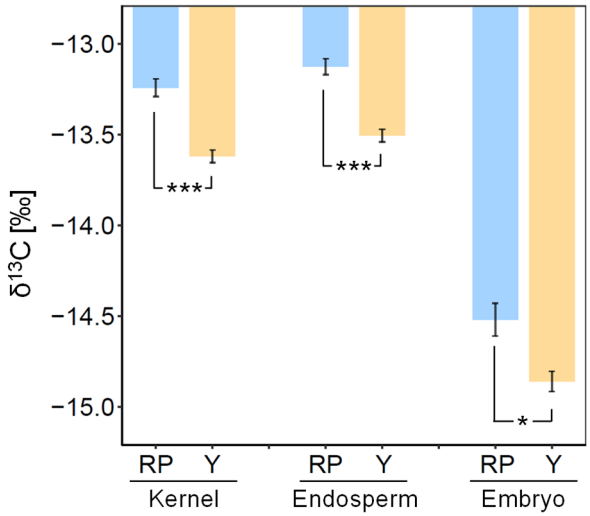

Figure 3.18: Carbon isotopic composition ($\delta^{13}C$) of total kernels and of endosperm and embryo fractions of the kernel of near isogenic line NIL Y and recurrent parent RP grown in the field in 2018.
Data are means ± SE. n=5. Significant differences compared to RP based on a Dunnett's test are indicated as *: $p<0.05$, ***: $p<0.001$.

Taken together, the fact that differences in $\delta^{13}C_{Kernel}$, kernel number and TKW between NIL Y and RP do not strictly co-occur and that NIL Y and RP do not differ in their proportion of the embryo and endosperm fraction, suggest that the differences in kernel number and TKW are not causative for the difference in $\delta^{13}C_{Kernel}$.

3.5 Genetic dissection of the segment on chromosome 1

The genetic composition of the NILs, with a limited number and size of well-defined introgressions associated with the $\delta^{13}C_{Kernel}$ difference, offers the opportunity to narrow down the causal genomic region by forward genetics making use of recombination. Generation and phenotyping of recombinant lines, which carry smaller sub-segments of the original introgression, allows to separate genetic factors, which might contribute to the phenotype. The $\delta^{13}C_{Kernel}$ differences can additionally be connected to a smaller genomic region, which might ultimately be small enough to identify potential candidate genes. The fine-mapping of the genomic region causing the $\delta^{13}C_{Kernel}$ difference in NIL B was carried out in a flanking project and is described in Blankenagel et al. (2022). To narrow down the respective region in NIL Y, NIL Y was backcrossed to RP and repeatedly self-pollinated in order to generate recombinant lines segregating for smaller overlapping segments of the original 27 Mb introgression on chromosome 1 (see chapter 2.1.2). In the F_2 generation, seven plants were selected based on genotyping with five markers for propagation and additional phenotyping experiments. These lines were named Yb-Yf, Yh and Yi. These recombinant lines were analyzed for $\delta^{13}C_{Kernel}$ in the greenhouse in winter, but no differences were detected among genotypes. Since values for $\delta^{13}C_{Kernel}$ were unusually low (-15.1 to -14.3‰), which was most likely due to the environmental conditions in the greenhouse in winter, the experiment was repeated in summer 2020 with the F_4 generation. F_5 plants were planted in the field trial in 2021 to analyze $\delta^{13}C_{Kernel}$ also on field-grown plants.

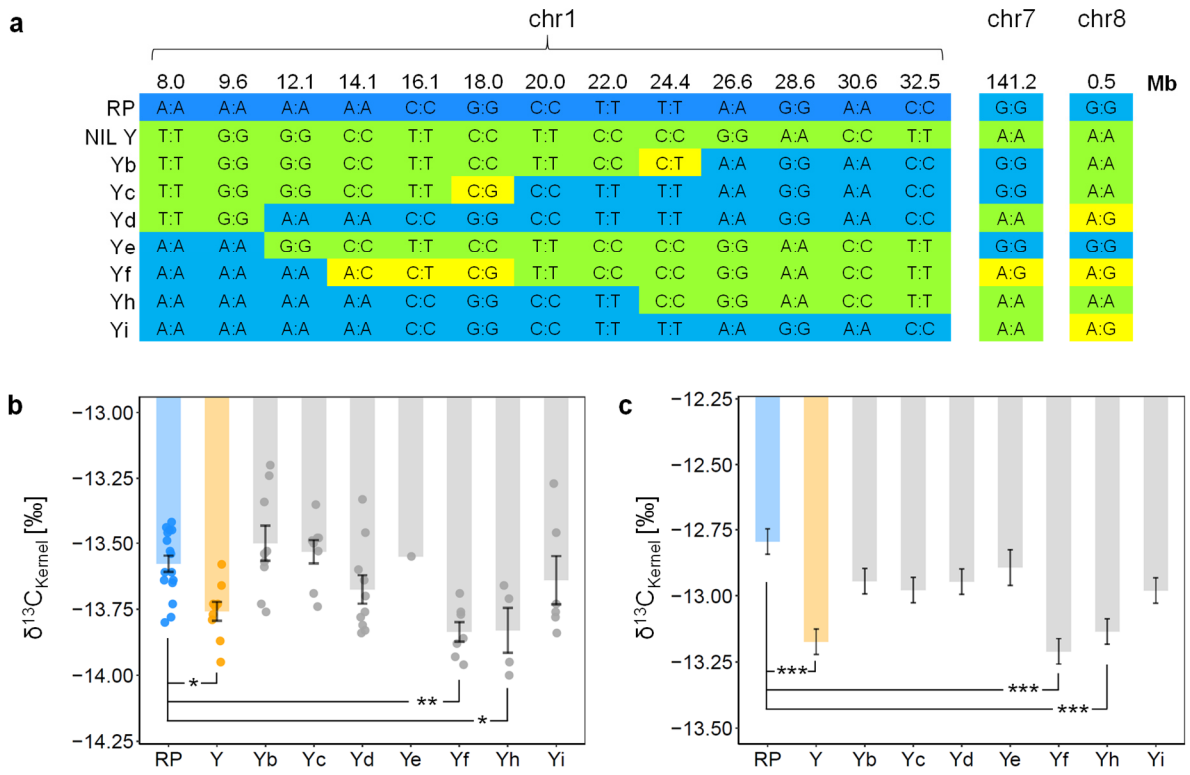

Figure 3.19: Genotyping data based on polymorphic markers in the NIL Y introgressions and kernel carbon isotopic composition ($\delta^{13}C_{Kernel}$) of recombinant lines derived from RP and NIL Y. Recombinant lines Yb-Yi carry smaller overlapping segments of the chromosome (chr) 1 introgression carried by NIL Y. a) Marker positions are given at the top in Mega bases (Mb). Marker results corresponding to the genotype of RP are marked in blue, marker results corresponding to the genotype of the donor parent in green. Marker positions that are yellow were heterozygous in the previous generation and segregate among individuals of the respective line. $\delta^{13}C_{Kernel}$ is shown of the lines grown in the greenhouse (b) and in the field (c). Bars show mean ± SE. In the greenhouse, 20 plants of RP and 10 of all other genotypes were grown, resulting in n for $\delta^{13}C$ of 1-16. Round symbols show $\delta^{13}C$ values of individual plants. For the field, means over six plots are shown, except for Ye, where three plots were included. Significant differences compared to RP based on a Dunnett's test are indicated as: *: p<0.05, **: p<0.01, ***: p<0.001.

The selected recombinant lines Yb-i were analyzed with KASP markers, spread over the chromosome 1 introgression and one each in the small chromosome 7 and chromosome 8 introgression. The lines were homozygous for the majority of the marker positions within the introgressions, particularly on chromosome 1 (Figure 3.19a). Yi differs from RP only in the small introgressions on chromosomes 7 and 8. Yb, Yc and Yd all carry the beginning of the chromosome 1 introgression in decreasing size, Ye, Yf and Yh carry the end of the chromosome 1 introgression in decreasing size. Of genotype Ye only one plant produced a sufficient number of seeds in the greenhouse.

NIL Y showed more negative $\delta^{13}C_{Kernel}$ than RP both in the greenhouse experiment in summer, as well as in the field, although in the greenhouse the difference was less pronounced

(Figure 3.19b,c). In addition to NIL Y, also Yf and Yh had significantly lower $\delta^{13}C_{Kernel}$ than RP both in the greenhouse and field experiment, while the other genotypes did not differ from RP.

Yf and Yh share the region on chromosome 1 between the marker at 22.0 Mb and the end of the introgression at 34.7 Mb, suggesting that this region might be associated with the decrease in $\delta^{13}C_{Kernel}$. Ye also carries the DP allele in that region, but did not differ from RP in $\delta^{13}C_{Kernel}$. However, Ye grew poorly in the greenhouse and produced very few kernels also in the field, so a lower number of replicates was included and conclusions based on this line should be drawn with caution.

Differences in $\delta^{13}C_{Kernel}$ were not systematically connected to changes in TKW or kernel number in the NIL Y recombinants (Figure S3). Under field conditions NIL Y, Yc, Ye, Yf and Yh produced fewer kernels than RP; and NIL Y and Yd showed significantly higher TKW. In the greenhouse experiment, there were no differences in kernel numbers and only Yf had a significantly higher TKW than RP.

Analysis of the recombinant lines derived from NIL Y allowed to narrow down the genetic region on chromosome 1 associated with the $\delta^{13}C_{Kernel}$ difference from 26.7 to 12.7 Mb. Under greenhouse and field conditions, the recombinant lines Yf and Yh confirmed that the introgression of the DP allele in the region between 22.0 and 34.7 Mb decreases $\delta^{13}C_{Kernel}$. This segment contains gene models for 286 protein-coding genes (based on B73 AGPv4, genes were extracted using the Biomart tool by Gramene, www.gramene.org). The line Yf or Yh can be used to generate additional recombinant lines for narrowing down the segment causal for the $\delta^{13}C_{Kernel}$ difference further. Analysis of 195 F_2 plants of the NIL Y x NIL B cross with five markers within 9.6 to 34.6 Mb in the chromosome 1 introgression (chapter 2.1.2) indicated a high recombination rate in this region, as 138 out of 195 individuals demonstrated recombination events. This demonstrates that there is a high chance for generating additional lines that segregate within the 12.7 Mb region shared between Yf and Yh by backcrossing one of these lines to RP.

4 Discussion

Carbon isotope discrimination during carbon fixation ($\Delta^{13}C_{Photosynthetic}$) of C_4 plants is shaped by processes that also determine water use and photosynthetic efficiency. The two main drivers of $\Delta^{13}C_{Photosynthetic}$ variation are the ratio of the intercellular to ambient CO_2 concentration (C_i/C_a), which is closely linked to plant water use efficiency (WUE_{plant}), and leakiness, which is linked to photosynthetic efficiency (Farquhar, 1983). However, their respective contribution to intraspecific variation in $\Delta^{13}C_{Photosynthetic}$ has not been established. Additionally, the relationship of $\Delta^{13}C_{Photosynthetic}$ and C_i/C_a can change its direction, depending on the extent of leakiness. If genotypic differences in $\Delta^{13}C_{Photosynthetic}$ are sufficiently pronounced and stably expressed, they can be reflected in the carbon isotopic composition ($\delta^{13}C$) of plant dry matter (Ghashghaie & Badeck, 2014). While in C_3 plants, $\delta^{13}C$ of dry matter is established to reliably reflect genotypic differences in intrinsic water use efficiency (iWUE; Condon et al., 2004), the extent to which $\delta^{13}C$ of C_4 plants reflects differences in gas exchange is not clear. This is because of the interacting effects of leakiness and C_i/C_a and the generally lower $\Delta^{13}C_{Photosynthetic}$ compared to C_3 plants (Farquhar, 1983). The aim of this study was to characterize the relationship of $\delta^{13}C$ and gas exchange in near isogenic lines of the C_4 plant maize.

4.1 Connection between genotypic differences in $\delta^{13}C$ and iWUE

4.1.1 Genetic variation in photosynthetic $\Delta^{13}C$ and C_i/C_a

The near isogenic maize lines NIL B and NIL Y and the recurrent parent RP were selected to study the connection of intraspecific variation in $\delta^{13}C$ and gas exchange. Selection of these lines was based on differences in $\delta^{13}C_{Kernel}$ of NIL B and NIL Y compared to RP in the field with effects in opposite directions, as well as higher $\delta^{13}C_{Leaf}$ in NIL B and a tendency for lower $\delta^{13}C_{Leaf}$ in NIL Y in a greenhouse experiment. NIL B carries a 55 Mb introgression from a flint donor parent (DP) on chromosome 7 and NIL Y carries a 27 Mb introgression from the same DP on chromosome 1. A hypothesis of this study was that the increased $\delta^{13}C_{Kernel}$ of NIL B and decreased $\delta^{13}C_{Kernel}$ of NIL Y compared to RP reflected differences in $\Delta^{13}C_{Photosynthetic}$.

Connection of differences in $\Delta^{13}C_{Photosynthetic}$, C_i/C_a and stomatal conductance between RP and NIL B

Intraspecific variation for $\Delta^{13}C_{Photosynthetic}$ of C_4 species has not been studied extensively so far. Some reports on intraspecific variation in $\delta^{13}C$ of maize (Araus et al., 2010; Eggels et al., 2021;

Gresset et al., 2014; Kolbe et al., 2018; Monneveux et al., 2007; Twohey et al., 2019) suggest variation for $\Delta^{13}C_{Photosynthetic}$, however, intraspecific variation for $\Delta^{13}C_{Photosynthetic}$ of different (non-mutant) genotypes measured on-line during gas exchange has only been described for sorghum (Henderson et al., 1998). Here, $\Delta^{13}C_{Photosynthetic}$ of the three maize lines were assessed at the vegetative stage V5/6 and varied between 3 and 5‰ (Figure 3.3). These values are in the range of values of 2-5‰ that are typically observed in interspecific studies of C_4 species (Cousins et al., 2008; Henderson et al., 1992). Literature reports for maize quantified $\Delta^{13}C_{Photosynthetic}$ to lie between 3.1‰ and 3.77‰ (Cousins et al., 2008; Henderson et al., 1992; Kubasek et al., 2007; Ubierna et al., 2018).

A main focus of this study was to investigate differences in $\Delta^{13}C_{Photosynthetic}$ between the maize lines as a cause for $\delta^{13}C$ segregation. NIL Y did not differ from RP in $\Delta^{13}C_{Photosynthetic}$ assessed in the growth chamber. In NIL B, $\Delta^{13}C_{Photosynthetic}$ was lower than in RP and NIL Y (Figure 3.3), which is in line with higher $\delta^{13}C_{Kernel}$ in NIL B. This was first strong evidence that the high $\delta^{13}C_{Kernel}$ in NIL B is caused by altered $\Delta^{13}C_{Photosynthetic}$. The difference in $\Delta^{13}C_{Photosynthetic}$ between NIL B and RP was thus examined in more detail. C_i/C_a was investigated as a potential driver for the changed $\Delta^{13}C_{Photosynthetic}$ of NIL B. Indeed, simultaneously to the low $\Delta^{13}C_{Photosynthetic}$, C_i/C_a was increased in NIL B compared to RP, suggesting a negative relationship of the two traits (Figure 3.3). A negative relationship between differences in $\Delta^{13}C_{Photosynthetic}$ and C_i/C_a of different genotypes was also observed in eight sorghum genotypes analyzed by Henderson et al. (1998).

Differences in C_i/C_a indicate a difference in the ratio of CO_2 assimilation rate (A) and stomatal conductance (g_s). In NIL B, high C_i/C_a resulted from increased g_s compared to RP (Figure 3.4). A/C_i curves demonstrated that in RP assimilation was close to CO_2 saturation at ambient CO_2 levels, so further increases in C_i through higher g_s in NIL B did not greatly improve A (Figure 3.4). Elevated g_s without an equivalent increase in A thus resulted in increased C_i/C_a, corresponding to reduced iWUE, in NIL B. The C_i of approximately 150 ppm in RP at ambient CO_2 of 400 ppm, is a typical value for C_4 plants (Blankenagel et al., 2018) and also saturation of CO_2 assimilation under current atmospheric conditions is a common phenomenon for C_4 species (Leakey, 2009). Thus, despite a tight connection between g_s and A, changes in their ratio, i.e. iWUE, as a result of an altered g_s are not uncommon (Brugière et al., 2017; Leakey et al., 2019). That NIL B did not differ from RP in activities of photosynthetic enzymes or chlorophyll content analyzed (Table 3.2) is in line with the primary role of the stomata for the high C_i/C_a in NIL B.

To further test the dependence of $\Delta^{13}C_{Photosynthetic}$ on stomata-related C_i/C_a differences, the effect of a short-term reduction in relative humidity (RH) on $\Delta^{13}C_{Photosynthetic}$ was tested. As expected, lowering RH caused all genotypes to restrict g_s. For NIL B this resulted in a decrease

in C_i/C_a to a value similar to that of RP and NIL Y at control RH (60%; Figure 3.3). Connected to this was an increase in $\Delta^{13}C_{Photosynthetic}$ in NIL B at low RH to a value similar to $\Delta^{13}C_{Photosynthetic}$ of RP and NIL Y at control RH. These results further supported a major role of g_s in causing the covariation of C_i/C_a and $\Delta^{13}C_{Photosynthetic}$ in NIL B, although they do not exclude an additional contribution of a changed leakiness.

Combined analyses of $\Delta^{13}C_{Photosynthetic}$, gas exchange and dry matter $\delta^{13}C$ of different genotypes have been lacking for maize to directly assess the connection between traits. In this thesis, on-line measurements on genetically well-defined material differing only in few clearly defined genomic segments demonstrated that differences in $\delta^{13}C_{Kernel}$ between maize genotypes can be indicative of differences in $\Delta^{13}C_{Photosynthetic}$ that are linked to altered C_i/C_a and g_s.

4.1.2 Genetic variation in leakiness

Potential contribution of leakiness to $\Delta^{13}C$ differences between genotypes

A negative relationship between $\Delta^{13}C_{Photosynthetic}$ and C_i/C_a is predicted from the simplified $\Delta^{13}C$ model (Equation 1) for leakiness values below 0.37 (von Caemmerer et al., 2014). Given low leakiness, the discrimination against ^{13}C that can be realized by Rubisco is low. Thus, the fractionations associated with CO_2 hydration and PEPC carboxylation, which result in an enrichment in ^{13}C, come into effect more (Farquhar, 1983). As a result, increases in C_i/C_a decrease $\Delta^{13}C_{Photosynthetic}$ at low leakiness. Leakiness of the genotypes under study was calculated from the simultaneous measurements of C_i/C_a and $\Delta^{13}C_{Photosynthetic}$ in two experiments and was indeed below 0.37 in NIL B, amounting to 0.27 and 0.30. Values of leakiness in RP and NIL Y were close to 0.37, especially in Exp. 1.1 (0.38 and 0.39 in Exp. 1.1, 0.34 and 0.32 in Exp. 1.2; Figure 3.3). Most reports of leakiness measurements in the literature are lower than 0.37, including those for maize of 0.22 to 0.27 (Cousins et al., 2008; Kubasek et al., 2007; Ubierna et al., 2018). On the other hand, higher leakiness values were calculated for other C_4 species by Cousins et al. (2008) and by Kubasek et al. (2007). Based on the leakiness values of RP and NIL Y a relationship of C_i/C_a and $\Delta^{13}C_{Photosynthetic}$ of close to zero would be expected in these two lines and changes in C_i/C_a should have almost no effect on $\Delta^{13}C_{Photosynthetic}$. The predicted relationship of $\Delta^{13}C_{Photosynthetic}$ and C_i/C_a of close to zero in RP and NIL Y results from $\Delta^{13}C_{Photosynthetic}$ being close to 4.4‰, which equals the fractionation factor of the diffusion of CO_2 in air and the y-intercept of the predicted line (Farquhar, 1983).

Since leakiness cannot be measured directly and the model comes with strong assumptions used for calculating it (Kromdijk et al., 2014), interpretation of the differences in leakiness between genotypes as well as absolute values are tricky. In order to calculate leakiness more

accurately, the CO_2 concentrations in bundle sheath and mesophyll cells and thus bundle sheath and mesophyll conductance would have to be known, as well as boundary layer conductance, respiratory and photorespiratory rates (Kromdijk et al., 2014). Additionally, the extended $\Delta^{13}C$ model described by Farquhar and Cernusak (2012) comprises a ternary correction for the effect of transpiration on CO_2 uptake and further fractionation factors associated with substeps of CO_2 diffusion and fixation. Not taking these factors into account likely leads to errors, when comparing leakiness values obtained under different environmental conditions (Kromdijk et al., 2014). Still, also absolute values under control conditions and differences between genotypes, as they were assessed in this study, might be affected by the simplifications, so conclusions should be drawn with caution. Regarding mesophyll conductance, no intraspecific differences were found between five maize lines by Kolbe and Cousins (2018).

Despite uncertainties regarding absolute values for leakiness and their influence on the relationship between $\Delta^{13}C_{Photosynthetic}$ and C_i/C_a, a negative relationship between $\Delta^{13}C_{Photosynthetic}$ and C_i/C_a was demonstrated in NIL B by lowering RH. The significant decrease in C_i/C_a under low RH compared to standard conditions was connected to a significant increase in $\Delta^{13}C_{Photosynthetic}$ in NIL B. In RP and NIL Y, the change in C_i/C_a by lowering RH was smaller than in NIL B due to the lower C_i/C_a under standard conditions, and was not connected to a significant change in $\Delta^{13}C_{Photosynthetic}$. The relationship between $\Delta^{13}C_{Photosynthetic}$ and C_i/C_a in RP and NIL Y could thus not be finally resolved.

That lower leakiness was determined in NIL B compared to RP and NIL Y indicates that, in addition to the higher C_i/C_a in NIL B, a difference in leakiness contributes to the $\Delta^{13}C_{Photosynthetic}$ difference. In studies of $\delta^{13}C$ of C_4 plants, it is often hypothesized that variation in leakiness could contribute to $\delta^{13}C$ variation and reduce the strength of the correlation with WUE_{plant} (Ellsworth et al., 2020; Twohey et al., 2019). Leakiness of different genotypes of the same species assessed by on-line $\Delta^{13}C$ measurements had only been described by Henderson et al. (1998) so far. In that study, no significant differences in leakiness were found between eight sorghum genotypes, which differed in C_i/C_a. While a lower leakiness could affect $\Delta^{13}C_{Photosynthetic}$ in NIL B independently of C_i/C_a, it might also be a result of the changed intercellular CO_2 concentration, as leakiness is influenced by the CO_2 concentration gradient between bundle sheath and mesophyll cells (von Caemmerer & Furbank, 2003). Low leakiness could be beneficial regarding photosynthetic efficiency, yet the effects of lower leakiness and higher g_s in NIL B on iWUE go in opposite directions. A lower leakiness would increase photosynthetic efficiency, whereas increased g_s lowers iWUE (Ellsworth et al., 2020). As iWUE is lower in NIL B compared to RP, no beneficial effect of a lower leakiness was observed. While no definite conclusions can be drawn regarding the absolute values for leakiness of the studied lines, the positive relationship of differences in iWUE and differences in $\Delta^{13}C_{Photosynthetic}$ between

genotypes and for NIL B under different measurement conditions point to the potential to detect differences in iWUE based on $\delta^{13}C$.

4.1.3 Connection between gas exchange and dry matter $\delta^{13}C$

$\delta^{13}C$ of plant dry matter can reflect differences in $\Delta^{13}C_{Photosynthetic}$ in a time-integrated manner (Ghashghaie & Badeck, 2014). However, additional post-photosynthetic isotopic fractionations lead to discrepancies between $\Delta^{13}C_{Photosynthetic}$ and the $\Delta^{13}C$ derived from dry matter $\delta^{13}C$. Particularly in C_4 species, in which the extent and variation of $\Delta^{13}C_{Photosynthetic}$ is lower than in C_3 plants, these post-photosynthetic fractionations might be of higher significance and the consistency of differences in $\Delta^{13}C_{Photosynthetic}$ and dry matter $\delta^{13}C$ is less clear (Henderson et al., 1998).

Consistent differences in $\delta^{13}C$ between NIL B and RP

With the lower $\Delta^{13}C_{Photosynthetic}$ found in NIL B compared to RP, a higher ^{13}C content in plant material and therefore higher $\delta^{13}C$ is expected (Farquhar et al., 1982). The high $\delta^{13}C_{Kernel}$ of NIL B in the initial field analysis thus matched the difference detected in $\Delta^{13}C_{Photosynthetic}$. Contrastingly, the low $\delta^{13}C_{Kernel}$ of NIL Y was not connected to a difference in $\Delta^{13}C_{Photosynthetic}$. Since $\Delta^{13}C_{Photosynthetic}$ is determined in a short period of minutes at the juvenile stage V5/6, one cannot directly draw conclusions on whether these measurements reflect the $\Delta^{13}C_{Photosynthetic}$ during the majority of the plant's lifecycle. Therefore, $\delta^{13}C$ of leaves and gas exchange were analyzed throughout the development.

$\delta^{13}C$ of the three analyzed genotypes varied mainly between -15 and -13‰ in leaves and -13.5 and -12‰ in kernels (Figure 3.2), which agrees with values commonly observed for C_4 plants (Cernusak et al., 2013; von Caemmerer et al., 2014). Differences in $\delta^{13}C$ of plant material between RP and NIL B, with higher values in NIL B, were consistently expressed throughout the lifecycle of the plants over different experiments, and in different environments, such as greenhouse and field. Additionally, iWUE was also stably lower in NIL B compared to RP at different developmental stages and environments (Figures 3.5, 3.7). Combined with the on-line $\Delta^{13}C$ measurements, these results present strong evidence that the changed $\delta^{13}C$ values of NIL B are a reflection of stably altered $\Delta^{13}C_{Photosynthetic}$ that is linked to differences in iWUE.

Differences in $\Delta^{13}C_{Photosynthetic}$ between NIL B and RP were more pronounced than those detected in dry matter $\delta^{13}C$, with a difference of approximately 1‰ and 0.4‰, respectively (Figures 3.2, 3.3). Measurement conditions in the leaf cuvette during on-line measurements might have promoted expression of differences compared to the conditions the plants

experienced, when assimilating carbon for production of the sampled dry matter. Additionally, post-photosynthetic fractionations affect the $\delta^{13}C$ of dry matter and might have attenuated differences that resulted directly from photosynthesis (Ghashghaie & Badeck, 2014). In the literature, weak correlations have been observed between on-line $\Delta^{13}C$ and dry matter $\delta^{13}C$ over different C_4 species and were ascribed to differences in post-photosynthetic fractionations between species (Cousins et al., 2008; Henderson et al., 1992). Given their high genetic similarity and the stable differences between NIL B and RP in on-line and leaf and kernel dry matter-derived $\Delta^{13}C$, it can be assumed that post-photosynthetic fractionations have only marginal effects on differences in $\delta^{13}C$ between these lines.

Consistent differences in iWUE between NIL B and RP

The strong consistency of $\delta^{13}C$ variation between RP and NIL B was matched by consistent differences in gas exchange. NIL B showed a pronounced elevation of g_s as well as reduction in iWUE compared to RP at developmental stage V5/6 and V7-9, under greenhouse, growth chamber and field conditions (Figure 3.5, Table S6). Only in one out of seven experiments, RP and NIL B did not differ in measurements of gas exchange, which were taken in Exp. 2.4 in the greenhouse at stage V9-12 (Figure 3.14). $\delta^{13}C$ values of the measured leaves in this experiment demonstrated a significant increase in NIL B compared to RP, as in other experiments. The strong covariation of both traits in all other measurement sets, as well as results from the coupled on-line $\Delta^{13}C$ and gas exchange measurements make it very likely that the discrepancy in Exp. 2.4 between lack of difference in gas exchange, but significant differences in $\delta^{13}C$, is caused by the difference in time integration between the two measures. Short-term measurements of gas exchange are more prone to environmental error than the $\delta^{13}C$ measurements, in which gas exchange differences over the time of tissue synthesis are integrated (Kubasek et al., 2007). Additionally, RP was on average one developmental stage further developed than NIL B in this experiment, leading to measurements on leaf 10-12 in RP and on leaf 9-11 in NIL B. Since gas exchange differs throughout plant development (Pimentel et al., 1999), these developmental differences could have attenuated the difference in g_s and iWUE between the two lines. As the developmental stage changed over the different measurement days, its effect could not be separated from variation caused by different weather conditions on different days. Errors associated with developmental variation were mostly avoided in measurements at the younger stage V5/6, when developmental differences between genotypes were less pronounced. The same plants of RP and NIL B that differed in leaf 9-12 $\delta^{13}C$, but not in gas exchange, had previously been analyzed for their gas exchange at stage V5/6 (Table S6). At that stage, g_s of NIL B was significantly higher and iWUE lower compared to RP. It is possible that the $\delta^{13}C$ of leaf 9-12 reflects the gas exchange difference

between RP and NIL B of a younger developmental stage, because the leaf dry matter carbon is in part derived from assimilates produced in older leaves (von Caemmerer et al., 2014). Thus, results in this thesis highlight the advantage of $\delta^{13}C_{Leaf}$ analyses over short-term gas exchange measurements, as they integrate environmental, developmental and diurnal fluctuations (Kubasek et al., 2007).

That iWUE is indeed lower in NIL B than in RP for a substantial part of the plants' lifecycle is demonstrated by lower WUE_{plant} (Figure 3.10). Higher g_s relative to A in NIL B compared to RP caused a lower accumulation of biomass with the same amount of water. As a result, the positive association of $\Delta^{13}C_{Photosynthetic}$ and iWUE translates into a negative association of leaf and kernel $\delta^{13}C$ with WUE_{plant} for the maize line NIL B. This demonstrates that both leaf and kernel $\delta^{13}C$ can serve as a proxy for WUE_{plant}. $\delta^{13}C_{Leaf}$ has the advantage that it can be assessed earlier in the lifecycle and will more closely reflect $\Delta^{13}C_{Photosynthetic}$. On the other hand, $\delta^{13}C_{Kernel}$ is less susceptible to error caused by environmental and developmental variation. This was evident in the present study by higher stability of the NIL B phenotype regarding $\delta^{13}C_{Kernel}$ compared to $\delta^{13}C_{Leaf}$ under field conditions.

Twohey et al. (2019) also investigated the relationship between $\delta^{13}C_{Leaf}$ and iWUE and WUE_{plant} with four recombinant inbred lines (RIL) derived from the maize NAM panel (Yu et al., 2008). Similarly to the results on NIL B and RP, the RIL with highest $\delta^{13}C_{Leaf}$ showed highest g_s, lowest leaf transpiration efficiency (ratio of assimilation and transpiration) and lowest WUE_{plant} among the four RILs. This is in line with a negative relationship of $\delta^{13}C_{Leaf}$ and both iWUE and WUE_{plant}, which is driven by g_s. However, among the other three RILs no clear relationship of these traits could be seen. Similarly, Henderson et al. (1998) observed negative correlations of both C_i/C_a and $\Delta^{13}C_{Photosynthetic}$ as well as $\delta^{13}C_{Leaf}$ and WUE_{plant} for eight and thirty sorghum genotypes, respectively. While the negative correlation of WUE_{plant} and $\delta^{13}C_{Leaf}$ was significant, it was weak, indicating that not all genotypes fit the relationship and additional factors contribute to $\delta^{13}C$ variation. Divergence from a tight negative correlation of $\delta^{13}C$ and WUE_{plant} is highlighted by the results of the present study on NIL Y, which, with exception of one out of seven experiments, had consistently lower $\delta^{13}C_{Kernel}$ than RP, but did not differ consistently in WUE_{plant} or iWUE.

Studies on genetic link between $\delta^{13}C$ and WUE_{plant} in C_4 species

The joined difference of $\delta^{13}C$ and WUE_{plant} in NIL B compared to RP motivated fine-mapping of the genetic region on chromosome 7 in a project described in Blankenagel et al. (2022). Through phenotyping of additional NILs carrying smaller overlapping introgressions, the genetic region on chromosome 7 associated with the $\delta^{13}C$ and WUE difference was narrowed

down sufficiently to identify the abscisic acid (ABA) 8'-hydroxylase-encoding *ZmAbh4* as causal for the difference in both traits. *ZmAbh4* acts through catabolism of the phytohormone ABA, which restricts g_s. Higher expression of functional *ZmAbh4* transcript in NIL B causes decreased ABA levels and thus increased g_s, decreased iWUE and increased $\delta^{13}C_{Kernel}$ in comparison to RP. Molecular and biochemical analyses in combination with the generation of additional recombinant lines and CRISPR/Cas9 mutants corroborated the causal role of *ZmAbh4*. Covariation of $\delta^{13}C_{Kernel}$, iWUE and WUE_{plant} in the NILs and mutants demonstrated the direct link of these traits through g_s via influence of a single gene. Although no significant difference was found in stomatal density between NIL B and RP in the greenhouse experiments in this thesis, NIL B showed higher stomatal density in a field experiment of this study and in experiments described in Avramova et al. (2019). Higher stomatal density could also contribute to the increased g_s of NIL B compared to RP. It remains to be shown if *ZmAbh4* or another candidate gene in the chromosome 7 genomic region is causative for this difference.

The introgression on chromosome 7 of NIL B associated with $\delta^{13}C$ and WUE_{plant} (also described in Avramova et al., 2019) overlaps with a QTL for $\delta^{13}C_{Leaf}$ of maize identified in a study by Sorgini et al. (2021). These authors used four RIL families derived from four maize NAM lines and B73 as a common parent for $\delta^{13}C_{Leaf}$ QTL mapping. Out of five identified QTL, one overlapped with the introgression on chromosome 7 and two further QTL overlapped with QTL for $\delta^{13}C_{Kernel}$ identified by Gresset et al. (2014). The identification of *ZmAbh4* in NIL B demonstrates the potential to identify genes with relevance for WUE_{plant} based on screening for $\delta^{13}C$ in C_4 plants and the overlap of QTL between the described studies by Sorgini et al. (2021) and Gresset et al. (2014) suggests that these might be relevant in different genetic backgrounds.

Co-localized QTL for $\delta^{13}C$ and WUE_{plant} of C_4 species were also recently identified in an interspecific *Setaria* RIL population (Ellsworth et al., 2020). All three QTL that were identified for $\delta^{13}C_{Leaf}$ overlapped with QTL for WUE_{plant} and/or transpiration. Additionally, a negative correlation of $\delta^{13}C_{Leaf}$ and WUE_{plant} was found among the genotypes of this RIL population, which supports the findings of this thesis that a negative relationship of these traits exists in maize.

4.1.4 Divergence of leaf- and kernel-derived measures of $\Delta^{13}C$

While the covariation of differences in $\delta^{13}C$ and WUE_{plant} between NIL B and RP demonstrated the connection of these traits through $\Delta^{13}C_{Photosynthetic}$ and iWUE, this dependence did not apply to NIL Y. Despite stably lower $\delta^{13}C_{Kernel}$ compared to RP, particularly under field conditions, no consistent differences in iWUE, WUE_{plant}, $\Delta^{13}C_{Photosynthetic}$ or $\delta^{13}C_{Leaf}$ were detected. While the

variable $\delta^{13}C_{Leaf}$ patterns in NIL Y (Figure 3.2) could indicate that leakiness is indeed around the value that causes the relationship of $\Delta^{13}C_{Photosynthetic}$ and C_i/C_a to be close to zero, also gas exchange measurements did not show consistent differences in iWUE for NIL Y and RP. In several experiments, both g_s and A were lower in NIL Y than in RP, but not connected to an altered iWUE and in other experiments no significant differences were observed for any gas exchange parameter (Table S6). There are several potential causes for the lack of connection between $\delta^{13}C_{Kernel}$ and leaf-level measurements in NIL Y.

Differences in time integration between measures of $\delta^{13}C$ and gas exchange

One factor that can cause divergence between measurements of gas exchange and $\delta^{13}C$ of plant dry matter mentioned above is the difference in time integration. Gas exchange measurements only capture the state of processes occurring during the measurement period of approximately 5 min (after 30 min equilibration). Stomatal conductance, assimilation rate and thus iWUE are strongly dependent on environmental conditions and also vary diurnally (Leakey et al., 2019; Medrano et al., 2015). Fluctuations in iWUE with influence on $\Delta^{13}C_{Photosynthetic}$ would integrate into $\delta^{13}C_{Leaf}$ and also into WUE_{plant}. In the case of NIL Y, lower g_s and A were observed than in RP in some experiments, but only in one experiment these changes led to a detectable increase in iWUE (Table S6). Since a tendency for lower g_s is often associated with increases in iWUE (Bertolino et al., 2019), it is possible that iWUE was higher in NIL Y for a significant period of the lifecycle, but not caught in the short-term measurements. That the chromosome 1 introgression of NIL Y can have a positive effect on iWUE is also supported by the comparison of NIL BY, which carries the chromosome 1 and 7 introgression, with NIL B, carrying only the chromosome 7 introgression. In a greenhouse experiment, iWUE of NIL BY was higher compared to NIL B (Figure 3.6) and in the field NIL B had lower iWUE than RP, but NIL BY did not (Figure 3.8).

However, no difference was found between NIL Y and RP in WUE_{plant} in the greenhouse (Figure 3.10). Moreover, in the greenhouse experiment including NIL BY (Exp. 2.5), differences between NIL BY and NIL B were not integrated into $\delta^{13}C_{Kernel}$ (Table S4), indicating they were not expressed for the majority of the growth conditions. Additionally, also NIL Y did not differ from RP in $\delta^{13}C_{Kernel}$ in that experiment. These results support that the $\delta^{13}C_{Kernel}$ difference between RP and NIL Y observed in the field and other greenhouse experiments cannot be exclusively explained by a difference in iWUE, and highlight a strong environmental dependence of the NIL Y phenotype.

Potential role for post-photosynthetic fractionations

In addition to divergence of instantaneous measures and measures of $\delta^{13}C$, the $\delta^{13}C$ of NIL Y relative to RP behaved differently in leaves and kernels, even within the same experiment (Figure 3.14). Divergence of $\delta^{13}C_{Leaf}$ and $\delta^{13}C_{Kernel}$ can be the consequence of post-photosynthetic fractionations (Ghashghaie & Badeck, 2014) that can occur during several metabolic reactions, particularly during synthesis of different plant compounds. These non-photosynthetic fractionations cause differences in isotopic signatures of different substances so that lipids, proteins and lignin are depleted in ^{13}C compared to sucrose, starch and cellulose (Hobbie & Werner, 2004; von Caemmerer et al., 2014). Even the same substance can show different $\delta^{13}C$ depending on its origin. Different $\delta^{13}C$ of e.g. sucrose can originate not only from different synthesis pathways, but also from changes in its signature throughout the development due to ontogenetic or environmental effects on iWUE (Cernusak et al., 2009; Francey et al., 1985; Pimentel et al., 1999; Rao et al., 1995).

If compounds with $\delta^{13}C$ different from the bulk leaf $\delta^{13}C$ are exported from the leaves or used for respiration, the bulk leaf signature will be affected (Cernusak et al., 2009; Ghashghaie & Badeck, 2014). Similarly, differences in $\delta^{13}C$ of carbon allocated for grain filling can influence the $\delta^{13}C_{Kernel}$ differently in different genotypes. Differential use of carbon metabolic pathways or differential carbon allocation between RP and NIL Y might serve as a potential explanation for different patterns of $\delta^{13}C_{Leaf}$ and $\delta^{13}C_{Kernel}$ in NIL Y in comparison to RP. Generally, further research on the contribution of post-photosynthetic fractionations to intraspecific variation in $\delta^{13}C$ is required. Kolbe et al. (2018) performed RNA-sequencing on diverse maize lines including the NAM panel to identify potential post-photosynthetic drivers of $\delta^{13}C$ variation, but did not detect any correlation of $\delta^{13}C$ with transcript levels with potential relevance for post-photosynthetic fractionation processes.

Developmental differences, which can also contribute to $\delta^{13}C$ variation (Rebetzke et al., 2008), are unlikely to have had a major effect on genotypic differences in $\delta^{13}C$ in the genetic material of this study. RP developed slightly faster than NIL B and NIL Y, but due to the high genetic similarity this variation was small and also flowering time did not differ consistently between the maize lines in this thesis (Table S3).

The impact of developmental and metabolic effects on $\delta^{13}C$ of all genotypes can be observed in the differences between $\delta^{13}C$ of leaf 6, the cobleaf, the kernel and different kernel compartments in the current study. Under field conditions, a shift towards more positive values was observed from leaf 6 to cobleaf $\delta^{13}C$ for all genotypes (Figures 3.2, 3.9). A switch towards more positive values between juvenile and adult maize leaves around V7 was also described by Twohey et al. (2019). Kernels show even higher $\delta^{13}C$, which mainly results from the difference in substance class composition, since starch as a main component of the kernel is

enriched in ^{13}C compared to bulk leaf material (von Caemmerer et al., 2014). This influence of substance class composition on total $\delta^{13}C$ is demonstrated by the distinctly lower $\delta^{13}C$ of the embryo, which has higher lipid and protein content, compared to the endosperm, which has higher starch content (Ai & Jane, 2016; Figure 3.18). Differences in kernel composition could potentially contribute to $\delta^{13}C_{Kernel}$ differences between genotypes, although to affect bulk kernel $\delta^{13}C$ this would require a considerable change in substance class distribution. No indications for this were observed in the current study as embryo and endosperm had similar proportions in RP and NIL Y and differences in $\delta^{13}C$ between RP and NIL Y were comparable in both compartments (Figure 3.18).

Association of $\delta^{13}C$ and kernel number in NIL Y

An indication for differences in carbon-related processes between RP and NIL Y that could be associated with post-photosynthetic fractionations is the observation of differences in kernel number and thousand kernel weight (TKW) between NIL Y and RP. NIL Y produced distinctly fewer kernels than RP under field conditions and showed higher TKW in many experiments (Figure 3.17, Table S7). $\delta^{13}C_{Kernel}$ and kernel number were positively correlated in field trials including lines derived from the same introgression library as NIL Y and NIL B (Figure 3.16). Gresset (2014) also found a positive correlation between kernel number and $\delta^{13}C_{Kernel}$ with the original introgression lines under control conditions in field and greenhouse.

Similarly to the negative correlation of yield and $\delta^{13}C$ that is often observed in C_3 species (Condon et al., 2004), a positive correlation in C_4 species might be interpreted as an indication for a connection between $\delta^{13}C$ and iWUE. Plants with high iWUE would be expected to have high $\delta^{13}C$ in C_3 species and low $\delta^{13}C$ in C_4 species, given leakiness is low (Cernusak et al., 2013). High iWUE is often the result of reduced g_s, which under well-watered conditions might lead to disadvantages in growth and yield compared to plants with high g_s and high assimilation (Condon et al., 2004). Under drought on the other hand, plants with high iWUE might have an advantage in yield, so the correlation of $\delta^{13}C$ and yield might change direction (Condon et al., 2004; Gresset, 2014). The negative relationship of $\delta^{13}C$ and ear weight of maize under drought observed by Monneveux et al. (2007) supports this hypothesis. In this thesis, correlations of $\delta^{13}C_{Kernel}$ and kernel number did not change direction under drought conditions, but were weaker compared to control conditions or abolished. Moreover, NIL Y, with lower $\delta^{13}C_{Kernel}$ and lower kernel number than RP under well-watered conditions, did not differ consistently from RP in iWUE or WUE_{plant}, and NIL B differed consistently in $\delta^{13}C$, iWUE and WUE_{plant}, but not in kernel number (Tables S3, S6, Figure 3.10). The results of this study thus did not provide conclusive evidence for a correlation of $\delta^{13}C$ and kernel number as a consequence of the common link to iWUE.

A difference in grain $\delta^{13}C$ between genotypes could not just result directly from differences in iWUE, but also from differential use of assimilates from stem reserves for grain filling or from differential access to soil water around flowering time (Condon et al., 2002). Lower CO_2 assimilation rate, lower chlorophyll content and higher specific leaf area (SLA) of NIL Y compared to RP under field conditions (Figure 3.8, Table 3.3) indicate potential differences in growth and assimilate use strategies that might influence both $\delta^{13}C$ and kernel number. However, this warrants further research as no significant differences between RP and NIL Y were observed in sugar contents of cobleaves (Table 3.4).

While the $\delta^{13}C_{Kernel}$ and kernel number difference in NIL Y compared to RP might be genetically connected, e.g. through differences in gas exchange, there was no conclusive co-occurrence of differences in these traits. In greenhouse Experiments 2.4 and 2.6, NIL Y and RP differed in $\delta^{13}C_{Kernel}$, but not in kernel number. Additionally, analysis of $\delta^{13}C_{Kernel}$ and kernel number of NIL Y-derived recombinant lines points against a connection of both traits. Under field conditions, several recombinant lines had lower kernel numbers and/or higher TKW than RP, but differences in the traits TKW, kernel number and $\delta^{13}C_{Kernel}$ did not consistently occur in the same genotypes. These results indicate that different factors contribute to the lower $\delta^{13}C_{Kernel}$ and to the difference in kernel traits in NIL Y compared RP.

Narrowing down the genetic region responsible for low $\delta^{13}C_{Kernel}$ in NIL Y

Despite the variable observations in NIL Y regarding gas exchange and $\delta^{13}C_{Leaf}$, the effect of the chromosome 1 introgression on $\delta^{13}C_{Kernel}$ was stable in the field. Additionally in the field, $\delta^{13}C_{Kernel}$ of NIL Y differed from RP to a similar extent as $\delta^{13}C_{Kernel}$ of NIL B, which showed stable gas exchange and $\delta^{13}C_{Leaf}$ differences (Figure 3.2). This finding was supported by the analysis of NIL BY in the field, which carries both introgressions and did not differ in $\delta^{13}C_{Kernel}$ from RP (Figure 3.9). To understand the mechanism that causes the $\delta^{13}C_{Kernel}$ difference to RP in NIL Y, a promising approach, particularly given the high genetic similarity of RP and NILY, is to identify the underlying genetic cause. This can be achieved by a fine-mapping approach, similar to that applied in NIL B that led to the identification of *ZmAbh4* (Blankenagel et al., 2022). For this purpose, seven recombinant lines derived from the backcross of NIL Y with RP were generated within this study and analyzed for $\delta^{13}C_{Kernel}$. Based on comparison of genotypes that carry overlapping subsegments of the chromosome 1 introgression, the effects of smaller chromosomal regions on $\delta^{13}C$ can be evaluated. Lines Yf and Yh had lower $\delta^{13}C_{Kernel}$ than RP, both in greenhouse and field conditions (Figure 3.19). This indicated that the region on chromosome 1 between 22.0 and 34.7 Mb, containing 286 gene models for protein encoding genes, controls the $\delta^{13}C_{Kernel}$ difference to RP, since both lines carry the donor parent allele in this region as does NIL Y. The fact that Ye also carries the same allele in this region,

but did not differ in $\delta^{13}C_{Kernel}$ from RP could be due to the low production of kernels in this line. Lines Yf and Yh might thus be backcrossed to RP for generation of further recombinant lines, which segregate within the 22.0 to 34.7 Mb region. The high percentage of plants showing recombination in the chromosome 1 introgression in the F_2 generation of the NIL Y x NIL B cross (138 out of 195) implies a high potential for generating additional recombinants. By analyzing additional recombinant lines, potential interacting factors with influence on $\delta^{13}C_{Kernel}$ that are in close genetic proximity can be separated and ultimately the genomic segment can be narrowed down further to identify potential candidate genes.

Overall, the results on NIL Y demonstrate that in maize $\delta^{13}C$ differences are not consistently indicative of differences in iWUE or WUE_{plant}. The variability of the phenotype of NIL Y highlights the difficulty in interpreting $\delta^{13}C$ differences in C_4 plants that is associated with the low magnitude of $\Delta^{13}C_{Photosynthetic}$, the uncertainty in the relationship with iWUE and the contribution of post-photosynthetic fractionations.

Environmental cues that are likely to occur in the field seem to trigger higher SLA, lower chlorophyll and lower g_s and A in NIL Y. Differences in these traits could lead to higher iWUE under some environmental conditions, as well as differences in carbon use or allocation that affect both kernel number and $\delta^{13}C_{Kernel}$. This study allows to explain the NIL Y phenotype based on the assessed traits, yet other mechanisms might be involved that could be revealed by identifying the causal gene(s).

4.2 Environmental effects on gas exchange and $\Delta^{13}C$

4.2.1 Effect of field conditions on genotypic differentiation in $\delta^{13}C$

Plant characteristics are often evaluated under controlled growth chamber or semi-controlled greenhouse conditions and the transferability of results to the field can be a concern (Poorter et al., 2016). In the present study, genotypic differences in gas exchange and in $\delta^{13}C$ between RP and NIL B were highly consistent between growth chamber, greenhouse and field experiments. Contrastingly, observations for NIL Y varied between experiments. Under growth chamber conditions, NIL Y did not show any differences in gas exchange or $\Delta^{13}C_{Photosynthetic}$ compared to RP, under field conditions g_s and A were lower in NIL Y than in RP (Table S6). In greenhouse experiments, results were variable, as NIL Y showed either reduced g_s and A or no difference compared to RP. In terms of $\delta^{13}C_{Kernel}$, NIL Y showed consistently lower values than RP in the field, whereas in the greenhouse the decrease in $\delta^{13}C_{Kernel}$ of NIL Y was

experiment-dependent. Therefore, some of the variability in the results might be attributable to differences in environmental conditions.

Differences in environmental conditions between controlled and field conditions and their effect on $\Delta^{13}C$

Generally, gas exchange, particularly CO_2 assimilation A, was the lowest under growth chamber and the highest under field conditions (Figure 3.7). In line with the high A, also chlorophyll content was higher in field-grown compared to greenhouse-grown plants (Tables 3.2, 3.3). Higher photosynthetic rates of field-grown plants compared to plants grown under controlled conditions are commonly observed (Poorter et al., 2016) and are likely mainly the result of the growth under higher light intensity. In the growth chamber, plants were grown at a light intensity of 800 µmol $m^{-2}s^{-1}$, whereas in the field light intensities of 1500 µmol $m^{-2}s^{-1}$ were common and probably frequently exceeded. Measurements of on-line $\Delta^{13}C$ and gas exchange in the growth chamber at light intensities of 800 and 1500 µmol $m^{-2}s^{-1}$ in the leaf cuvette, revealed lower C_i/C_a in all three genotypes at lower light intensities, but no distinct differences in $\Delta^{13}C_{Photosynthetic}$ or leakiness between the conditions and also no effect of the light intensity on differences in $\Delta^{13}C_{Photosynthetic}$ between genotypes (Figure 3.3).

Many reports have found that leakiness and thus $\Delta^{13}C_{Photosynthetic}$ increase at low light intensities (Kromdijk et al., 2014). While part of this increase has been assigned to modeling errors (Ubierna et al., 2011), some increase likely does occur. An increase in leakiness has also been reported in response to high VPD, which might also transiently occur under field conditions (Gong et al., 2017). Several other reports suggested leakiness to be relatively stable under different environmental conditions and to adapt to most environmental changes (Ellsworth & Cousins, 2016; Henderson et al., 1992; Kromdijk et al., 2014). Short-term fluctuations, as they oftentimes occur under field conditions, might however transiently disrupt the balance of the C_3 and C_4 cycle and thus affect leakiness (Bellasio & Griffiths, 2014) and the relationship between $\Delta^{13}C_{Photosynthetic}$ and C_i/C_a. The high variability of conditions in the field is a main difference to controlled conditions. Amplitudes of variation in e.g. temperature are much higher in the field than in the growth chamber and greenhouse and additionally change more throughout the day. The same holds true for light intensities. Short-term changes are not only due to weather conditions, but also due to the variable self-shading because of leaf movement by wind.

Another major difference is given by the growth under controlled conditions in pots with homogeneous and soft substrate, to which water and nutrients are supplied regularly in high availability, and restricted root growth. While root growth is less restricted in the field, access

to water and nutrients is less regular. Furthermore, CO_2 concentrations in growth chambers and closed greenhouses can differ from that under field conditions.

Most of these environmental parameters can influence $\Delta^{13}C_{Photosynthetic}$, not only by potentially influencing leakiness, but also particularly through their effect on C_i/C_a. For example, C_i/C_a is expected to decrease at low relative humidity or low water availability due to the reduced g_s (Farquhar et al., 1989b). Low light intensities can increase C_i/C_a by decreasing A, whereas above a certain light intensity this effect might disappear (Cernusak et al., 2013). High nitrogen content may decrease C_i/C_a by increasing photosynthetic capacity and also at high temperatures decreased values for C_i/C_a have been observed (Kubasek et al., 2007). In addition to its effect on C_i/C_a, temperature can influence $\Delta^{13}C_{Photosynthetic}$ of C_4 plants through its effect on the fractionation during CO_2 dissolution and hydration, with the fractionation factor in favor of ^{13}C decreasing by 1‰ between 20 °C and 30 °C (Farquhar, 1983).

Effect of field conditions on genotypic differences in $\Delta^{13}C$

While the differences in environmental conditions between growth chamber, greenhouse and field experiments are the same for all analyzed maize lines, different genotypes often react differently to certain environmental cues. It is thus possible that certain genotypic differences can only be observed under field and not growth chamber conditions, since certain environmental triggers are necessary for expression of these differences (Poorter et al., 2016).

One indication for a differential influence of the field conditions on the genotypes under study comes from differences in specific leaf area SLA. SLA was lower under field conditions for all genotypes compared to growth chamber conditions (Tables 3.3, S5). Increased SLA of plants in the growth chamber is a common observation, which can probably be attributed to lower light, higher temperature and higher nutrient and water availability in the growth chamber (Poorter et al., 2016). In the present study, genotypes did not differ in SLA under growth chamber conditions, yet under field conditions, NIL Y had significantly higher SLA than RP and NIL B (Tables 3.3, S5). Since SLA and A per area are often negatively correlated (Evans & Poorter, 2001; Poorter et al., 2016; Rao et al., 1995), the higher SLA of NIL Y compared to RP might partially explain the lower A in NIL Y compared to RP under field conditions. This is supported by the result that A per dry weight did not differ between RP and NIL Y. It is possible that under environmental conditions where A is not primarily limited by g_s the tendency to lower g_s and A in NIL Y might result in increased iWUE and thus higher $\Delta^{13}C_{Photosynthetic}$ in NIL Y. Differences in SLA might also influence leaf-internal CO_2 diffusion and thereby cause differences in $\delta^{13}C$ between genotypes (Sorgini et al., 2021). Beyond this study, more research

is needed on the influence of anatomical features on carbon isotope fractionations (Retta et al., 2016).

Due to the high number of interacting environmental factors, which differ between controlled and field conditions and their high variability in the field, it is difficult to identify, which might be the critical factor that promotes expression of differences between NIL Y and RP under field conditions compared to greenhouse and growth chamber conditions. When comparing results from greenhouse and field experiments, Gresset et al. (2014) did not observe significant genotype-by-environment interactions, yet several other studies on WUE_{plant} and $\delta^{13}C$ have observed some extent of genotype-by-environment interaction for different environments (Chen et al., 2011; Henderson et al., 1998; Twohey et al., 2019). The environmental dependence of the NIL Y phenotype highlights the relevance of performing analyses under field conditions, as results might strongly differ from controlled environmental setups. For the assessment of $\delta^{13}C$, phenotyping under field conditions is easily achievable.

4.2.2 Effect of drought on genotypic differentiation in $\delta^{13}C$

A main interest in $\delta^{13}C$ lies in its connection to WUE_{plant} and its assessment under field conditions, which might be associated with temporary water deficit. A crucial question is, whether genotypic differences in $\delta^{13}C$ that are detected under control conditions will also be detectable and relevant under drought. First, this would require that genotypic differences in gas exchange that underlie the $\delta^{13}C$ differentiation are sufficiently expressed under drought to still be detectable in dry matter $\delta^{13}C$ under drought. Second, the relationship between C_i/C_a and $\Delta^{13}C_{Photosynthetic}$, and thus leakiness, would need to be stable under both conditions.

Effect of water deficit on gas exchange

How genotypic differences in iWUE are affected by drought will depend on the cause for the iWUE differentiation. In the case of NIL B, the decreased iWUE compared to RP resulted from increased g_s (Figure 3.4). This high g_s was caused at least partially by lower ABA levels due to higher ABA 8'-hydroxylase 4 activity (Avramova et al., 2019; Blankenagel et al., 2022).

In growth chamber and greenhouse experiments of this thesis, in which stable drought conditions were induced, water deficit led to a reduction in g_s in all genotypes to values of approximately 0.13 mol $m^{-2}s^{-1}$. In the growth chamber experiment, genotypic differences in g_s and iWUE disappeared under drought (Figure 3.12). In the greenhouse experiment at stage V9-12, NIL B had by tendency higher g_s only under drought, which led to a significant difference in iWUE under drought, but not under control conditions (Figure 3.14). Under drought, the

effect of lower initial ABA levels and higher ABA 8'-hydroxylase 4 activity in NIL B (Blankenagel et al., 2022) might have led to a detectable difference in gas exchange between NIL B and RP. Whether NIL B and RP will differ in g_s under drought will most likely be very specific to the time of measurement and intensity, duration and type of drought. Two contrasting effects on g_s are likely to interact. The increased g_s under control conditions can lead to higher, earlier water loss, so NIL B might experience water deficit earlier. This was observed, when g_s was measured during progressive drought (Figure 3.11). On the other hand, at the same level of water availability, g_s might be higher in NIL B compared to RP under drought because of generally higher expression of functional ABA 8'-hydroxylase 4 transcript in NIL B than in RP (Blankenagel et al., 2022). Results of the controlled drought treatment in the growth chamber, in which strong developmental effects were avoided by measuring at a young developmental stage, indicate that genotypic differences in g_s and iWUE are overall reduced under water deficit and disappear if the drought is severe and permanent (Figure 3.12).

Relationship of C_i/C_a and $\Delta^{13}C_{Photosynthetic}$ under drought

During transient or mild drought, persisting differences in iWUE might still result in differences in $\delta^{13}C$. For the interpretation of $\delta^{13}C$ of plants grown under drought conditions the effect of water limitation on the relationship between $\Delta^{13}C_{Photosynthetic}$ and C_i/C_a is of relevance. If changes in leakiness under water deficit cause a switch in the sign of the relationship between C_i/C_a and $\Delta^{13}C_{Photosynthetic}$, it will not be possible to draw conclusions from $\delta^{13}C$ under drought conditions on iWUE. With a predicted relationship of $\Delta^{13}C_{Photosynthetic}$ and C_i/C_a in RP and NIL Y close to zero, this is a critical aspect. $\Delta^{13}C_{Photosynthetic}$ and C_i/C_a were assessed under water deficit in the growth chamber at stage V5/6. In all analyzed maize lines, C_i/C_a was drastically decreased under drought, because of the reduced g_s (Figure 3.12). Along with this decrease in C_i/C_a, $\Delta^{13}C_{Photosynthetic}$ increased significantly for all genotypes (Figure 3.13). This supports a negative relationship of $\Delta^{13}C_{Photosynthetic}$ and C_i/C_a that is predicted by low leakiness. Increases in $\Delta^{13}C_{Photosynthetic}$ were stronger than predicted from the simplified $\Delta^{13}C$ model based on the leakiness calculated under control conditions (Figure 3.13). As a consequence, estimated leakiness values were higher under drought, with no differences between genotypes (Table S5). In RP and NIL Y, mean values shifted from <0.37 to ≥0.37, though as explained above, conclusions based on absolute leakiness values calculated from the simplified $\Delta^{13}C$ model should be drawn with caution. It is possible that both changes in C_i/C_a and leakiness are causing the shift in $\Delta^{13}C_{Photosynthetic}$ to higher values and that the leakiness change might even be causally connected to the change in C_i/C_a. The effect of water deficit on leakiness has also been investigated in sorghum by Sonawane and Cousins (2020). In that study, $\delta^{13}C_{Leaf}$ was decreased under drought, indicating higher $\Delta^{13}C_{Photosynthetic}$, but no change in leakiness in

response to water deficit was observed. Also in several other studies on C_4 species, a decrease in $\delta^{13}C_{Leaf}$ under drought has been found and interpreted mainly as a consequence of the decreased C_i/C_a (Ellsworth et al., 2017; Ellsworth et al., 2020; Ghannoum et al., 2002; Twohey et al., 2019). Contrastingly, Zhang et al. (2015) attribute higher $\delta^{13}C_{Leaf}$ under drought to decreases in leakiness, however leakiness was not assessed from $\Delta^{13}C_{Photosynthetic}$ in that study, so this result warrants further research.

The ranking of genotypes regarding C_i/C_a and $\Delta^{13}C_{Photosynthetic}$ was not changed by the drought treatment. While the genotypic differences in C_i/C_a and $\Delta^{13}C_{Photosynthetic}$ are reduced under drought, NIL B still tends to show highest C_i/C_a and lowest $\Delta^{13}C_{Photosynthetic}$, until differences in both C_i/C_a and $\Delta^{13}C$ between genotypes are no more observable at a certain drought level (Figures 3.12-3.13). These results indicate that genotypic differences in iWUE and $\Delta^{13}C_{Photosynthetic}$ will be harder to detect under drought conditions, but genotypic differences in $\Delta^{13}C_{Photosynthetic}$ that persist under drought will most likely follow the same directions as under control conditions.

Effect of water deficit on dry matter $\delta^{13}C$

In the greenhouse and most field experiments, genotypic differences in dry matter $\delta^{13}C$ between RP and NIL B persisted in plants exposed to water limitation. The effect of the drought treatment on $\Delta^{13}C_{Photosynthetic}$ can be seen in the decrease of both $\delta^{13}C_{Leaf}$ and $\delta^{13}C_{Kernel}$ (Figures 3.14, 3.15), which is in agreement with the increase in $\Delta^{13}C_{Photosynthetic}$ observed in the on-line measurements (Figure 3.13). However, differences in $\delta^{13}C$ between RP and NIL B were only slightly affected (Figure 3.14, 3.15). In the greenhouse, this is likely due to the short duration of the drought treatment of six days. Also in the field, the drought treatment was moderate and restricted to the time period before flowering to ensure production of seeds. The presence of differences in RP and NIL B under drought in $\delta^{13}C$ can either indicate that differences in iWUE between these lines persisted at the respective drought level or that a transient absence of genotypic differentiation in iWUE and $\Delta^{13}C_{Photosynthetic}$ did not significantly impact the differentiation in dry matter $\delta^{13}C$. Particularly when measured in kernels, $\delta^{13}C$ likely was in part derived from assimilates produced when plants were not yet or no longer stressed. These results indicate that genotypic differences in $\delta^{13}C$ that are indicative of a difference in iWUE are also detectable under transient or mild drought conditions. Under severe and persistent drought, however, differentiation in $\delta^{13}C$ will likely be abolished as indicated by the measurements of on-line $\Delta^{13}C$ and the observations in previous field trials (Avramova et al., 2019) and other studies (Ellsworth et al., 2020), in which genotypic differences in $\delta^{13}C_{Kernel}$ did not persist under water limitation.

Connection of oxygen isotopic composition ($\delta^{18}O$) and transpiration

The oxygen isotopic composition ($\delta^{18}O$) of plant dry matter can provide time-integrated information on stomatal conductance and was investigated in this thesis. In contrast to $\delta^{13}C$, $\delta^{18}O$ is not affected by photosynthetic processes, but to a large extent influenced by transpiration (Cabrera-Bosquet et al., 2009b). Interest in $\delta^{18}O$ is based on the enrichment of liquid water in ^{18}O relative to ^{16}O by the predominant loss of $H_2{}^{16}O$ during evaporation (Barbour et al., 2000). $\delta^{18}O$ of leaf water depends on the $\delta^{18}O$ of the source water taken up by the plant, the evaporative enrichment during transpiration and the Péclet number (Ellsworth et al., 2017). The evaporative enrichment at the site of transpiration depends on temperature and the ratio of ambient to intercellular air vapor mole fraction. The Péclet number describes the mixing behavior of source water from the xylem and enriched water from the sites of transpiration and is dependent on transpiration rate and effective path length that water moves from veins to the site of evaporation (Ellsworth et al., 2017). The Péclet number increases with transpiration rates, and the contribution of the ^{18}O enrichment at the site of transpiration decreases with increasing Péclet number. Thus, $\delta^{18}O$ of leaf water decreases with increasing transpiration (if path length remains constant). The $\delta^{18}O$ of leaf water is passed onto the $\delta^{18}O$ of the bulk leaf material through oxygen exchange, however, additional fractionations can occur during biochemical reactions for synthesis of organic matter (Cabrera-Bosquet et al., 2009b). While generally a negative relationship between transpiration and $\delta^{18}O$ is expected, different observations have been made in different studies. A negative relationship of $\delta^{18}O$ and g_s was observed in cotton and wheat (Barbour & Farquhar, 2000; Barbour et al., 2000) and a negative correlation between $\delta^{18}O$ and yield was found in wheat and durum wheat (Araus et al., 2013; Barbour et al., 2000). On the other hand, positive correlations between $\delta^{18}O$ and transpiration have been observed for cowpea, groundnut and rice (Sheshshayee et al., 2005). Ellsworth et al. (2017) found the correlation of $\delta^{18}O$ and g_s over different watering regimes to be species-dependent for the genus *Setaria* and Ghannoum et al. (2002) did not observe a significant effect of drought on $\delta^{18}O_{Leaf}$ of different C_4 grasses.

Here, $\delta^{18}O$ was analyzed in dry matter of leaves and kernels of the maize lines to examine whether it correlates with the short-term measurements of g_s and provides a time-integrated picture on transpiration of the genotypes. Different results were obtained in different experiments. At stage V5/6, a negative relationship was found between genotypic differences in g_s and $\delta^{18}O_{Leaf}$ in the greenhouse. NIL B with higher g_s demonstrated lower $\delta^{18}O_{Leaf}$ and NIL Y with lower g_s had higher $\delta^{18}O_{Leaf}$ than RP (Figure 3.5). This indicates that $\delta^{18}O_{Leaf}$ might reflect differences in g_s and supported the hypothesis that differences in gas exchange observed in the short-term measurements are representative for a significant period of leaf development. The negative relationship of $\delta^{18}O_{Leaf}$ and g_s was further supported by experiments on leaves at stage V9-12 under control and drought conditions. The decrease in

g_s by water deficit resulted in a clear increase in $\delta^{18}O_{Leaf}$ for all genotypes (Figure 3.14). No differences between genotypes were observed in $\delta^{18}O_{Leaf}$ at that stage, although NIL Y showed lower g_s compared to RP in the short-term measurements. This indicates that for $\delta^{18}O_{Leaf}$ to reliably reflect differences in g_s they have to be strongly pronounced. Cabrera-Bosquet et al. (2009b) and Sanchez-Bragado et al. (2016) also studied $\delta^{18}O$ of maize and observed a negative relationship of $\delta^{18}O_{Leaf}$ and $\delta^{18}O_{Kernel}$ and g_s over different watering regimes.

In the present study, $\delta^{18}O$ was also analyzed in kernels, but no connection of $\delta^{18}O_{Kernel}$ with g_s could be detected. The lack of a clear treatment effect, when comparing plants grown in the well-watered control field and plants grown under drought in the rain-out shelter (Figure 3.15), might be a consequence of differences in experimental sites and water sources between the control field and the rain-out shelter. Thus, it is difficult to make comparisons between different field trials. Within the same experiment in both greenhouse and field, $\delta^{18}O_{Kernel}$ did not meet expectations of a negative relationship with g_s under control conditions. In both environments, NIL Y showed lower $\delta^{18}O_{Kernel}$ than RP and lower or similar $\delta^{18}O_{Kernel}$ compared to NIL B (Figure 3.15, Table S4). Lower $\delta^{18}O_{Kernel}$ in NIL Y would imply a higher transpiration rate compared to RP and NIL B. Since in all measurements of short-term gas exchange NIL Y showed lower or unchanged g_s compared to RP and consistently lower g_s compared to NIL B, it is unlikely that the low $\delta^{18}O_{Kernel}$ in NIL Y is the consequence of a higher transpiration. Also in the study by Barbour et al. (2000), in which a negative correlation of $\delta^{18}O_{Leaf}$ with g_s and yield was found, the correlation with grain $\delta^{18}O$ was less clear. Sanchez-Bragado et al. (2016) attributed poor correlations between $\delta^{18}O_{Leaf}$ and $\delta^{18}O_{Kernel}$ to the additional metabolic conversions of translocated compounds and associated opportunities for oxygen exchange with water during grain filling and the different time scales for development. Nevertheless, a negative correlation of $\delta^{18}O$ and yield across 17 genotypes of maize analyzed under well-watered conditions and intermediate stress by Cabrera-Bosquet et al. (2009b) indicated that the negative relationship of $\delta^{18}O$ and g_s across different genotypes might persist in kernels.

Overall, differences in g_s seem to require a certain magnitude to be reliably reflected in $\delta^{18}O$ of plant dry matter, which indicates that $\delta^{18}O$ might be more suitable for comparison of different environmental conditions and watering regimes rather than of genotypes with generally smaller differences in gas exchange. Additional metabolic conversions that can affect $\delta^{18}O_{Kernel}$ complicate the interpretation of $\delta^{18}O_{Kernel}$ and suggest that $\delta^{18}O_{Leaf}$ might allow more reliable conclusions on g_s.

4.3 Conclusions

Characterization of near isogenic maize lines with contrasting differences in $\delta^{13}C_{Kernel}$ compared to their recurrent parent RP revealed a genotype-specific association between $\delta^{13}C$ and iWUE. Line NIL B had been selected based on increased leaf and kernel $\delta^{13}C$ and a priori knowledge of a QTL affecting $\delta^{13}C_{Kernel}$ located in its introgression on chromosome 7 (Avramova et al., 2019; Gresset et al., 2014). Investigation of different measures of $\Delta^{13}C$ and gas exchange in several environments demonstrated a strong connection between differences in $\delta^{13}C$, $\Delta^{13}C_{Photosynthetic}$ and iWUE in NIL B that is driven by g_s. Low $\Delta^{13}C_{Photosynthetic}$ caused consistently higher $\delta^{13}C$ of leaves and of kernels compared to its RP. $\Delta^{13}C_{Photosynthetic}$ demonstrated a positive relationship with iWUE, both with respect to variation of these parameters within NIL B as well as with respect to differences between the genotypes NIL B and RP. The association of these two traits measured directly during gas exchange has not previously been demonstrated in well-defined genetic material of C_4 species with minimal genetic background effects. The decrease in iWUE in NIL B was caused by an increased g_s and led to lower WUE_{plant}. Thus, the positive relationship of differences in $\Delta^{13}C_{Photosynthetic}$ and iWUE between RP and NIL B translated into a reliable negative relationship of $\delta^{13}C$ and WUE_{plant}. Fine-mapping of the underlying genetic region in a flanking project identified higher amounts of functional transcript of the ABA 8'-hydroxylase *ZmAbh4* as causing lower ABA levels and higher g_s in NIL B (Avramova et al., 2019; Blankenagel et al., 2022). Thus, the $\delta^{13}C_{Kernel}$ screen led to the identification of a gene with relevance for WUE_{plant}, demonstrating the potential use of $\delta^{13}C$ for studies of WUE_{plant} also in C_4 plants. Drought increased $\Delta^{13}C_{Photosynthetic}$ and removed genotypic differences in $\Delta^{13}C_{Photosynthetic}$ beyond a certain severity. Nevertheless, genotypic differentiation in dry matter $\delta^{13}C$ persisted under moderate or transient drought conditions.

In addition to the altered iWUE, NIL B also showed lower leakiness than RP. The low leakiness might have contributed to the $\Delta^{13}C_{Photosynthetic}$ difference and led to stronger changes in $\Delta^{13}C_{Photosynthetic}$ and $\delta^{13}C$ in response to iWUE in this line. Since iWUE and WUE_{plant} were still reduced compared to RP, no considerable positive effect of the potentially reduced leakiness was detected. Thus, in the specific case of NIL B in comparison to RP, a potential interaction of changes in iWUE and leakiness did not compromise the stable relationship between differences in $\delta^{13}C$, and iWUE as well as WUE_{plant}.

The consistent negative relationship of $\delta^{13}C$ and WUE_{plant} did not hold for the second line, NIL Y, which was selected based on decreased $\delta^{13}C_{Kernel}$ compared to RP. This suggests that results of NIL B might not be transferable to all maize genotypes. Nevertheless, recent studies on $\delta^{13}C$ in C_4 species from other groups suggest that the dependence of $\delta^{13}C$ and WUE_{plant} is not unique for NIL B. Sorgini et al. (2021) identified QTL for $\delta^{13}C_{Leaf}$ in maize, which overlapped

with QTL identified for $\delta^{13}C_{Kernel}$ by Gresset et al. (2014), demonstrating transferability of maize $\delta^{13}C$ QTL between tissues and genetic backgrounds. Twohey et al. (2019) also found support for a negative link between $\delta^{13}C_{Leaf}$ and iWUE and WUE_{plant} in maize. And Ellsworth et al. (2020) detected co-localization of three QTL for $\delta^{13}C_{Leaf}$ and WUE_{plant} and/or transpiration in *Setaria*. Together, the results from this thesis and recent other studies support that screening for $\delta^{13}C$ can reveal genotypes with altered WUE_{plant}, although the link to WUE_{plant} needs to be confirmed for the genetic material under study.

In NIL Y, consistently lower $\delta^{13}C_{Kernel}$ compared to RP in the field was not matched by differences in $\Delta^{13}C_{Photosynthetic}$ or gas exchange in the growth chamber. Stomatal conductance and assimilation rate were lower than in RP in some greenhouse experiments and in the field and $\delta^{13}C_{Leaf}$ varied between experiments. Results suggested a strong environmental influence on differences in gas exchange, presumably leading to higher iWUE under conditions where assimilation is not primarily limited by g_s. WUE_{plant} did not differ between NIL Y and RP in the greenhouse and divergent patterns for genotypic differences in $\delta^{13}C_{Leaf}$ and $\delta^{13}C_{Kernel}$ suggested an involvement of post-photosynthetic fractionations in contributing to $\delta^{13}C$ variation between these genotypes. The association of a lower $\delta^{13}C_{Kernel}$ and a lower kernel number in NIL Y compared to RP under field conditions warrants further investigation to resolve whether changes in the two traits are pleiotropic or caused by different genetic factors in the same region.

Recombinant lines carrying smaller sub-segments of the chromosome 1 introgression of NIL Y were generated in this study and allowed to narrow down the genetic region responsible for the $\delta^{13}C_{Kernel}$ difference. The analysis of the recombinant lines pointed to a 12.7 Mb region, which provides a starting point for separating potentially interacting traits influenced by this region and for identifying the gene causing the $\delta^{13}C_{Kernel}$ difference.

The phenotype of NIL Y highlights the challenges associated with the low magnitude of $\Delta^{13}C_{Photosynthetic}$, its potentially variable relationship with iWUE and an unknown contribution of post-photosynthetic fractionations, when analyzing $\delta^{13}C$ of C_4 plants. The number of studies focusing on the contribution of post-photosynthetic fractionations to intraspecific variation in C_4 plants is limited. Further investigations on the contribution of different anatomical and post-photosynthetic components to intraspecific variation of $\delta^{13}C$ and on the universality of the relationship between $\Delta^{13}C_{Photosynthetic}$ and iWUE are thus needed in C_4 plants. This thesis established the potential of identifying genotypes with altered WUE_{plant} based on a $\delta^{13}C_{Kernel}$ screen and demonstrated the direct connection of the two traits to $\Delta^{13}C_{Photosynthetic}$ and g_s for defined genetic material. With the advantage of simple assessment under field conditions, $\delta^{13}C$ can be of use to identify genotypes that are of interest for studies of WUE_{plant} and

photosynthetic efficiency and is worth being explored further for a potential use in breeding of C_4 crops.

5 References

Adiredjo, A. L., Navaud, O., Munos, S., Langlade, N. B., Lamaze, T., & Grieu, P. (2014). Genetic control of water use efficiency and leaf carbon isotope discrimination in sunflower (*Helianthus annuus* L.) subjected to two drought scenarios. *PLoS One*, *9*(7), e101218. https://doi.org/10.1371/journal.pone.0101218

Ai, Y., & Jane, J. L. (2016). Macronutrients in Corn and Human Nutrition. *Compr Rev Food Sci Food Saf*, *15*(3), 581-598. https://doi.org/10.1111/1541-4337.12192

Araus, J. L., Cabrera-Bosquet, L., Serret, M. A. D., Bort, J., & Nieto-Taladriz, M. A. T. (2013). Comparative performance of $\delta^{13}C$, $\delta^{18}O$ and $\delta^{15}N$ for phenotyping durum wheat adaptation to a dryland environment. *Funct Plant Biol*, *40*(6), 595-608. https://doi.org/10.1071/FP12254

Araus, J. L., Sanchez, C., & Cabrera-Bosquet, L. (2010). Is heterosis in maize mediated through better water use? *New Phytol*, *187*(2), 392-406. https://doi.org/10.1111/j.1469-8137.2010.03276.x

Arrivault, S., Obata, T., Szecowka, M., Mengin, V., Guenther, M., Hoehne, M., Fernie, A. R., & Stitt, M. (2017). Metabolite pools and carbon flow during C_4 photosynthesis in maize: $^{13}CO_2$ labeling kinetics and cell type fractionation. *J Exp Bot*, *68*(2), 283-298. https://doi.org/10.1093/jxb/erw414

Avramova, V., Meziane, A., Bauer, E., Blankenagel, S., Eggels, S., Gresset, S., Grill, E., Niculaes, C., Ouzunova, M., Poppenberger, B., Presterl, T., Rozhon, W., Welcker, C., Yang, Z., Tardieu, F., & Schön, C. C. (2019). Carbon isotope composition, water use efficiency, and drought sensitivity are controlled by a common genomic segment in maize. *Theor Appl Genet*, *132*(1), 53-63. https://doi.org/10.1007/s00122-018-3193-4

Baca Cabrera, J. C., Hirl, R. T., Zhu, J., Schäufele, R., & Schnyder, H. (2020). Atmospheric CO_2 and VPD alter the diel oscillation of leaf elongation in perennial ryegrass: compensation of hydraulic limitation by stored-growth. *New Phytol*, *227*(6), 1776-1789. https://doi.org/10.1111/nph.16639

Barbour, M. M., Bachmann, S., Bansal, U., Bariana, H., & Sharp, P. (2016). Genetic control of mesophyll conductance in common wheat. *New Phytologist*, *209*(2), 461-463.

Barbour, M. M., & Farquhar, G. D. (2000). Relative humidity- and ABA- induced variation in carbon and oxygen isotope ratios of cotton leaves. *Plant Cell Environ*, *23*(5), 473-485.

Barbour, M. M., Fischer, R. A., Sayre, K. D., & Farquhar, G. D. (2000). Oxygen isotope ratio of leaf and grain material correlates with stomatal conductance and grain yield in irrigated wheat. *Functional Plant Biology*, *27*(7), 625-637.

Barbour, M. M., Warren, C. R., Farquhar, G. D., Forrester, G., & Brown, H. (2010). Variability in mesophyll conductance between barley genotypes, and effects on transpiration efficiency and carbon isotope discrimination. *Plant Cell Environ*, *33*(7), 1176-1185. https://doi.org/10.1111/j.1365-3040.2010.02138.x

Bazzer, S. K., Kaler, A. S., Ray, J. D., Smith, J. R., Fritschi, F. B., & Purcell, L. C. (2020). Identification of quantitative trait loci for carbon isotope ratio $\delta^{13}C$ in a recombinant inbred population of soybean. *Theor Appl Genet*, *133*(7), 2141-2155. https://doi.org/10.1007/s00122-020-03586-0

Bellasio, C., & Griffiths, H. (2014). Acclimation to low light by C_4 maize: implications for bundle sheath leakiness. *Plant Cell Environ*, *37*(5), 1046-1058. https://doi.org/10.1111/pce.12194

Bertolino, L. T., Caine, R. S., & Gray, J. E. (2019). Impact of Stomatal Density and Morphology on Water-Use Efficiency in a Changing World. *Front Plant Sci*, *10*, 225. https://doi.org/10.3389/fpls.2019.00225

Blankenagel, S., Eggels, S., Frey, M., Grill, E., Bauer, E., Dawid, C., Fernie, A. R., Haberer, G., Hammerl, R., Medeiros, D. B., Ouzunova, M., Presterl, T., Ruß, V., Schäufele, R., Schlüter, U., Tardieu, F., Urbany, C., Urzinger, S., Weber, A. P. M., Schön, C. C., Avramova, V. (2022). Natural alleles of the abscisic acid catabolism gene *ZmAbh4*

modulate water use efficiency and carbon isotope discrimination in maize. *Manuscript accepted at The Plant Cell*.

Blankenagel, S., Yang, Z., Avramova, V., Schön, C. C., & Grill, E. (2018). Generating Plants with Improved Water Use Efficiency. *Agronomy*, *8*(9). https://doi.org/10.3390/agronomy8090194

Brück, H., Payne, W., & Sattelmacher, B. (2000). Effects of phosphorus and water supply on yield, transpirational water-use efficiency, and carbon isotope discrimination of pearl millet. *Crop science*, *40*(1), 120-125.

Brugière, N., Zhang, W., Xu, Q., Scolaro, E. J., Lu, C., Kahsay, R. Y., Kise, R., Trecker, L., Williams, R. W., Hakimi, S., Niu, X., Lafitte, R., & Habben, J. E. (2017). Overexpression of RING Domain E3 Ligase ZmXerico1 Confers Drought Tolerance through Regulation of ABA Homeostasis. *Plant Physiol*, *175*(3), 1350-1369. https://doi.org/10.1104/pp.17.01072

Cabrera-Bosquet, L., Sanchez, C., & Araus, J. L. (2009a). How yield relates to ash content, $\Delta^{13}C$ and $\Delta^{18}O$ in maize grown under different water regimes. *Ann Bot*, *104*(6), 1207-1216. https://doi.org/10.1093/aob/mcp229

Cabrera-Bosquet, L., Sanchez, C., & Araus, J. L. (2009b). Oxygen isotope enrichment ($\Delta^{18}O$) reflects yield potential and drought resistance in maize. *Plant Cell Environ*, *32*(11), 1487-1499. https://doi.org/10.1111/j.1365-3040.2009.02013.x

Cano, F. J., Sharwood, R. E., Cousins, A. B., & Ghannoum, O. (2019). The role of leaf width and conductances to CO_2 in determining water use efficiency in C_4 grasses. *New Phytol*, *223*(3), 1280-1295. https://doi.org/10.1111/nph.15920

Cernusak, L. A., Tcherkez, G., Keitel, C., Cornwell, W. K., Santiago, L. S., Knohl, A., Barbour, M. M., Williams, D. G., Reich, P. B., & Ellsworth, D. S. (2009). Why are non-photosynthetic tissues generally ^{13}C enriched compared with leaves in C_3 plants? Review and synthesis of current hypotheses. *Functional Plant Biology*, *36*(3), 199-213.

Cernusak, L. A., Ubierna, N., Winter, K., Holtum, J. A., Marshall, J. D., & Farquhar, G. D. (2013). Environmental and physiological determinants of carbon isotope discrimination in terrestrial plants. *New Phytol*, *200*(4), 950-965. https://doi.org/10.1111/nph.12423

Chen, J., Chang, S. X., & Anyia, A. O. (2011). Gene discovery in cereals through quantitative trait loci and expression analysis in water-use efficiency measured by carbon isotope discrimination. *Plant Cell Environ*, *34*(12), 2009-2023. https://doi.org/10.1111/j.1365-3040.2011.02397.x

Chen, J., Chang, S. X., & Anyia, A. O. (2012). Quantitative trait loci for water-use efficiency in barley (*Hordeum vulgare* L.) measured by carbon isotope discrimination under rain-fed conditions on the Canadian Prairies. *Theor Appl Genet*, *125*(1), 71-90. https://doi.org/10.1007/s00122-012-1817-7

Chen, J., Zhang, L., Liu, S., Li, Z., Huang, R., Li, Y., Cheng, H., Li, X., Zhou, B., & Wu, S. (2016). The genetic basis of natural variation in kernel size and related traits using a four-way cross population in maize. *PLoS One*, *11*(4), e0153428.

Condon, A. G., Richards, R., Rebetzke, G., & Farquhar, G. D. (2002). Improving intrinsic water-use efficiency and crop yield. *Crop science*, *42*(1), 122-131.

Condon, A. G., Richards, R. A., Rebetzke, G. J., & Farquhar, G. D. (2004). Breeding for high water-use efficiency. *J Exp Bot*, *55*(407), 2447-2460. https://doi.org/10.1093/jxb/erh277

Cousins, A. B., Badger, M. R., & von Caemmerer, S. (2008). C_4 photosynthetic isotope exchange in NAD-ME- and NADP-ME-type grasses. *J Exp Bot*, *59*(7), 1695-1703. https://doi.org/10.1093/jxb/ern001

Dercon, G., Clymans, E., Diels, J., Merckx, R., & Deckers, J. (2006). Differential ^{13}C Isotopic Discrimination in Maize at Varying Water Stress and at Low to High Nitrogen Availability. *Plant and Soil*, *282*(1-2), 313-326. https://doi.org/10.1007/s11104-006-0001-8

Eggels, S., Blankenagel, S., Schön, C. C., & Avramova, V. (2021). The carbon isotopic signature of C_4 crops and its applicability in breeding for climate resilience. *Theor Appl Genet*, *134*(6), 1663-1675. https://doi.org/10.1007/s00122-020-03761-3

Ellsworth, P. Z., & Cousins, A. B. (2016). Carbon isotopes and water use efficiency in C_4 plants. *Curr Opin Plant Biol*, *31*, 155-161. https://doi.org/10.1016/j.pbi.2016.04.006

Ellsworth, P. Z., Ellsworth, P. V., & Cousins, A. B. (2017). Relationship of leaf oxygen and carbon isotopic composition with transpiration efficiency in the C_4 grasses *Setaria viridis* and *Setaria italica*. *J Exp Bot*, *68*(13), 3513-3528. https://doi.org/10.1093/jxb/erx185

Ellsworth, P. Z., Feldman, M. J., Baxter, I., & Cousins, A. B. (2020). A genetic link between leaf carbon isotope composition and whole-plant water use efficiency in the C_4 grass *Setaria*. *Plant J*, *102*(6), 1234-1248. https://doi.org/10.1111/tpj.14696

Evans, J., & Poorter, H. (2001). Photosynthetic acclimation of plants to growth irradiance: the relative importance of specific leaf area and nitrogen partitioning in maximizing carbon gain. *Plant Cell Environ*, *24*(8), 755-767.

Farquhar, G. D. (1983). On the nature of carbon isotope discrimination in C_4 species. *Functional Plant Biology*, *10*(2), 205-226.

Farquhar, G. D., & Cernusak, L. A. (2012). Ternary effects on the gas exchange of isotopologues of carbon dioxide. *Plant Cell Environ*, *35*(7), 1221-1231. https://doi.org/10.1111/j.1365-3040.2012.02484.x

Farquhar, G. D., Ehleringer, J. R., & Hubick, K. T. (1989a). Carbon isotope discrimination and photosynthesis. *Annual review of plant biology*, *40*(1), 503-537.

Farquhar, G. D., Hubick, K., Condon, A., & Richards, R. (1989b). Carbon isotope fractionation and plant water-use efficiency. In *Stable isotopes in ecological research* (pp. 21-40). Springer.

Farquhar, G. D., O'Leary, M. H., & Berry, J. A. (1982). On the relationship between carbon isotope discrimination and the intercellular carbon dioxide concentration in leaves. *Functional Plant Biology*, *9*(2), 121-137.

Farquhar, G. D., & Richards, R. A. (1984). Isotopic composition of plant carbon correlates with water-use efficiency of wheat genotypes. *Functional Plant Biology*, *11*(6), 539-552.

Feldman, M. J., Ellsworth, P. Z., Fahlgren, N., Gehan, M. A., Cousins, A. B., & Baxter, I. (2018). Components of Water Use Efficiency Have Unique Genetic Signatures in the Model C_4 Grass *Setaria*. *Plant Physiol*, *178*(2), 699-715. https://doi.org/10.1104/pp.18.00146

Francey, R., Gifford, R., Sharkey, T., & Weir, B. (1985). Physiological influences on carbon isotope discrimination in huon pine (*Lagarostrobos franklinii*). *Oecologia*, *66*(2), 211-218.

Furbank, R. T. (2011). Evolution of the C_4 photosynthetic mechanism: are there really three C_4 acid decarboxylation types? *J Exp Bot*, *62*(9), 3103-3108. https://doi.org/10.1093/jxb/err080

Furbank, R. T., & Kelly, S. (2021). Finding the C_4 sweet spot: cellular compartmentation of carbohydrate metabolism in C_4 photosynthesis. *J Exp Bot*, *72*(17), 6018-6026. https://doi.org/10.1093/jxb/erab290

Ghannoum, O., von Caemmerer, S., & Conroy, J. P. (2002). The effect of drought on plant water use efficiency of nine NAD-ME and nine NADP-ME Australian C_4 grasses. *Funct Plant Biol*, *29*(11), 1337-1348. https://doi.org/10.1071/FP02056

Ghashghaie, J., & Badeck, F. W. (2014). Opposite carbon isotope discrimination during dark respiration in leaves versus roots - a review. *New Phytol*, *201*(3), 751-769. https://doi.org/10.1111/nph.12563

Gibon, Y., Blaesing, O. E., Hannemann, J., Carillo, P., Hohne, M., Hendriks, J. H., Palacios, N., Cross, J., Selbig, J., & Stitt, M. (2004). A Robot-based platform to measure multiple enzyme activities in Arabidopsis using a set of cycling assays: comparison of changes of enzyme activities and transcript levels during diurnal cycles and in prolonged darkness. *Plant Cell*, *16*(12), 3304-3325. https://doi.org/10.1105/tpc.104.025973

Gong, X. Y., Schäufele, R., Feneis, W., & Schnyder, H. (2015). $^{13}CO_2$ /$^{12}CO_2$ exchange fluxes in a clamp-on leaf cuvette: disentangling artefacts and flux components. *Plant Cell Environ*, *38*(11), 2417-2432. https://doi.org/10.1111/pce.12564

Gong, X. Y., Schäufele, R., & Schnyder, H. (2017). Bundle-sheath leakiness and intrinsic water use efficiency of a perennial C_4 grass are increased at high vapour pressure deficit during growth. *J Exp Bot*, *68*(2), 321-333. https://doi.org/10.1093/jxb/erw417

Gresset, S. (2014). Genetische Analyse der stabilen Kohlenstoffisotopendiskriminierung in einer Mais (Zea mays L.) Introgressionsbibliothek. *Dissertation, Technische Universität München.*

Gresset, S., Westermeier, P., Rademacher, S., Ouzunova, M., Presterl, T., Westhoff, P., & Schön, C. C. (2014). Stable carbon isotope discrimination is under genetic control in the C_4 species maize with several genomic regions influencing trait expression. *Plant Physiol*, *164*(1), 131-143. https://doi.org/10.1104/pp.113.224816

Hammer, G. L., Farquhar, G. D., & Broad, I. J. (1997). On the extent of genetic variation for transpiration efficiency in sorghum. *Australian Journal of Agricultural Research*, *48*(5), 649-656.

Hatch, M. D. (1987). C_4 photosynthesis: a unique blend of modified biochemistry, anatomy and ultrastructure. *Biochimica et Biophysica Acta (BBA)-Reviews on Bioenergetics*, *895*(2), 81-106.

Henderson, S., von Caemmerer, S., Farquhar, G. D., Wade, L., & Hammer, G. (1998). Correlation between carbon isotope discrimination and transpiration efficiency in lines of the C_4 species *Sorghum bicolor* in the glasshouse and the field. *Functional Plant Biology*, *25*(1), 111-123.

Henderson, S. A., von Caemmerer, S., & Farquhar, G. D. (1992). Short-term measurements of carbon isotope discrimination in several C_4 species. *Functional Plant Biology*, *19*(3), 263-285.

Hobbie, E. A., & Werner, R. A. (2004). Intramolecular, compound-specific, and bulk carbon isotope patterns in C_3 and C_4 plants: a review and synthesis. *New Phytologist*, *161*(2), 371-385.

Jiao, Y., Peluso, P., Shi, J., Liang, T., Stitzer, M. C., Wang, B., Campbell, M. S., Stein, J. C., Wei, X., Chin, C. S., Guill, K., Regulski, M., Kumari, S., Olson, A., Gent, J., Schneider, K. L., Wolfgruber, T. K., May, M. R., Springer, N. M., . . . Ware, D. (2017). Improved maize reference genome with single-molecule technologies. *Nature*, *546*(7659), 524-527. https://doi.org/10.1038/nature22971

Kolbe, A. R., & Cousins, A. B. (2018). Mesophyll conductance in *Zea mays* responds transiently to CO_2 availability: implications for transpiration efficiency in C_4 crops. *New Phytol*, *217*(4), 1463-1474. https://doi.org/10.1111/nph.14942

Kolbe, A. R., Studer, A. J., & Cousins, A. B. (2018). Biochemical and transcriptomic analysis of maize diversity to elucidate drivers of leaf carbon isotope composition. *Funct Plant Biol*, *45*(5), 489-500. https://doi.org/10.1071/FP17265

Kromdijk, J., Schepers, H. E., Albanito, F., Fitton, N., Carroll, F., Jones, M. B., Finnan, J., Lanigan, G. J., & Griffiths, H. (2008). Bundle sheath leakiness and light limitation during C_4 leaf and canopy CO_2 uptake. *Plant Physiol*, *148*(4), 2144-2155. https://doi.org/10.1104/pp.108.129890

Kromdijk, J., Ubierna, N., Cousins, A. B., & Griffiths, H. (2014). Bundle-sheath leakiness in C_4 photosynthesis: a careful balancing act between CO_2 concentration and assimilation. *J Exp Bot*, *65*(13), 3443-3457. https://doi.org/10.1093/jxb/eru157

Kubasek, J., Setlik, J., Dwyer, S., & Santrucek, J. (2007). Light and growth temperature alter carbon isotope discrimination and estimated bundle sheath leakiness in C_4 grasses and dicots. *Photosynth Res*, *91*(1), 47-58. https://doi.org/10.1007/s11120-007-9136-6

Leach, K. A., & Braun, D. M. (2016). Soluble Sugar and Starch Extraction and Quantification from Maize (*Zea mays*) Leaves. *Curr Protoc Plant Biol*, *1*(1), 139-161. https://doi.org/10.1002/cppb.20018

Leakey, A. D. B. (2009). Rising atmospheric carbon dioxide concentration and the future of C_4 crops for food and fuel. *Proc Biol Sci*, *276*(1666), 2333-2343. https://doi.org/10.1098/rspb.2008.1517

Leakey, A. D. B., Ferguson, J. N., Pignon, C. P., Wu, A., Jin, Z., Hammer, G. L., & Lobell, D. B. (2019). Water Use Efficiency as a Constraint and Target for Improving the Resilience and Productivity of C_3 and C_4 Crops. *Annu Rev Plant Biol*, *70*, 781-808. https://doi.org/10.1146/annurev-arplant-042817-040305

Lenth, R. V. (2022). emmeans: Estimated Marginal Means, aka Least-Squares Means. *R package version 1.7.2. https://CRAN.R-project.org/package=emmeans*.

Lichtenthaler, H. K. (1987). Chlorophylls and carotenoids: pigments of photosynthetic biomembranes. In *Methods in enzymology* (Vol. 148, pp. 350-382). Elsevier.

Medrano, H., Tomás, M., Martorell, S., Flexas, J., Hernández, E., Rosselló, J., Pou, A., Escalona, J.-M., & Bota, J. (2015). From leaf to whole-plant water use efficiency (WUE) in complex canopies: Limitations of leaf WUE as a selection target. *The Crop Journal*, *3*(3), 220-228.

Mertz, R. A., & Brutnell, T. P. (2014). Bundle sheath suberization in grass leaves: multiple barriers to characterization. *J Exp Bot*, *65*(13), 3371-3380. https://doi.org/10.1093/jxb/eru108

Monneveux, P., Sheshshayee, M. S., Akhter, J., & Ribaut, J.-M. (2007). Using carbon isotope discrimination to select maize (*Zea mays* L.) inbred lines and hybrids for drought tolerance. *Plant Science*, *173*(4), 390-396. https://doi.org/10.1016/j.plantsci.2007.06.003

Pimentel, C., Laffray, D., & Louguet, P. (1999). Intrinsic water use efficiency at the pollination stage as a parameter for drought tolerance selection in Phaseolus vulgaris. *Physiologia Plantarum*, *106*(2), 184-189.

Poorter, H., Fiorani, F., Pieruschka, R., Wojciechowski, T., van der Putten, W. H., Kleyer, M., Schurr, U., & Postma, J. (2016). Pampered inside, pestered outside? Differences and similarities between plants growing in controlled conditions and in the field. *New Phytol*, *212*(4), 838-855. https://doi.org/10.1111/nph.14243

R Core Team, R. (2019). R: A language and environment for statistical computing. *R Foundation for Statistical Computing, Vienna, Austria. URL https://www.R-project.org/.*

Rao, R. N., Udaykumar, M., Farquhar, G., Talwar, H., & Prasad, T. (1995). Variation in carbon isotope discrimination and its relationship to specific leaf area and ribulose-1, 5-bisphosphate carboxylase content in groundnut genotypes. *Functional Plant Biology*, *22*(4), 545-551.

Rebetzke, G., Condon, A. G., Richards, R., & Farquhar, G. (2002). Selection for reduced carbon isotope discrimination increases aerial biomass and grain yield of rainfed bread wheat. *Crop science*, *42*(3), 739-745.

Rebetzke, G. J., Condon, A. G., Farquhar, G. D., Appels, R., & Richards, R. A. (2008). Quantitative trait loci for carbon isotope discrimination are repeatable across environments and wheat mapping populations. *Theor Appl Genet*, *118*(1), 123-137. https://doi.org/10.1007/s00122-008-0882-4

Retta, M., Ho, Q. T., Yin, X., Verboven, P., Berghuijs, H. N. C., Struik, P. C., & Nicolai, B. M. (2016). A two-dimensional microscale model of gas exchange during photosynthesis in maize (*Zea mays* L.) leaves. *Plant Sci*, *246*, 37-51. https://doi.org/10.1016/j.plantsci.2016.02.003

RStudio Team, R. (2021). Integrated Development Environment for R. *RStudio, PBC, Boston, MA URL http://www.rstudio.com/*.

Ryan, A. C., Dodd, I. C., Rothwell, S. A., Jones, R., Tardieu, F., Draye, X., & Davies, W. J. (2016). Gravimetric phenotyping of whole plant transpiration responses to atmospheric vapour pressure deficit identifies genotypic variation in water use efficiency. *Plant Sci*, *251*, 101-109. https://doi.org/10.1016/j.plantsci.2016.05.018

Sage, R. F. (2017). A portrait of the C_4 photosynthetic family on the 50th anniversary of its discovery: species number, evolutionary lineages, and Hall of Fame. *J Exp Bot*, *68*(2), 4039-4056. https://doi.org/10.1093/jxb/erx005

Saghai-Maroof, M. A., Soliman, K. M., Jorgensen, R. A., & Allard, R. (1984). Ribosomal DNA spacer-length polymorphisms in barley: Mendelian inheritance, chromosomal location, and population dynamics. *Proceedings of the National Academy of Sciences*, *81*(24), 8014-8018.

Sales, C. R. G., Wang, Y., Evers, J. B., & Kromdijk, J. (2021). Improving C_4 photosynthesis to increase productivity under optimal and suboptimal conditions. *J Exp Bot*, *72*(17), 5942-5960. https://doi.org/10.1093/jxb/erab327

Saliendra, N. Z., Meinzer, F. C., Perry, M., & Thom, M. (1996). Associations between partitioning of carboxylase activity and bundle sheath leakiness to CO_2, carbon isotope

discrimination, photosynthesis, and growth in sugarcane. *Journal of Experimental Botany*, *47*(7), 907-914.

Sanborn, L. H., Reid, R. E. B., Bradley, A. S., & Liu, X. (2021). The effect of water availability on the carbon and nitrogen isotope composition of a C_4 plant (pearl millet, *Pennisetum glaucum*). *Journal of Archaeological Science: Reports*, *38*. https://doi.org/10.1016/j.jasrep.2021.103047

Sanchez-Bragado, R., Araus, J. L., Scheerer, U., Cairns, J. E., Rennenberg, H., & Ferrio, J. P. (2016). Factors preventing the performance of oxygen isotope ratios as indicators of grain yield in maize. *Planta*, *243*(2), 355-368. https://doi.org/10.1007/s00425-015-2411-4

Schlüter, U., Brautigam, A., Droz, J. M., Schwender, J., & Weber, A. P. M. (2019). The role of alanine and aspartate aminotransferases in C_4 photosynthesis. *Plant Biol*, *21* 64-76. https://doi.org/10.1111/plb.12904

Schneider, C. A., Rasband, W. S., & Eliceiri, K. W. (2012). NIH Image to ImageJ: 25 years of image analysis. *Nat Methods*, *9*(7), 671-675. https://doi.org/10.1038/nmeth.2089

Sharwood, R. E., Sonawane, B. V., & Ghannoum, O. (2014). Photosynthetic flexibility in maize exposed to salinity and shade. *J Exp Bot*, *65*(13), 3715-3724. https://doi.org/10.1093/jxb/eru130

Sheshshayee, M. S., Bindumadhava, H., Ramesh, R., Prasad, T. G., Lakshminarayana, M. R., & Udayakumar, M. (2005). Oxygen isotope enrichment $\Delta^{18}O$ as a measure of time-averaged transpiration rate. *J Exp Bot*, *56*(422), 3033-3039. https://doi.org/10.1093/jxb/eri300

Signorell et mult. al., A. (2020). DescTools: Tools for descriptive statistics. *R package version 0.99.32*.

Sonawane, B. V., & Cousins, A. B. (2020). Mesophyll CO_2 conductance and leakiness are not responsive to short- and long-term soil water limitations in the C_4 plant *Sorghum bicolor*. *Plant J*. https://doi.org/10.1111/tpj.14849

Sorgini, C. A., Roberts, L. M., Sullivan, M., Cousins, A. B., Baxter, I., & Studer, A. J. (2021). The genetic architecture of leaf stable carbon isotope composition in *Zea mays* and the effect of transpiration efficiency on leaf elemental accumulation. *G3 (Bethesda)*, *11*(9). https://doi.org/10.1093/g3journal/jkab222

Sulpice, R., Tschoep, H., M, V. O. N. K., Bussis, D., Usadel, B., Hohne, M., Witucka-Wall, H., Altmann, T., Stitt, M., & Gibon, Y. (2007). Description and applications of a rapid and sensitive non-radioactive microplate-based assay for maximum and initial activity of D-ribulose-1,5-bisphosphate carboxylase/oxygenase. *Plant Cell Environ*, *30*(9), 1163-1175. https://doi.org/10.1111/j.1365-3040.2007.01679.x

Sun, W., Ubierna, N., Ma, J. Y., & Cousins, A. B. (2012). The influence of light quality on C_4 photosynthesis under steady-state conditions in *Zea mays* and *Miscanthus* x *giganteus*: changes in rates of photosynthesis but not the efficiency of the CO_2 concentrating mechanism. *Plant Cell Environ*, *35*(5), 982-993. https://doi.org/10.1111/j.1365-3040.2011.02466.x

Twohey, R. J., 3rd, Roberts, L. M., & Studer, A. J. (2019). Leaf stable carbon isotope composition reflects transpiration efficiency in *Zea mays*. *Plant J*, *97*(3), 475-484. https://doi.org/10.1111/tpj.14135

Ubierna, N., Gandin, A., & Cousins, A. B. (2018). The response of mesophyll conductance to short-term variation in CO_2 in the C_4 plants *Setaria viridis* and *Zea mays*. *J Exp Bot*, *69*(5), 1159-1170. https://doi.org/10.1093/jxb/erx464

Ubierna, N., Sun, W., & Cousins, A. B. (2011). The efficiency of C_4 photosynthesis under low light conditions: assumptions and calculations with CO_2 isotope discrimination. *J Exp Bot*, *62*(9), 3119-3134. https://doi.org/10.1093/jxb/err073

Ubierna, N., Sun, W., Kramer, D. M., & Cousins, A. B. (2013). The efficiency of C_4 photosynthesis under low light conditions in *Zea mays, Miscanthus* x *giganteus* and *Flaveria bidentis*. *Plant Cell Environ*, *36*(2), 365-381. https://doi.org/10.1111/j.1365-3040.2012.02579.x

Unterseer, S., Bauer, E., Haberer, G., Seidel, M., Knaak, C., Ouzunova, M., Meitinger, T., Strom, T. M., Fries, R., & Pausch, H. (2014). A powerful tool for genome analysis in

maize: development and evaluation of the high density 600 k SNP genotyping array. *BMC genomics*, *15*(1), 1-15.

Vadez, V., Choudhary, S., Kholova, J., Hash, C. T., Srivastava, R., Kumar, A. A., Prandavada, A., & Anjaiah, M. (2021). Transpiration efficiency: insights from comparisons of C_4 cereal species. *J Exp Bot*, *72*(14), 5221-5234. https://doi.org/10.1093/jxb/erab251

Vadez, V., Kholova, J., Medina, S., Kakkera, A., & Anderberg, H. (2014). Transpiration efficiency: new insights into an old story. *J Exp Bot*, *65*(21), 6141-6153. https://doi.org/10.1093/jxb/eru040

von Caemmerer, S. (2021). Updating the steady-state model of C_4 photosynthesis. *J Exp Bot*, *72*(17), 6003-6017. https://doi.org/10.1093/jxb/erab266

von Caemmerer, S., & Furbank, R. T. (2003). The C_4 pathway: an efficient CO_2 pump. *Photosynthesis research*, *77*(2), 191-207.

von Caemmerer, S., Ghannoum, O., Pengelly, J. J., & Cousins, A. B. (2014). Carbon isotope discrimination as a tool to explore C_4 photosynthesis. *J Exp Bot*, *65*(13), 3459-3470. https://doi.org/10.1093/jxb/eru127

Werner, R. A., & Rossmann, A. (2015). Multi element (C, H, O) stable isotope analysis for the authentication of balsamic vinegars. *Isotopes Environ Health Stud*, *51*(1), 58-67. https://doi.org/10.1080/10256016.2015.1011154

Westgate, M. E., & Boyer, J. S. (1985). Carbohydrate Reserves and Reproductive Development at Low Leaf Water Potentials in Maize. *Crop science*, *25*(5), 762-769.

Wickham, H. (2016). ggplot2: Elegant Graphics for Data Analysis. *Springer-Verlag New York. ISBN 978-3-319-24277-4, https://ggplot2.tidyverse.org.*

Williams, D., Gempko, V., Fravolini, A., Leavitt, S., Wall, G., Kimball, B., Pinter Jr, P., LaMorte, R., & Ottman, M. (2001). Carbon isotope discrimination by *Sorghum bicolor* under CO_2 enrichment and drought. *New Phytologist*, *150*(2), 285-293.

Xie, J., Fernandes, S. B., Mayfield-Jones, D., Erice, G., Choi, M., A, E. L., & Leakey, A. D. B. (2021). Optical topometry and machine learning to rapidly phenotype stomatal patterning traits for maize QTL mapping. *Plant Physiol*, *187*(3), 1462-1480. https://doi.org/10.1093/plphys/kiab299

Xu, X., Martin, B., Comstock, J. P., Vision, T. J., Tauer, C. G., Zhao, B., Pausch, R. C., & Knapp, S. (2008). Fine mapping a QTL for carbon isotope composition in tomato. *Theor Appl Genet*, *117*(2), 221-233. https://doi.org/10.1007/s00122-008-0767-6

Yang, Z., Liu, J., Tischer, S. V., Christmann, A., Windisch, W., Schnyder, H., & Grill, E. (2016). Leveraging abscisic acid receptors for efficient water use in *Arabidopsis*. *Proc Natl Acad Sci U S A*, *113*(24), 6791-6796. https://doi.org/10.1073/pnas.1601954113

Yu, J., Holland, J. B., McMullen, M. D., & Buckler, E. S. (2008). Genetic design and statistical power of nested association mapping in maize. *Genetics*, *178*(1), 539-551. https://doi.org/10.1534/genetics.107.074245

Zhang, C., Zhang, J., Zhang, H., Zhao, J., Wu, Q., Zhao, Z., & Cai, T. (2015). Mechanisms for the relationships between water-use efficiency and carbon isotope composition and specific leaf area of maize (*Zea mays* L.) under water stress. *Plant Growth Regulation*, *77*(2), 233-243. https://doi.org/10.1007/s10725-015-0056-8

6 Supplement

Supplementary Figures

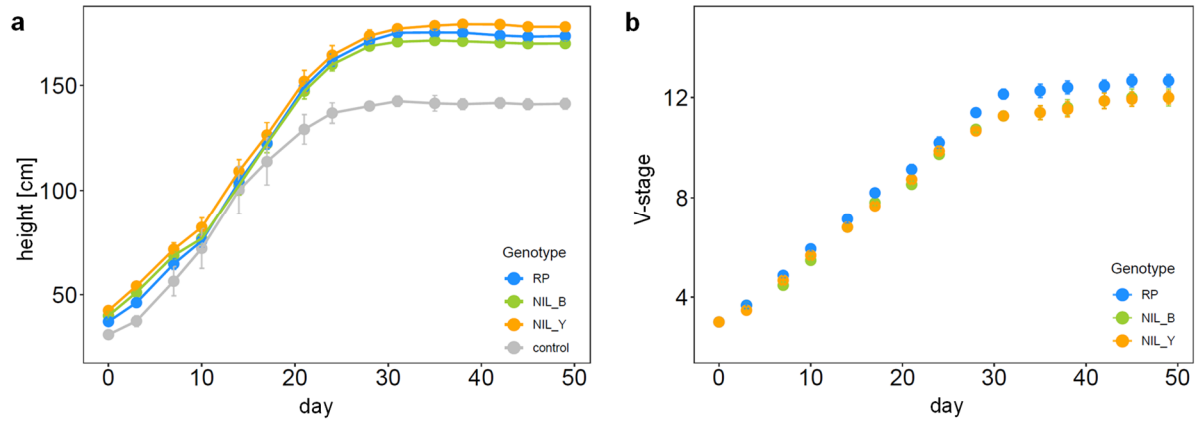

Figure S1: Plant height (a) and average vegetative developmental stage (V-stage, b) of near isogenic lines NIL B and NIL Y and recurrent parent RP during a progressive drought experiment for determining whole plant water use efficiency.
At day 0, two-week-old plants were watered to field capacity, covered with foil and not watered further until the end of the experiment. Pots of "control" plants (grey) were not covered with foil. Plant height and V-stage were scored every three to four days until the end of the experiment, when plants had stopped growing. Shown are means ± SE. n=14-15, for control n=5.

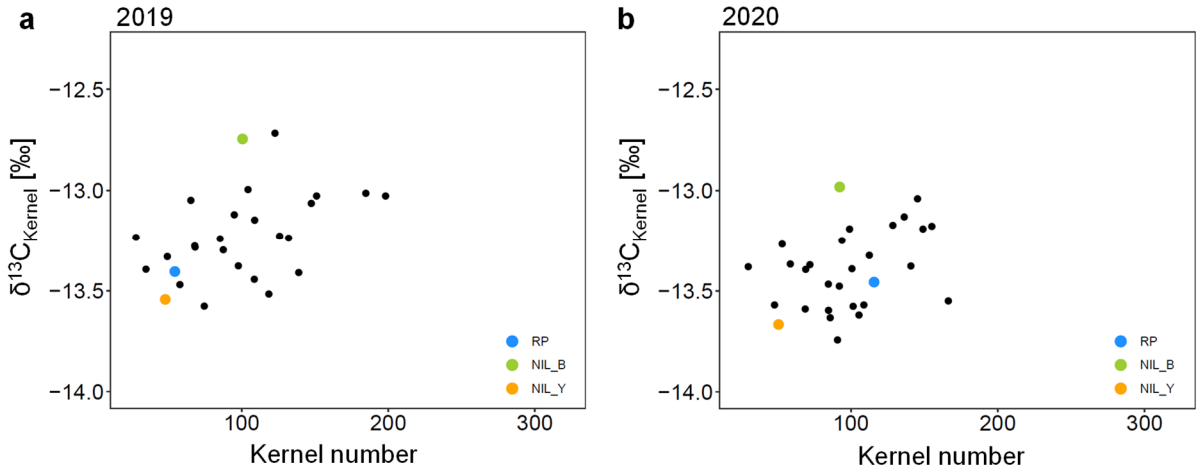

Figure S2: Mean carbon isotopic composition of kernels ($\delta^{13}C_{Kernel}$) plotted against the mean kernel number per plant of the respective genotype in the field trials 2019 (a) and 2020 (b) under water-limited conditions.
Shown are data of 25 and 27 introgression lines, in 2019 and 2020 respectively, and their common recurrent parent (RP) and donor parent. Data for RP, NIL B and NIL Y are highlighted by colored symbols of bigger size. Data are means over three or six plots adjusted for the block effect of the experimental design. Watering was restricted between developmental stage V9 and R1. For 2019, r^2=0.17 (p=0.019), for 2020, correlation was not significant (p=0.061). For values of means ± SE see Table S8.

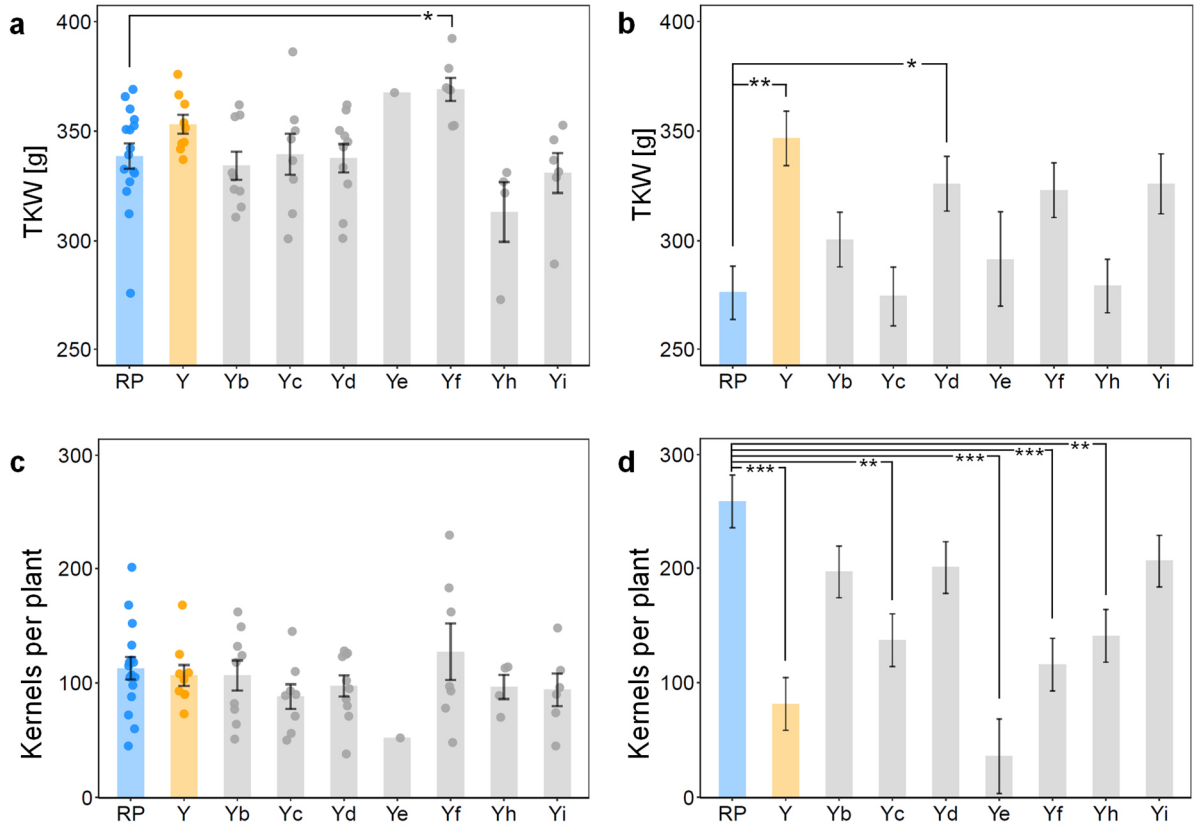

Figure S3: Thousand kernel weight (TKW) and kernel number per plant of NIL Y-derived recombinant lines grown in the greenhouse (a, c, Exp. 2.6) and field (b, d, 2021).
Bars show mean ± SE, a) and c) round symbols show values of individual plants. In the greenhouse, 20 plants of RP and 10 of all other genotypes were grown, resulting in n for kernel traits of 1-16. For the field, means over six plots are shown, except for Ye, where three plots were included. Significant differences compared to RP based on a Dunnett's test are indicated as: *: p<0.05, **: p<0.01, ***: p<0.001.

.

Supplementary tables

Table S1: Introgressions of NIL C, NIL W and NIL X with starting and end coordinates on the respective chromosomes (chr) in bp. Coordinates are based on B73 AGPv4.

	NIL C	NIL W	NIL X
	borders [bp]	borders [bp]	borders [bp]
chr 2	-	-	37,549 - 421,419
chr 3	-	22,276,445 - 22,476,752	-
	-	23,172,062 - 24,345,266	-
chr 8	-	181,189 - 1,591,008	-
chr 10	5,012,724 - 110,663,362	134,353,678 - 137,260,558	824,847 - 12,278,265
	138,709,471 - 140,554,980	-	-

Table S2: Primer sequences for KASP markers used for generation of NIL BY and recombinant lines derived from NIL Y with marker coordinates (B73 AGPv4) on the respective chromosome (chr). Nucleotide bases differing between recurrent parent and the donor parent given in brackets.

ID	chr	position [bp]	sequence
AX-90528533	1	8,048,178	CAAGACCCTATATTTCCTAATAGAATAAATTTGTG[A/T]ACGAGCCTTTACCTACTAAAATGCCACACTAATAT
AX-90528544	1	9,638,977	TCAACTCCAGCATGAATCCGTTTTCATCTATGCTC[A/G]TCCCTGTGCTTGCATTGTACGAAAGGGCAGCATCT
AX-90564732	1	12,146,599	CGGGAGACTAGGGAGAATGGTATGGAATGGATTGC[A/G]AGCGCAGCCGCTCCTCCTCCCCCTCCCTGTTGGAC
AX-90598853	1	14,082,518	TTGGCTTTCCCTCCGCTATACTTCTTGGAAAAATC[A/C]TCCTTGACTCTTTCAATAAATCCAACTGGAAG
AX-91456390	1	16,129,251	ACCTGTTGGAGCCTAGCTCCCTTGTACGTGCTCCA[C/T]TTGGCCTATAAAAGTGAGGACACATGTGTT
AX-91456763	1	18,001,999	GGTTTTGACTTGACGACCACTGCAACACAATCCAC[C/G]CCACCAGCAGAACTTTCTTTTGCTTGGGAGCCGGG
AX-90570846	1	20,022,709	TATAGCCCCTCCAGGTAACTTGTTTTATTGCCAAG[C/T]GTTGATCGTACCATACCAACTGAAGCTGAAGGCCT
AX-91457497	1	22,006,632	ATTTTTTGAGTGCATATCAACCATAGGAGCGGCCC[C/T]TCTTACCTGCAGTCGCTGCAGTTGGTGTATACAGA
AX-90656493	1	24,417,904	AGCAAGGGTGGTCGGACTACGTGATTTGATAACTT[C/T]CAGAGGGTCTGTTTGCAAATATTTAGTGCAGGAGA
AX-90528796	1	26,609,865	TCTTGGGAGAATCTCGGCCGCAAATGGATCGGACG[A/G]AAGTTGGGAATGAATAAAGGCCGCAATGACGGCGA
AX-90526031	1	28,638,770	TCTCGAGACTAGACCACTGGCAATACATTACGCTG[A/G]AAAGCATACCTCATTTACACACCTAAACTACTCGG
AX-90528864	1	30,554,699	TTTATGCAGCCGACGATCGATCCAGTACTACTCTA[A/C]TAGTAGAGTATGTGATTGGCGATAGGTAACGACGA
AX-90528910	1	32,474,714	TTAATGGCATAAATTGATAATATATCTGCATATGA[C/T]CATCATTTAGCAGCTAGTGTGGTTTCTAGCACTAG
AX-90528942	1	34,592,871	TGTGAGATAAGCCTTGTTTAGCCTCTGTTGATACT[G/T]GGCGTCTTCTATTAAAGCTGCACGCTGAAAACAAT
AX-91393015	3	212,550,017	GCTGATCGCTCCCCTTCCATGGCCTTGCGCCTTCC[C/G]GTCCATCAGCGAGGCTAGATAAACGGTGATCAGTA
AX-90607846	3	215,865,146	GCCAGCTTTGTCCAGTGTGCGCATTCCAGACACAA[C/T]GATGAAACCATGTGTGAGCACCGGTAGTGACTTCA
AX-91355356	7	4,233,140	TATATTCGAAGCTAAGGTTACCAGTAGTGGTGTCA[C/T]TGCCACACCATATGGTAATAACCGCTCAGACTGAC
AX-90570605	7	5,052,968	CAGATGGTTAACTAAGGCAAGCGAATTGATCGAGG[A/G]CGTGCGCCGGTTGCATGCTCCGTAAGTTACCTGCT
AX-91356933	7	118,512,477	GGTAAACCTTACACACAATAACCGGCAAGACAGGA[A/C]AAAGGAGTAGCCTACAGCATCATGAAACCATAAAT
AX-90552118	7	124,341,628	CTGTCCCACCACCACTTGTTCAGCTGCACTTCGAC[C/T]CAATACATGTGGATTGGGGTGGATTAGAGTGGAGC
AX-90527158	7	132,117,607	TTCTGACCTGACCTAGTTTATAGCACCTGATCGGA[A/G]TGGCGTCCATTCTTCTCGCTGAGAAGGTCGTTCTG
AX-90552405	7	141,161,954	TGTGACCTGTATTACACTCAAGAAGCTATCAGCAA[A/G]TACCTGGTAGCTCTGCCAATAACTTCACCATTAGC
AX-90572351	7	155,419,484	ATTCAAAAATTGGATCTGGTGAGGGTGATTGTGTC[A/G]CTACCCCAGCACCCCCATCCATTGAAGCTTCACCT
AX-90552866	7	173,286,556	AATTGACCACGTTAAAGATCACTTCTCTAGTACTA[A/G]AAATCTAGAACCCACCCGTTTAGCAGAATTCCCAG
AX-90553010	8	494,673	TGTCGCTTACCAGCGCGCACAGATTGGATCAGATC[A/G]GTGATCGGGTGAAGGAAGGAGACATCCGGAGATAT

Table S3: Kernel isotopic compositions and growth- and yield-related traits of RP, NIL B and NIL Y grown in field trials 2019 and 2020 under well-watered (control) and semi-controlled drought conditions.

$\delta^{13}C_{Kernel}$, kernel carbon isotopic composition, $\delta^{18}O_{Kernel}$, kernel oxygen isotopic composition, TKW, thousand kernel weight, final PH, final plant height, DTS, days to silking, DTT, days to tasseling, SPAD, chlorophyll meter measurements at developmental stages V6, V9 and R1. Numbers for DTS and DTT refer to the day number of the year. Listed are means over six plots ± SE. Significant differences compared to RP based on a Dunnett's test are indicated as *: p<0.05, **: p<0.01, ***: p<0.001. ns, not significant. $\delta^{13}C_{Kernel}$ data of RP and NIL B for 2019, control also published in Blankenagel et al. (2022).

		$\delta^{13}C_{Kernel}$ [‰]	$\delta^{18}O_{Kernel}$ [‰]	Kernel number	TKW [g]	final PH [cm]	DTS	DTT	SPAD V6	SPAD V9	SPAD R1
2019 control	RP	-12.93 ± 0.03	27.32 ± 0.10	224 ± 25	300 ± 7	203.8 ± 3.2	212 ± 1	214 ± 1	32.2 ± 0.9	34.2 ± 1.3	48.1 ± 0.7
	NIL B	-12.37 ± 0.03***	26.68 ± 0.10***	205 ± 25 ns	284 ± 7 ns	196.1 ± 3.2 ns	209 ± 1 ns	210 ± 1*	30.0 ± 0.8 ns	32.3 ± 1.3 ns	49.3 ± 0.7 ns
	NIL Y	-13.19 ± 0.03***	25.80 ± 0.10***	135 ± 25*	322 ± 7 ns	183.6 ± 3.2**	211 ± 1 ns	213 ± 1 ns	25.9 ± 0.8***	28.2 ± 1.3*	46.2 ± 0.7 ns
2019 drought	RP	-13.41 ± 0.04	26.44 ± 0.10	54 ± 10	249 ± 10	155.6 ± 4.3	217 ± 1	214 ± 1	30.0 ± 0.7	35.2 ± 1.1	42.2 ± 0.9
	NIL B	-12.75 ± 0.04***	26.65 ± 0.10 ns	101 ± 10**	287 ± 10*	167.5 ± 4.3 ns	213 ± 1*	209 ± 1**	27.5 ± 0.7 ns	28.3 ± 1.1**	43.9 ± 0.8 ns
	NIL Y	-13.54 ± 0.04*	25.55 ± 0.10***	48 ± 10 ns	310 ± 10**	176.1 ± 4.3*	213 ± 1*	211 ± 1 ns	25.5 ± 0.8**	30.8 ± 1.1*	42.6 ± 0.8 ns
2020 control	RP	-13.18 ± 0.04		160 ± 16	317 ± 6	165.6 ± 5.9	215 ± 1	215 ± 1	24.8 ± 1.1	29.9 ± 1.2	41.0 ± 1.4
	NIL B	-12.76 ± 0.04***		150 ± 16 ns	313 ± 6 ns	168.6 ± 5.9 ns	216 ± 1 ns	215 ± 1 ns	23.8 ± 1.1 ns	29.1 ± 1.2 ns	41.1 ± 1.4 ns
	NIL Y	-13.41 ± 0.04**		46 ± 16***	362 ± 6***	168.1 ± 5.9 ns	211 ± 1**	212 ± 1*	26.5 ± 1.1 ns	28.1 ± 1.2 ns	38.2 ± 1.4 ns
2020 drought	RP	-13.46 ± 0.07		116 ± 6	261 ± 4	169.2 ± 5.1	215 ± 1	216 ± 1	27.8 ± 0.7	35.4 ± 0.9	38.5 ± 0.8
	NIL B	-12.98 ± 0.07***		92 ± 6*	266 ± 4 ns	161.4 ± 5.1 ns	216 ± 1*	215 ± 1 ns	24.8 ± 0.7*	32.2 ± 0.9 ns	40.3 ± 0.8 ns
	NIL Y	-13.67 ± 0.07 ns		51 ± 6***	305 ± 4***	153.9 ± 5.1 ns	211 ± 1 ns	213 ± 1 ns	25.9 ± 0.7 ns	30.6 ± 0.9**	36.0 ± 0.8 ns

Table S4: Stomatal density (St. density) and isotopic compositions of RP, NIL B, NIL Y and NIL BY grown in the greenhouse (Exp. 2.5).
St. density was determined on the youngest fully developed leaf at stage V5/6 (n=14-15). Carbon isotopic composition ($\delta^{13}C$) of the cobleaf was determined at flowering before pollination (n=9). $\delta^{13}C_{Kernel}$, carbon isotopic composition of kernels, $\delta^{18}O_{Kernel}$, oxygen isotopic composition of kernels (n=8-17). Listed are means ± SE. For stomatal density, means are adjusted for the developmental stage. Significant differences based on a Tukey test for st. density and based on pairwise t-tests for isotopic compositions are indicated by different letters ($p<0.05$).

	st. density [mm^{-2}]	$\delta^{13}C_{Cobleaf}$ [‰]	$\delta^{13}C_{Kernel}$ [‰]	$\delta^{18}O_{Kernel}$ [‰]
RP	75 ± 2 a	-13.83 ± 0.04 a	-13.52 ± 0.06 a	30.11 ± 0.26 a
NIL B	76 ± 2 a	-13.63 ± 0.05 bc	-12.90 ± 0.05 b	28.61 ± 0.18 b
NIL Y	68 ± 2 b	-13.74 ± 0.04 ab	-13.53 ± 0.03 a	28.56 ± 0.08 b
NIL BY	80 ± 2 a	-13.55 ± 0.05 c	-12.94 ± 0.04 b	28.21 ± 0.17 b

Table S5: Photosynthetic carbon isotope discrimination ($\Delta^{13}C_{Photosynthetic}$), ratio of intercellular to ambient CO_2 concentration (C_i/C_a) and leakiness of RP, NIL B and NIL Y measured concurrently at stage V5/6 in growth chamber Exp. 1.1 and 1.2.
Measurements were performed on well-watered plants and drought-treated (drought) plants. Conditions for relative humidity (RH) and photosynthetically active radiation (PAR) refer to the conditions in the leaf cuvette. If not otherwise indicated, RH=60% and PAR=1500 µmol $m^{-2}s^{-1}$. Specific leaf area (SLA) listed for well-watered plants. Depicted are means ± SE. Significant differences compared to RP based on a Dunnett's test are indicated as ***: $p<0.001$. ns, not significant. For Exp. 1.1 n=12-14. For Exp. 1.2 n=12-15, except RH 35%, n=9-10. Data of RP and NIL B in Exp. 1.2 under control conditions also published in Blankenagel et al. (2022).

	Experiment 1.1			**Experiment 1.2**		
	RP	**NIL B**	**NIL Y**	**RP**	**NIL B**	**NIL Y**
	control (RH 60%, PAR 1500 µmol $m^{-2}s^{-1}$)			control (RH 60%, PAR 1500 µmol $m^{-2}s^{-1}$)		
$\Delta^{13}C_{Photosynthetic}$ [‰]	4.49 ± 0.09	3.51 ± 0.13 ***	4.64 ± 0.08 ns	4.06 ± 0.10	3.21 ± 0.06***	3.93 ± 0.06 ns
C_i/C_a	0.36 ± 0.01	0.45 ± 0.01 ***	0.37 ± 0.01 ns	0.35 ± 0.01	0.44 ± 0.01***	0.36 ± 0.01 ns
leakiness	0.38 ± 0.01	0.30 ± 0.01***	0.39 ± 0.01 ns	0.34 ± 0.01	0.27 ± 0.01***	0.32 ± 0.01 ns
	PAR 800 µmol $m^{-2}s^{-1}$			RH 35%		
$\Delta^{13}C_{Photosynthetic}$ [‰]	4.32 ± 0.14	3.50 ± 0.14***	4.57 ± 0.16 ns	4.02 ± 0.08	3.79 ± 0.11 ns	4.25 ± 0.16 ns
C_i/C_a	0.30 ± 0.01	0.42 ± 0.01***	0.32 ± 0.09 ns	0.28 ± 0.01	0.35 ± 0.01***	0.29 ± 0.00 ns
leakiness	0.36 ± 0.02	0.29 ± 0.01**	0.39 ± 0.02 ns	0.32 ± 0.01	0.31 ± 0.01 ns	0.35 ± 0.02 ns
				drought		
$\Delta^{13}C_{Photosynthetic}$ [‰]				4.49 ± 0.17	4.16 ± 0.13 ns	4.33 ±0.10 ns
C_i/C_a				0.30 ± 0.01	0.33 ± 0.01 ns	0.30 ± 0.01 ns
leakiness				0.39 ± 0.02	0.35 ± 0.01 ns	0.37 ± 0.01 ns
SLA [cm^2/g], well-watered	322 ± 10	317 ± 9 ns	307 ± 6 ns	346 ± 7	352 ± 7 ns	362 ± 10 ns

Table S6: Gas exchange parameters of RP, NIL B and NIL Y measured on the youngest fully developed leaf around developmental stage V6 in different experiments.
For growth chamber and greenhouse experiment: V5/6, for field 2021: V6/7. g_s=stomatal conductance, A=assimilation rate, iWUE= intrinsic water use efficiency. Listed are means ± SE. Significant differences compared to RP are indicated as *: p<0.05, **: p<0.01, ***: p<0.001. ns, not significant. In Exp. 2.4 and field 2021 significance levels are based on pairwise t-tests (including the genotype NIL BY), for other experiments a Dunnett's test was used. n=12-14 for Exp.1.1, n=14 for Exp. 1.2, n=16-20 for Exp. 2.3, n=13-20 for Exp. 2.4, n=14-15 for Exp. 2.5, n=14-15 for field 2021. Data of RP and NIL B in Exp. 2.3 also published in Blankenagel et al. (2022).

Environment	Experiment	Genotype	g_s [mol $m^{-2}s^{-1}$]	A [µmol $m^{-2}s^{-1}$]	iWUE [µmol CO_2 / mol H_2O]
Growth chamber	Exp. 1.1	RP	0.193 ± 0.005	28.60 ± 0.51	148.2 ± 1.8
		NIL B	0.240 ± 0.006***	30.23 ± 0.42*	126.5 ± 2.2***
		NIL Y	0.192 ± 0.005 ns	28.01 ± 0.37 ns	146.5 ± 1.9 ns
Growth chamber	Exp. 1.2	RP	0.189 ± 0.007	28.14 ± 0.71	150.2 ± 2.7
		NIL B	0.220 ± 0.008**	28.21 ± 0.76	128.6 ± 2.2***
		NIL Y	0.193 ± 0.005 ns	28.29 ± 0.42	147.2 ± 2.4 ns
Greenhouse	Exp. 2.3	RP	0.220 ± 0.004	32.75 ± 0.30	149.9 ± 3.2
		NIL B	0.280 ± 0.004***	35.08 ± 0.77*	126.9 ± 3.2***
		NIL Y	0.187 ± 0.006**	28.67 ± 0.70***	154.7 ± 3.6 ns
Greenhouse	Exp. 2.4	RP	0.245 ± 0.004	36.68 ± 0.45	150.1 ± 1.8
		NIL B	0.312 ± 0.005***	40.13 ± 0.34***	129.0 ± 2.0***
		NIL Y	0.212 ± 0.006***	33.91 ± 0.71***	160.7 ± 2.6**
Greenhouse	Exp. 2.5	RP	0.196 ± 0.004	33.61 ± 0.51	172.1 ± 2.9
		NIL B	0.258 ± 0.005***	36.84 ± 0.26***	143.5 ± 2.8***
		NIL Y	0.196 ± 0.005 ns	33.57 ± 0.71 ns	171.4 ± 3.0 ns
Field	2021	RP	0.253 ± 0.010	44.21 ± 1.12	176.0 ± 2.9
		NIL B	0.293 ± 0.011*	46.99 ± 1.06 ns	162.0 ± 3.4**
		NIL Y	0.224 ± 0.007 ns	38.69 ± 1.20**	173.2 ± 2.2 ns

Table S7: Thousand kernel weight (TKW) and kernel number of greenhouse-grown plants of RP and NIL Y.
One ear per plant was manually pollinated. Cobs with less than 30 kernels were excluded. Listed are means ± SE. Significant differences based a Student's t-test indicated as ***: p<0.001. ns, not significant. For Exp. 2.4 n=7-10, for Exp. 2.5 n=9-17, for Exp. 2.6 n=9-16.

	Experiment 2.4		Experiment 2.5		Experiment 2.6	
	RP	NIL Y	RP	NIL Y	RP	NIL Y
Kernel number	122 ± 12	102 ± 15 ns	96 ± 17	94 ± 9 ns	113 ± 10	107 ± 9 ns
TKW [g]	292 ± 10	363 ± 9***	299 ± 7	357 ± 4***	339 ± 6	353 ± 4 ns

Table S8: Carbon isotopic composition of kernels ($\delta^{13}C_{Kernel}$) and kernel number per plant of 25 and 27 introgression lines, in 2019 and 2020 respectively, and their common recurrent parent (RP) and donor parent (DP).

Plants were grown under well-watered conditions (control) or with limited watering between developmental stage V9 and R1 (drought). Data are means over three to six plots ± SE.

	2019, control		2019, drought		2020, control		2020, drought	
Genotype	$\delta^{13}C_{Kernel}$ [‰]	Kernel number	$\delta^{13}C_{Kernel}$ [‰]	Kernel number	$\delta^{13}C_{Kernel}$ [‰]	Kernel number	$\delta^{13}C_{Kernel}$ [‰]	Kernel number
RP	-12.93 ± 0.03	224 ± 19	-13.41 ± 0.05	54 ± 10	-13.18 ± 0.04	160 ± 17	-13.46 ± 0.05	116 ± 9
NIL_B	-12.37 ± 0.03	205 ± 19	-12.75 ± 0.05	101 ± 10	-12.76 ± 0.04	150 ± 17	-12.98 ± 0.05	92 ± 9
NIL_Y	-13.19 ± 0.03	135 ± 19	-13.54 ± 0.05	48 ± 10	-13.41 ± 0.04	46 ± 17	-13.67 ± 0.05	51 ± 9
BxY	-12.69 ± 0.03	286 ± 19	-13.05 ± 0.05	65 ± 10	-12.99 ± 0.04	116 ± 17	-13.25 ± 0.05	94 ± 9
DP	-12.89 ± 0.04	203 ± 27	-13.23 ± 0.08	126 ± 14	-12.96 ± 0.06	125 ± 24	-13.27 ± 0.07	53 ± 12
IL1_004	-12.93 ± 0.04	181 ± 27	-13.38 ± 0.08	98 ± 14	-13.08 ± 0.06	85 ± 24	-13.47 ± 0.07	85 ± 12
IL1_005	-12.30 ± 0.04	252 ± 27	-12.72 ± 0.08	123 ± 14	-12.56 ± 0.06	308 ± 24	-13.04 ± 0.07	145 ± 12
IL1_006	-12.73 ± 0.04	176 ± 27	-13.28 ± 0.08	68 ± 14	-13.11 ± 0.06	70 ± 24	-13.39 ± 0.07	69 ± 12
IL1_007	-12.94 ± 0.04	127 ± 27	-13.23 ± 0.08	28 ± 14	-13.01 ± 0.06	40 ± 24	-13.38 ± 0.07	30 ± 12
IL1_025	-13.17 ± 0.04	163 ± 27	-13.52 ± 0.08	119 ± 14	-13.31 ± 0.06	83 ± 24	-13.63 ± 0.07	86 ± 12
IL1_040	-13.09 ± 0.04	153 ± 27	-13.27 ± 0.08	68 ± 14	-13.32 ± 0.06	85 ± 24	-13.62 ± 0.07	105 ± 12
IL1_049	-12.59 ± 0.04	154 ± 27	-13.12 ± 0.08	95 ± 14	-12.90 ± 0.06	126 ± 24	-13.19 ± 0.07	99 ± 12
IL1_053	-12.78 ± 0.04	174 ± 27	-13.30 ± 0.08	87 ± 14	-13.13 ± 0.06	105 ± 24	-13.37 ± 0.07	72 ± 12
IL1_057	-12.69 ± 0.04	264 ± 27	-13.01 ± 0.08	185 ± 14	-13.10 ± 0.06	150 ± 24	-13.19 ± 0.07	149 ± 12
IL1_058	-12.69 ± 0.04	237 ± 27	-13.03 ± 0.08	198 ± 14	-13.03 ± 0.06	151 ± 24	-13.39 ± 0.07	101 ± 12
IL1_063	-12.94 ± 0.04	185 ± 27	-13.44 ± 0.08	109 ± 14	-13.32 ± 0.06	77 ± 24	-13.60 ± 0.07	85 ± 12
IL1_071	-12.95 ± 0.04	217 ± 27	-13.41 ± 0.08	139 ± 14	-13.39 ± 0.06	188 ± 24	-13.55 ± 0.07	166 ± 12
IL1_072	-12.71 ± 0.04	297 ± 27	-13.24 ± 0.08	132 ± 14	-13.03 ± 0.06	220 ± 24	-13.38 ± 0.07	141 ± 12
IL1_080	-12.49 ± 0.04	142 ± 27	-13.03 ± 0.08	151 ± 14	-12.80 ± 0.06	190 ± 24	-13.18 ± 0.07	155 ± 12
IL1_081	-12.98 ± 0.04	221 ± 27	-13.24 ± 0.08	85 ± 14	-13.23 ± 0.06	120 ± 24	-13.58 ± 0.07	101 ± 12
IL1_082	-13.06 ± 0.04	197 ± 27	-13.58 ± 0.08	75 ± 14	-13.39 ± 0.06	82 ± 24	-13.74 ± 0.07	91 ± 12
NIL A	-12.58 ± 0.03	309 ± 21	-13.00 ± 0.05	104 ± 10	-12.85 ± 0.04	156 ± 17	-13.17 ± 0.05	129 ± 9
NIL D	-12.75 ± 0.04	207 ± 27	-13.06 ± 0.08	148 ± 14	-13.09 ± 0.06	97 ± 24	-13.32 ± 0.07	113 ± 12
NIL E	-13.10 ± 0.04	182 ± 33	-13.39 ± 0.08	35 ± 14	-13.33 ± 0.06	106 ± 24	-13.37 ± 0.07	59 ± 12
NIL F	-12.97 ± 0.04	144 ± 27	-13.33 ± 0.08	49 ± 14	-13.07 ± 0.06	52 ± 24	-13.57 ± 0.07	48 ± 12
NIL G	-13.15 ± 0.04	128 ± 27	-13.47 ± 0.08	58 ± 14	-13.40 ± 0.06	46 ± 24	-13.59 ± 0.07	69 ± 12
NIL W	-12.83 ± 0.04	231 ± 27	-13.15 ± 0.08	109 ± 14	-13.08 ± 0.06	126 ± 24	-13.48 ± 0.07	92 ± 12
F1_(NIL B xRP)					-12.82 ± 0.04	247 ± 17	-13.13 ± 0.05	136 ± 9
F1_(NIL Y xRP)					-13.19 ± 0.04	160 ± 17	-13.57 ± 0.05	109 ± 9

7 Acknowledgements

Special thanks go to…

…Prof. Chris-Carolin Schön for the opportunity to work on this topic, as well as for constant trust, support and great professional advice.

…Prof. Thorsten Grams and Prof. Patrick Bienert for participating in my thesis examination committee.

…Dr. Viktoriya Avramova for always taking time to answer questions, for guidance and for many helpful suggestions and to Dr. Claudiu Niculaes for the initial introduction to this work.

…Dr. Monika Frey for always showing interest in discussing results and for sharing many ideas.

…Dr. Urte Schlüter for guidance on gas exchange measurements, for mentoring and extensive scientific feedback and also to all other FullThrottle project partners for suggestions and inspiring discussions.

…Dr. Rudi Schäufele for guidance on on-line $\Delta^{13}C$ measurements and helpful scientific input.

…Stefan Schwertfirm, Sylwia Schepella and all other former and current technicians for their motivation and skill in technical assistance, particularly genotyping in the lab and phenotyping in the field.

…my office mate Sonja Blankenagel and all other former and current fellow PhD students for helpful discussions on science and everything beyond and also to every other Plant Breeding group member for all the support.

…all gardeners at the Gewächshauslaborzentrum Dürnast for taking great care of plants in the greenhouse and to many students for helping with data collection.

Majority of this research was funded by the Federal Ministry of Education and Research (BMBF) within the project “Maximizing photosynthetic efficiency in Maize (FullThrottle)” (Funding ID: 031B0205C) as part of the funding initiative Plant Breeding Research for the Bioeconomy.